

# MinPet2015

**Montanuniversität Leoben**  
**September 10<sup>th</sup> - 13<sup>th</sup>**  
**Leoben**

*Abstracts*



*Montan University of Leoben, Peter-Tunner-Building (Applied Geosciences)*  
*picture by Kristina Stocker*



## PHASE EVOLUTION OF FE-TI-OXIDE MICRO-INCLUSIONS AND PLAGIOCLASE HOST IN OCEANIC GABBRO-PLAGIOGRANITE

Ageeva, O.<sup>1,2</sup>, Topa, D.<sup>3</sup> & Abart, R.<sup>1</sup>

<sup>1</sup>Department of Lithospheric Research, University of Vienna, Althanstrasse 14, A-1090 Wien, Austria

<sup>2</sup>IGEM RAS, Staromonetny 35, 119017, Moscow, Russia

<sup>3</sup>Naturhistorisches Museum Wien, Austria

e-mail: agolga7@yandex.ru

Fe,Ti- oxides carry most of the paleomagnetic record of magmatic rocks. Understanding the genesis and evolution of Fe-Ti oxides is of key importance for interpreting paleomagnetic data. We report on Fe,Ti-oxide micro-inclusions with specific regularities in shape, size, crystallographic and shape orientation which are hosted in rock-forming plagioclase of gabbro intruded by oceanic plagiogranite (OPG) veinlets from the Mid Atlantic Ridge at 13°34' N. Based on element mapping and point analyses at high spatial resolution using FEG-EMPA the chemical, and phase, evolution of the micro-inclusions during OPG magmatism and subsequent hydrothermal alteration was reconstructed.

The micro-inclusions are represented by (i) homogeneous ilmenite (Ilm) plates, and (ii) magnetite (Mt) needles/plates with ilmenite lamellae. Magnetite of Mt-Ilm micro-inclusions has close to magnetite end-member compositions. In the ilmenite lamellae the concentrations of Mg and Mn are elevated relative to the concentrations of these elements in magnetite. The plagioclase host is calcic (An<sub>63</sub>), but towards the magnetite-ilmenite inclusion a subtle decrease in anorthite content (down to An<sub>53</sub>) is observed in an about 5 micrometers wide zone. A more pronounced decrease of anorthite content (down to An<sub>42</sub>) and a concomitant increase in K-content occur around homogenous Ilm plates. Moreover, additional phases (amphibole, biotite and potassium feldspar) were identified at the interface between Ilm inclusions and plagioclase host. These characteristics allow to relate the formation of ilmenite with the OPG stage, which produces similar plagioclase chemistry and mineral assemblage features.

The distribution of Fe in plagioclase in domains surrounding the micro-inclusions is of particular interest. The concentration of FeO<sub>T</sub> in plagioclase surrounding Ilm progressively increases from 0.17 to 0.43wt% toward the ilm plate. This Fe-increase is positively correlated with Na concentrations. This contradicts the general trend of chemical evolution from gabbroic (An<sub>65-55</sub>) to OPG (An<sub>50-32</sub>) and hydrothermal (An<sub>26-13</sub>) generations of plagioclase showing negative correlation between Fe and Na. The increase of Fe concentration in plagioclase surrounding Ilm plates can be considered as result of re-deposition of this element from previous Fe-rich phase (presumably magnetite) into surrounding plagioclase which occurs in the OPG stage of rock formation.

The evolution of the micro-inclusions starts with abundant finest dust-like inclusions of Ti-bearing magnetite in plagioclase or initial gabbro. The most probable formation mechanism being exsolution of Fe,Ti-bearing plagioclase under sub-solidus conditions. In the next stage break-down of Ti-bearing magnetite into Mt-Ilm intergrowths, their subsequent growth succeeded by disappearance of the Mt phase and re-crystallization of Ilm lamellas into separated plates is attributed to the OPG stage. Finally hydrothermal alteration lead to complete cleaning of plagioclase from any micro-inclusions.

## MINERALOGY AND LEACHABILITY OF AUSTRIAN ROCKS USED IN ROAD CONSTRUCTION

Altenburger, I.<sup>1</sup>, Schweiger, G.<sup>1</sup>, Aldrian, A.<sup>2</sup> & Höllen, D.<sup>2</sup>

<sup>1</sup> Fachhochschule Technikum Wien, Institute of Biochemical Engineering, Hochstädtplatz 6, 1200 Wien, Austria

<sup>2</sup> Chair of Waste Processing Technology and Waste Management, Montanuniversität Leoben,

Franz-Josef-Str. 18, 8700 Leoben, Austria

e-mail: daniel.hoellen@unileoben.ac.at

Natural rocks and recycling materials compete with each other as aggregate for road construction in Austria. Recycling materials like slags or construction and demolition waste must fulfill the requirements of the Austrian Recycling Building Materials Directive, whereas natural rocks are not obliged to fulfill these requirements. Consequently, data regarding the leachability of rocks used in road construction are scarce (e.g., TOSSAVAINEN & FORSSBERG, 1999) and not available for Austrian rocks.

In this work the mineralogical composition and leachability of four Austrian rocks used in road construction are investigated. X-ray diffraction (XRD) including Rietveld refinement could not confirm the presence of stoichiometrically heavy metal bearing phases (e.g., chromite,  $\text{FeCr}_2\text{O}_4$ ). This is due to the detection limit of this method of about 2 wt.-% and possibly due to the incorporation of heavy metals in other phases; e.g., Ni was confirmed in lizardite ( $\text{Mg}_3\text{Si}_2\text{O}_5(\text{OH})_4$ ). Inductively coupled plasma mass spectrometry (ICP-MS) indicates that the total contents of most heavy metals are underneath the limit values of the Austrian Recycling Building Materials directive, but the investigated serpentinite exceeds the limit values of Cr and Ni for the quality class U-A by more than one order of magnitude. However, leaching tests of this rock according to EN 12457-4 indicate, that besides Ni it is not Cr, but Cu which exceeds the limit values in the leachate (Fig. 1).

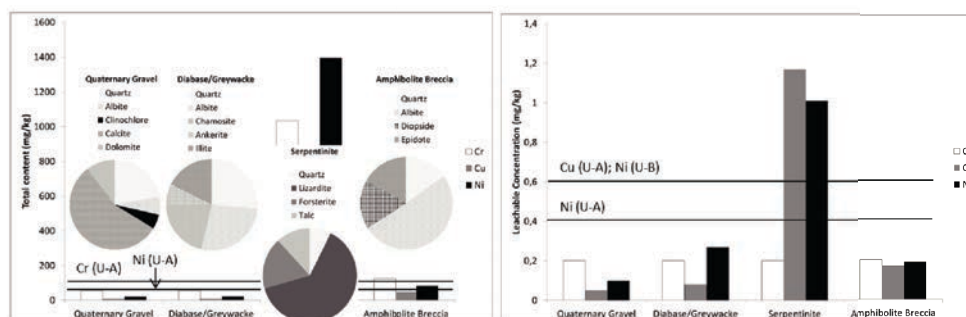


Figure 1. Comparison of total (left) and leachable (right) content of heavy metals from Austrian rocks with limit values for the quality classes U-A and U-B from the Austrian Recycling Building Materials Directive.

ALTENBURGER, I. (2015): Mineralogie und Auslaugbarkeit natürlicher im Straßenbau eingesetzter Gesteine Österreichs. Master Thesis. Fachhochschule Technikum Wien.

TOSSAVAINEN, M., FORSSBERG, E. (1999): The Science of the Total Environment 239, 31-47.



## NONOXIDES IN ORDINARY REFRACTORY CERAMICS – PHASES, COMPOSITIONS AND ANALYSIS

Atzenhofer, C.<sup>1</sup>, Gschiel, S.<sup>2</sup> & Harmuth, H.<sup>1</sup>

<sup>1</sup>Department Mineral Resources and Petroleum Engineering, Chair of Ceramics, Montanuniversität Leoben, Peter-Tunner-Straße 5, 8700 Leoben, Austria

<sup>2</sup>RHI Technology Center Leoben, Magnesitstraße 2, 8700 Leoben, Austria  
e-mail: christina.atzenhofer@unileoben.ac.at

Nonoxide phases in ordinary refractory materials may be either added to the mixture composition or are formed in-situ during service. The in-situ phase formation depends on the recipe, the temperature and the atmosphere. The occurring nonoxides can be carbides, nitrides, oxycarbides and oxycarbonitrides. This work deals with the identification of these in-situ formed nonoxide phases by X-ray diffraction analysis, microscopical investigations and with the help of EDX measurements.

Identifying these nonoxides can be a challenging task because on the one hand some of these phases possess similar X-ray diffraction spectra and on the other hand EDX analysis of light weight elements containing phases like carbides and nitrides are difficult.

This contribution deals with MgAlON, MgSiAlON, oxycarbide and oxycarbonitride bonded refractories. The identification of MgAlON and MgSiAlON is difficult due to the existence of several solid solutions. Furthermore, the determination of  $\text{Al}_4\text{O}_4\text{C}$ ,  $\text{Al}_2\text{OC}$  and  $\text{Al}_{28}\text{O}_{21}\text{C}_6\text{N}_6$  in refractory materials causes problems because their X-ray diffraction patterns can be mistaken with other phases like AlN,  $\text{Al}_4\text{CN}_3\text{O}$  and  $\text{Al}_3\text{OCN}$ . Another problem that arises is that the phases are in most cases very small and difficult to distinguish. An EDX analysis of a single phase is sometimes impossible.

For the analysis of carbon containing phases with EDX gold sputtered samples are used but the gold coating influences the measurement of the light elements (C and N). For a detailed phase analysis, a combination of several investigation methods is therefore always necessary.

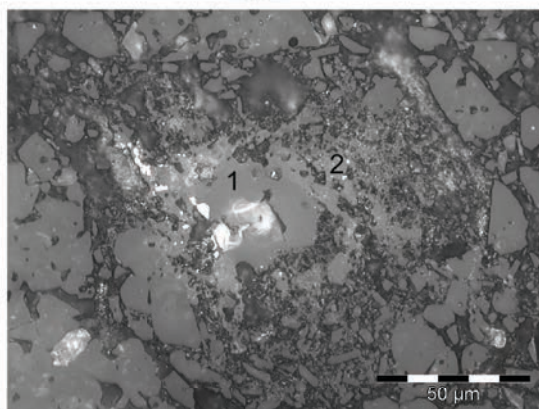


Figure 1. Reflected light microphotograph of refractory material containing  $\text{Al}_4\text{O}_4\text{C}$  (1) and  $\text{Al}_{28}\text{O}_{21}\text{C}_6\text{N}_6$  (2).

## VERIFICATION “CHEMICAL PARAMETER” FOR SOLVING CHEMICAL ATTACK OF CONCRETE

Bachhuber, P.<sup>1</sup>, Rümmele, F.<sup>1</sup>, Nickel, C.<sup>2</sup> & Klammer, D.<sup>1</sup>

<sup>1</sup>Institute of Applied Geosciences, University of Technology Graz, Rechbauerstrasse 12, 8010 Graz, Austria

<sup>2</sup>Institute of Technology and Testing of Building Materials, University of Technology Graz, Inffeldgasse 24,  
8010 Graz, Austria

e-Mail: dietmar.klammer@tugraz.at

The action against climate change affects production in concrete industry immensely. From there reducing the emission of carbon dioxide is a major goal in the scientific project „Performance oriented durability testing of eco-concrete for the precast industry” (JUHART et al., 2014). Among others, one of the aims of this project is to develop new so called eco-concretes. Goal of our research was to compare a proven concrete CEM 1 (equals B24) to the new developed, low CO<sub>2</sub> emitting concretes (equals B26, B29) in exposure to hydrogen carbon acidic solutions (pH within the range of 4.5–4.7). Within 6 weeks certain parameters were constantly monitored like pH, temperature and conductivity. Liquide samples were analysed by IC and ICP-OES to quantify the amount of dissolved ions. Solid analyses directly on the surface of the concrete pieces were performed before and after the experiment using IR and XRD Spectrometry to evaluate the damaged caused.

In the beginning of the experimental test the concretes were exposed to lower concentrated solutions. Resulting out of higher pumping rates in the experiment, samples were taken every hour on day. IC- and ICP-OES-analyses showed that dissolved ions concentration was at its peak after one day and fell off in the following days. Therefore sampling was reduced to once a day down respectively finally once in 3 days due to the constant test results and the stable state of chemical equilibration within the solution process. After three weeks the pumping rate was changed to increase the concentration of the acting solutions again with the effect that the ion concentration was three times higher than the values previously determined. Same mechanism of quick solution sampling in the beginning up to reaching a peak and reaching chemical balance was monitored. By the end of the experiment on all three different types of concrete specimen damages were visible, part wise as expected covered by a brown crust (probably iron phases). First XRD as well as IR-analyses showed that these analyse techniques unfortunately were not suited to show off the new built phases on the surface of the specimen since during the sample preparations mixing could not be prevented with the sample matrix. How was visible after sawing the test pieces the cause should be different profound dissolving processes where by the different height packing density of the concrete plays an essential role. On the 20<sup>th</sup> of March the pump was changed and thereafter the ion concentration increased again. The chemical balance adjusted in the following days.

Further detailed studies as well as other analytical methods are planned to be able to clarify exactly the formation and identification of solid samples formed during the dissolving process.

JUHART, J., G.-A. D. (2014): Mitt. Österr. Miner. Ges., 138, 179-196.

## H<sub>2</sub>O-NaCl FLUID INCLUSIONS IN WONDERLAND

Bakker, R.J.<sup>1</sup>

<sup>1</sup>Chair of Resource Mineralogy, Montanuniversität Leoben, Peter-Tunner-Str. 5, 8700 Leoben, Austria  
e-mail: bakker@unileoben.ac.at

The fluid system H<sub>2</sub>O-NaCl has been subject of investigation for many years in chemistry and physics, and is of special interest to fluid inclusion studies. Both components occur in the majority of fluid inclusions known to geologists. The properties of this fluid system are of major importance to interpret trapping conditions of fluid inclusions in many types of rock. The principle objective of the present study was to investigate experimental re-equilibration behaviour of synthetic H<sub>2</sub>O-NaCl-rich fluid inclusions. The study was orientated towards detecting diffusion processes, brittle deformation processes (micro-cracking), and fluid inclusion wall re-crystallization in and around synthetic fluid inclusions with well-defined composition and density under well-defined temperature-pressure-fugacity conditions. In due course of the project, a number of additional objectives were defined due to unexpected results: 1. Do synthetic H<sub>2</sub>O-NaCl fluid inclusions have densities that corresponds to the experimental T-P conditions?; and 2. How can I change fluid inclusion compositions against the applied gradients in fugacity compared to an external fluid? The synthesis of pure H<sub>2</sub>O and H<sub>2</sub>O-NaCl fluid inclusions was performed according to the descriptions in the PhD thesis of Gerald Doppler. Fluid inclusions were synthesized at 600°C and 337MPa, within the  $\alpha$ -quartz stability field. These experimental conditions were monitored accurately with an internal thermocouple. Fluid properties were calculated with software to handle complex but accurate equations of state, which are available at the web-site <http://fluids.unileoben.ac.at>. The re-equilibration experiments were designed at constant temperature (600°C) and constant pressure (337MPa) and specific fugacity gradients of H<sub>2</sub>O. The modifications of H<sub>2</sub>O-NaCl inclusion that are re-equilibrated in pure H<sub>2</sub>O environment are significant, both  $T_m$ 's and  $T_h$ 's are strongly affected. The intensity of modification is directly related to experimental run time, which may imply diffusion processes. All the experiments reveal a relative loss of H<sub>2</sub>O in individual inclusions. Close examination of the outcome of these experiments reveals a number of enigmas. First, fugacity gradients must result in diffusion of H<sub>2</sub>O into the inclusions resulting in a relative decrease of salinity, that correspond to higher  $T_m$ 's. Second,  $T_m$ 's decrease to values below the eutectic temperature of the binary H<sub>2</sub>O-NaCl system. Third, short term experiments have a reversed modification of  $T_h$  compared to long term experiments. Fifth, theoretical modelling of H<sub>2</sub>O diffusion out of the inclusions (calculated with the programs *AqSo DH* and *ReqDif*, <http://fluids.unileoben.ac.at>) result in a completely different trend of paired  $T_h$  and  $T_m$  modifications. The observed modifications in microthermometrical data can only be obtained by preferential H<sub>2</sub>O loss. However, bulk H<sub>2</sub>O diffusion alone cannot account for these modifications, but a paired process of H<sub>2</sub>O loss and SiO<sub>2</sub> gain result in observed trend of  $T_h$  and  $T_m$ . This process is not driven by H<sub>2</sub>O-fugacity gradients and only occurs with H<sub>2</sub>O-NaCl bearing fluid inclusions. Any pressure difference between fluid inclusions and pore fluids is inhibiting bulk-diffusion processes of fluid components through quartz. This work is supported by the FWF, project P224460-N21, as part of the PhD thesis of Gerald Doppler.

**COMPARISON OF FLUID INCLUSION STUDIES IN CORDIERITE-ANDALUSITE-RICH LEUCOGRANITE DYKES AND TOURMALINE-BEARING APLITE-PEGMATITE DYKES (ELBA, ITALY)**

Bakker, R.J.<sup>1</sup> & Schilli, S.E.<sup>1</sup>

<sup>1</sup>Chair of Resource Mineralogy, Montanuniversität Leoben, Peter-Tunner-Str. 5, 8700 Leoben, Austria  
e-mail: bakker@unileoben.ac.at

The late magmatic-hydrothermal stage of the Monte Capanne pluton (Elba, Italy) is associated with abundant fluid sources, of which the remnants are present in numerous fluid inclusion assemblages in associated leucogranite dykes, and aplite-pegmatite dykes and veins. They are mainly located in the pluton and its thermometamorphic aureole close to the pluton's contact. The studied dykes were sampled in serpentinitic host rock. The leucogranite dyke contains abundant andalusite and cordierite (peraluminous). The pegmatite vein is mainly composed of coarse-grained quartz, plagioclase and foitic tourmaline. A variety of fluid inclusion assemblages were observed in andalusite-plagioclase-quartz (leucogranite) and tourmaline-quartz (aplite-pegmatite). The contents of fluid inclusions were detected with microthermometry and Raman spectroscopy. Complex gas mixtures of CO<sub>2</sub>, CH<sub>4</sub>, H<sub>2</sub>, N<sub>2</sub>, and locally H<sub>2</sub>S and alkanes were detected in the vapour phase of all types of inclusions. Anhydrous inclusions in andalusite contain a low density CO<sub>2</sub>-rich gas-mixture and abundant accidentally trapped mica's. Some inclusions contain diaspore and quartz, which are reaction products of H<sub>2</sub>O (completely consumed) and host mineral. Type 1 inclusions in quartz contain a mixture of H<sub>2</sub>O and H<sub>2</sub>, and usually an accidentally trapped mica, which can only be detected by Raman. Type 2 inclusions have a CO<sub>2</sub>-CH<sub>4</sub>-rich vapour phase with up to 16mole% H<sub>2</sub> and N<sub>2</sub>. Some minor amounts of dissolved sassolite (H<sub>3</sub>BO<sub>3</sub>, <2.5mass%) and NaCl are detected in the liquid phase. Tourmaline from the aplite-pegmatite contains exceptional large fluid inclusions. The liquid phase contains higher concentrations of sassolite (4 to 6mass%), which nucleate to crystals by Raman laser irradiation at room temperatures. Arsenolite and arsenic was observed in some inclusions. The bulk fluid properties are similar to Type 2 from quartz in the leucogranite. Also the fluid inclusions in quartz from the aplite-pegmatite contain traces of sassolite (H<sub>3</sub>BO<sub>3</sub> < 2.5 mass%), and the vapour phase is CO<sub>2</sub>-rich, with minor amounts of CH<sub>4</sub>. Other gases were not detected in these inclusions. Both types of rock (leucogranite and aplite-pegmatite) reveal similar fluids in inclusions, which may imply a similar origin. H<sub>2</sub>O is the most important component of all fluid inclusion assemblage. The absence of melt inclusions in both rock types emphasizes their hydrothermal origin. Details about accessory components such as NaCl, H<sub>3</sub>BO<sub>3</sub> and gas-compositions in different fluid inclusion assemblages illustrate the development of rock-forming conditions. Whereas the CO<sub>2</sub>-rich fluids in andalusite suggest a magmatic source, a highly reduced fluid (H<sub>2</sub> and CH<sub>4</sub>) that is found in early assemblages in quartz and plagioclase illustrates the strong influence of fluid properties from the surrounding host rock (serpentinites). The fluid sources of both rock types are poor in NaCl. The solvus boundary of a Boron-H<sub>2</sub>O rich granitic melt, the presence of andalusite, and the specific molar volume of homogeneous fluid inclusion assemblage restrict formation conditions of both leucogranite and aplite-pegmatite to a narrow T-P window at about 650°C and 300MPa.

## GRAPHENE AND MoS<sub>2</sub> 2D CRYSTALS FOR ELECTRONIC DEVICES

Bayer, B.C.<sup>1</sup> & Kaindl, R.<sup>2</sup>

<sup>1</sup>University of Vienna, Faculty of Physics, Boltzmannngasse 5, A-1090 Vienna, AUSTRIA

<sup>2</sup>JOANNEUM RESEARCH, MATERIALS – Institute for Surface Technologies and Photonics,

Leobner Straße 94, A-8712 Niklasdorf, AUSTRIA

bernhard.bayer@univie.ac.at, reinhard.kaindl@joanneum.at

Electronic devices based on novel two-dimensional (2D) nanomaterials are set to revolutionise ICT towards high performance, mechanical flexibility and cost effectiveness. To date however, industrially scalable fabrication routes to realise such 2D electronics remain severely limited. Within a funded project (FFG 848152) a proof-of-principle field effect transistor device based on scalable synthesised 2D heterostructures of graphene layers with the semiconducting transition metal dichalcogenide MoS<sub>2</sub> should be manufactured. Synthesis of graphene and MoS<sub>2</sub> and their heterostructures will employ, amongst others, industrially scalable Physical Vapour Deposition (PVD) methods (magnetron sputtering).

Raman spectroscopy and Scanning Electron Microscopy with Energy Dispersive X-ray spectroscopy of PVD MoS<sub>2</sub> films deposited at room temperature (RT) confirm Raman peaks around 370 and 400 cm<sup>-1</sup>, typical for MoS<sub>2</sub> crystals and S/Mo ratio of 2.1±0.1. However, compared to exfoliated 2D MoS<sub>2</sub> the peaks are shifted and broadened indicating much lower crystallinity of RT PVD films. In-situ annealing in air under high laser power results in immediate development of new Raman peaks, which can be assigned to Mo-oxides or –hydroxides (SEGUIN et al., 1995). At 400°C deposition peak positions and lower full width at half maximum indicate higher crystallinities of PVD MoS<sub>2</sub> films. The peaks do not undergo any change upon high laser power irradiation, showing the higher stability compared to RT PVD films. Scanning transmission electron microscopy (STEM) indicates electron beam induced crystallisation of the initially largely amorphous MoS<sub>2</sub> structure at atomic resolution (Fig. 1).

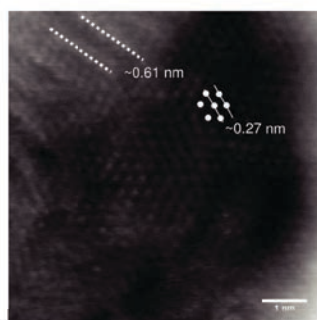


Figure 1. STEM image of electron-beam-induced crystallized RT PVD MoS<sub>2</sub> on CVD graphene. Layers perpendicular and parallel to substrate with the typical lattice distances (~0.61 and ~0.27 nm) are indicated.

SEGUIN, L., FIGLARZ, M. CAVAGNAT, R. LASSÉGUES, J.C. (1995): Spectrochim. Acta A, 51, 1323-1344.



# **POLYPHASE METAMORPHIC EVOLUTION OF METABASIC ROCKS FROM THE SONGSHUGOU OPHIOLITE, QINLING OROGEN, CHINA**

Belic, M.<sup>1</sup>, Hauzenberger, Ch.<sup>1</sup>, Dong, Y.<sup>2</sup> & Danling, Ch.<sup>2</sup>

<sup>1</sup>Institute for Earth Sciences, University of Graz, Universitätsplatz 2, 8010 Graz, Austria

<sup>2</sup>State Key Laboratory of Continental Dynamics, Department of Geology, Northwest University,

229 North Taibai Avenue, Xi'an, China

e-mail: belic.maximilian@gmail.com

The Proterozoic Songshugou ophiolite comprises a series of ultrabasic and metabasic rocks, which were emplaced as a lense shaped body into the southern margin of the Qinling Group during the Proterozoic closure of the Songshugou Ocean (DONG et al., 2008). The metabasic rocks contain the mineral assemblage garnet+amphibole+symplectitic pyroxenes+ilmenite+apatite±zoisite±sphene and display a strong retrograde metamorphic overprint. Garnet cores are typically full with inclusions (actinolite, pargasite, epidote, albite and sphene); their rims in turn are almost inclusion-free. Garnet zoning patterns, as well as garnet breakdown reactions and symplectitic pyroxenes indicate a polymetamorphic history of the metabasic rocks. Garnets clearly show a discontinuous growth displayed by a sudden increase in grossular and decrease in almandine components at the rims (Fig.1), and Y-rich cores. Based on symplectitic pyroxenes a high pressure metamorphic event can be concluded (ZHANG et al., 1999), supported by garnet isopleth geothermobarometry, where garnet core isopleths indicate an older amphibolite facies metamorphic event. Garnet-rim isopleths represent eclogite facies conditions. Different stages of garnet breakdown to plagioclase+amphibole+thin plagioclase rims surrounding the garnets or plagioclase rich pseudomorphs, are observed in various samples. The age of the metamorphic event is probably related to the closure of the Shangdan Ocean during the early Paleozoic. The financial support by Eurasia-Pacific Uninet is gratefully acknowledged.

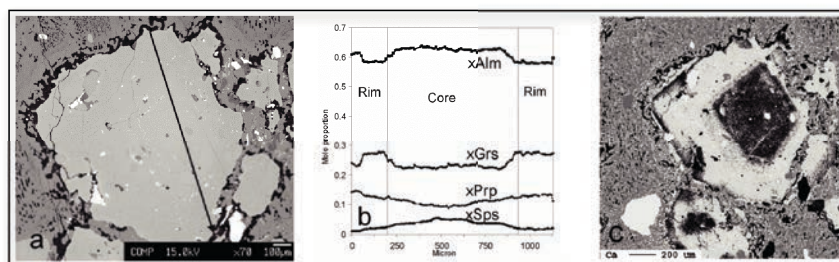


Figure 1. a: BSE image of garnet, b: garnet profile, c: Ca distribution image showing Ca-rich garnet rims.

DONG, Y.P., ZHOU, M.F., ZHANG, G.W., ZHOU, D.W., LIU, L., ZHANG, Q. (2008): Journal of Asian Earth Science 32, 325–335.

ZHANG, Z.J. (1999): The Island Arc, 8, 259–280.

**GEOHERMAL SCALING FORMATION: FIRST RESULTS FROM HIGH-RESOLUTION CHEMICAL, ISOTOPIC AND PETROGRAPHIC STUDIES**

Boch, R.<sup>1</sup>, Dietzel, M.<sup>1</sup>, Deák, J.<sup>2</sup>, Mindszenty, A.<sup>3</sup>, Szanyi, J.<sup>4</sup>, Leis, A.<sup>5</sup> & Demeny, A.<sup>6</sup>

<sup>1</sup>Graz University of Technology, Institute of Applied Geosciences, Rechbauerstr. 12, 8010 Graz, Austria

<sup>2</sup>GWIS – Ground Water Isotope Studies Ltd., Alkotmány u. 45, 2120 Dunakeszi, Hungary

<sup>3</sup>Eötvös L. University, Dept. of Physical and Applied Geology, Pázmány P. sétány 1/c, 1117 Budapest, Hungary

<sup>4</sup>University of Szeged, Dept. of Mineralogy, Geochemistry & Petrology, Egyetem u. 2, 6722 Szeged, Hungary

<sup>5</sup>Joanneum Research, Resources – Inst. f. Water, Energy & Sustainability, Elisabethstr. 18, 8010, Graz, Austria

<sup>6</sup>Hungarian Academy of Sciences, Inst. f. Geol. & Geochem. Research, Budaorsi ut 45, 1112 Budapest, Hungary  
e-mail: ronny.boch@tugraz.at

Water discharging from geothermal wells of hundreds to thousands meters depth tends to precipitate chemical sediments (scaling) resulting from high total dissolved solid and gas contents in aqueous solution at increased temperature and pressure. Clogging of boreholes, downhole pumps, transport pipes and heat exchangers from precipitation of carbonates, sulfates, sulfides and silica is a major problem at many sites of geothermal heat- and electric power production. In particular, scaling reduces the volume and efficiency of energy extraction and can even question the economic viability of installations.

In order to better constrain the natural and technological environmental conditions promoting scaling formation we collected mineral precipitates from different boreholes of nine selected sites distributed over Hungary. Samples of up to 8 cm thickness were recovered from different positions of the geothermal systems and precipitated from waters covering a broad temperature range (40-120°C), depth (1000-2500m), discharge (30-80m<sup>3</sup>/h), working-pressure and variable chemical composition. Although the scalings consist of all-dominant calcium carbonate reflecting the regional aquifer host rocks they show remarkable differences in macro- and microscopic appearance. Most of them show distinct lamination patterns including successions of calcite and aragonite within the same sample. Depending on the position and study site, mineral deposition from weeks up to 45 years is represented. Importantly, these chemical sediments constitute an archive capturing solid-fluid interaction and thus the determining but changing natural and production conditions over time. We therefore attempt to reconstruct particular scaling growth conditions at high spatiotemporal resolution applying state-of-the-art analytical techniques including laser-ablation mass-spectrometry and electron microprobe for minor- and trace-elemental compositions, micromill-sampling for stable carbon and oxygen isotope analysis, micro-XRD and petrographic methods (SEM, micro-CT). Analytical and geothermal plant-specific data combined with hydrogeochemical modelling will help to better understand changes in fluid chemistry, temperature, pressure, pH, degassing rate (CO<sub>2</sub>) and flow rate in the context of short-term versus long-term geothermal production dynamics. An ultimate goal aside from fundamental research interests persists in retarding and preventive measures of scaling formation in geothermal and other (e.g. oil production) applications.

**IKAITE ( $\text{CaCO}_3 \cdot 6\text{H}_2\text{O}$ ) CRYSTALLIZATION IN A MAN-MADE RIVER BED:  
CONCRETE LEACHING AND HYDROCHEMICAL ALTERATION**

Boch, R.<sup>1</sup>, Dietzel, M.<sup>1</sup>, Reichl, P.<sup>2</sup>, Leis, A.<sup>2</sup>, Baldermann, A.<sup>1</sup> & Pölt, P.<sup>3</sup>

<sup>1</sup>Graz University of Technology, Institute of Applied Geosciences, Rechbauerstr. 12, 8010 Graz, Austria

<sup>2</sup>Joanneum Research, Resources – Inst. f. Water, Energy & Sustainability, Elisabethstr. 18, 8010, Graz, Austria

<sup>3</sup>Graz University of Technology, Austrian Centre f. Electron Microscopy & Nanoanalysis, Steyrergasse 17,  
8010 Graz, Austria

e-mail: ronny.boch@tugraz.at

During repository building measures a natural river was relocated and the water was directed through a new artificial river bed lined with a concrete basement and local colluvium. Shortly after, centimetre-thick, beige-colored crusts were observed in the river bed and made a clarification at the construction-site necessary. A monitoring program launched to understand the rapid precipitation process revealed pH up to 12.9 and high  $\text{Ca}^{2+}$  concentrations (196mg/l) at near-freezing water-temperatures. A first set of crystal aggregates collected was found to disintegrate into a light-colored calcite powder at ambient temperature within few days only. Therefore, the metastable crusts were recovered in original solution and stored in a constantly-cooled refrigerator box. Immediate XRD, FT-IR and ESEM analyses revealed ikaite being the particular and rarely documented mineral which was never reported from such an environmental setting before. Ikaite typically forms in a narrow temperature range (<4–8 °C) from strongly supersaturated solutions, e.g. some specific lake-, sea- and spring-water mixing locations, as well as in brine pockets during Arctic- and Antarctic sea-ice formation. In our case, enhanced portlandite ( $\text{Ca}[\text{OH}]_2$ ) dissolution from the concrete river basement by water inflowing during wintertime provided exceptional hydrochemical conditions promoting rapid ikaite precipitation, e.g. up to  $2 \text{ kgd}^{-1}\text{m}^{-2}$  in a particular stream section. Sampling sites where ikaite occurred yielded pH>10.5 probably reflecting a lower limit. Our findings do not support  $\text{CaCO}_3$  nucleation inhibitors (phosphate, magnesium, sulfate, organic constituents), strongly elevated ionic strength (brines), or specific water-mixing as a crucial demand for ikaite formation. In this “natural laboratory” distinct ikaite vs. calcite spatial distribution encountered along the stream, and consequently the spatiotemporal evolution of fluid-solid interaction could be studied. Stable H and O isotopic compositions of aqueous solutions show rather constant values ranging from -74.3 to -71.7 and -10.9 to -10.4‰ VSMOW, respectively, while the  $\delta^{13}\text{C}_{\text{DIC}}$  values reveal pronounced variations of -15.8 to -5.9‰ VPDB, depending on the location and hydrochemical evolution along the stream. Similarly,  $\delta^{13}\text{C}$  and  $\delta^{18}\text{O}$  of ikaite and calcite precipitates show large ranges of -15.0 to -10.0 and -17.9 to -4.2‰ VPDB, respectively. The very low values strongly indicate  $\text{CO}_2$  absorption from the atmosphere (and associated isotope fractionation) playing an important role in the aqueous carbonate budget and efficient formation of these chemical sediments.

Finally, the prominent and widespread ikaite crusts vanished rapidly during pronounced springtime air- and water-temperature rise (>6°C) superimposed on more gradual hydrochemical changes, e.g. decrease of pH and  $\text{Ca}^{2+}$  concentration. The latter development highlights the critical temperature restriction of ikaite occurrence and stability. Observations made in this study are of interest for both applied (construction-engineering) and fundamental environmental research.



**INTERNAL MICROSTRUCTURES AND BREAKDOWN OF GARNET FROM  
MOLDANUBIAN GRANULITES (GFÖHL UNIT, DUNKELSTEINER WALD,  
NIEDERÖSTERREICH)**

Bourgin, N.<sup>1</sup>, Abart, R.<sup>1</sup> & Petrakakis, K.<sup>2</sup>

<sup>1</sup>Dep. of Lithospheric Research, Althanstraße 14 (UZA 2), 1090 Vienna, Austria

<sup>2</sup>Dep. of Geodynamics and Sedimentology, Althanstraße 14 (UZA 2), 1090 Vienna, Austria  
e-mail: a0542762@unet.univie.ac.at

Some conspicuous symplectite-bearing granulite-facies rocks from the Moldanubian Gföhl Unit show an unusual bulk composition with very high Mg and Ca contents and 14mole% normative corundum. They contain garnets ( $X_{\text{Py}} > 0.55$ ), clinopyroxene ( $X_{\text{Di}} > 0.7$ ;  $X_{\text{CaTs}} > 0.2$ ), pargasitic hornblende, and plagioclase ( $X_{\text{An}} > 0.75$ ). The primary microstructure is granular and well equilibrated.

Garnets of about 2cm size are common. Often they are resorbed and thus significantly smaller. The garnets show internal deformation which is expressed by non-coaxial strain around a common rotation axis approximately parallel to [211] of the garnet lattice of the different domains. From crystal orientation imaging incipient polygonalization of garnet during crystal plastic deformation under high-grade metamorphic conditions is inferred.

Along garnet margins and within cracks, various replacement symplectites were formed comprising distinct assemblages of orthopyroxene+spinel+anorthite±Al-rich amphibole±tschermakitic diopside±sapphirine±corundum. Symplectite formation was probably induced by decompression and fluid input. The last peak metamorphic conditions of the Gföhl Unit has been estimated in previous studies with pressures and temperatures around 0.8-1.1GPa and 700-800°C. The rocks then experienced isothermal decompression followed by isobaric cooling down to 0.5-0.6GPa (PETRAKAKIS, 1997). The temperature during the formation of the symplectites has been estimated using Grt-Opx- and Grt-Cpx-thermometry and resulted in values of approx. 700°C for the pressure-range of 0.5-0.6GPa, indicating essentially isothermal decompression.

Towards the interface with the symplectites, garnets show secondary diffusional zoning, which is most likely related to symplectite formation. This zoning is characterized by increasing Fe and decreasing Mg towards the garnet rim and can be used for geospeedometry modelling. Diffusion modelling yields a time interval for symplectite formation of about 1000 years, which thus represents an ephemeral episode during decompression within the geological time frame. Preservation of the delicate symplectite microstructures and the lack of penetrative deformation are consistent with isobaric cooling at 0.5-0.6GPa as suggested earlier.

PETRAKAKIS, K. (1997): J. Metam. Geol. 15, 203-222.

**JAVANESE KRIS DAGGERS AND THE USE OF METEORITIC IRON:  
PRELIMINARY RESULTS OF AN XRF STUDY**

Brandstätter, F.<sup>1</sup>, Padilla-Alvarez, R.<sup>2</sup>, Giester G.<sup>3</sup>, Karydas, A.<sup>2</sup>, Kuhnt-Saptodewo, S.<sup>4</sup>,  
Visser, S.<sup>5</sup> & Koeberl, C.<sup>1,6</sup>

<sup>1</sup>Department of Mineralogy and Petrography, Natural History Museum, Burgring 7, 1010 Wien, Austria

<sup>2</sup>Department of Nuclear Sciences and Applications, International Atomic Energy Agency, Vienna International  
Centre, PO Box 100, 1400 Wien, Austria

<sup>3</sup>Institute of Mineralogy and Crystallography, University of Vienna, Althanstrasse 14, 1090 Wien, Austria

<sup>4</sup>Weltmuseum Wien, Neue Burg, Heldenplatz, 1010 Wien, Austria

<sup>5</sup>Bellevuedreef 40, 2970 Schilde (Antwerp), Belgium

<sup>6</sup>Department of Lithospheric Research, University of Vienna, Althanstrasse 14, 1090 Vienna, Austria  
e-mail: Franz.Brandstaetter@nhm-wien.ac.at

The “Weltmuseum Wien” owns a large collection of kris daggers. These objects are famous for their metal blades consisting of numerous layers made by a complicated forging process involving repeated folding and welding of the individual layers. Of special interest are kris daggers from Java, as it is known that some blades were made by adding meteoritic nickel-iron to terrestrial iron during forging. Most meteoritic metal was taken from the Prambanan iron meteorite, which fell in central Java and is known since 1784 (COHEN, 1905). The aim of the present study is to identify daggers in the collection of the Weltmuseum Wien that contain nickel-iron metal from the Prambanan meteorite. However, due to several restrictions the identification of a meteoritic admixture in the kris blades is not a trivial task (NEČEMER et al., 2013). The main complications comprise the exclusive use of a non-destructive method, the size of the objects being ~30 cm in length, the location of suitable areas/spots for chemical analysis, and the limitations inherent to the applied method. This study was performed using a handheld XRF instrument, as this technique has already proven useful for the basic classification of meteorites (e.g., DAVIAU et al., 2012). In a first step, blades of ~200 krisses were checked for areas having significant Ni-contents (in the wt%-range) by using a Bruker Tracer IV-SD XRF analyzer. After this preselection, 7 krisses (inventory numbers 8.044, 23.606, 23.646, 46.049, 119.014, 125.117, 900.382) with the apparently highest Ni-contents were selected for more detailed investigations. These measurements were performed using a Thermo Scientific Niton Xlt XRF analyzer (with an Au anode operated at maximum values of 50 kV and a current not producing more than 2 W). The apparent concentrations (in wt%) for Fe, Ni, and Co were calculated using a manufacturer-provided calibration for metals. For a Prambanan test sample the calculated values for Ni (9.6 wt%) and Co (0.83 wt%) are in good agreement with the bulk data of KRACHER et al. (1980). Altogether 39 spots (~3 mm in diameter) on both sides of the kris blades were analyzed, yielding significant Ni concentrations, from ~ 0.4 to 12.5 wt%. The corresponding Co values range from below detection limit to 1.5 wt%, indicating a possible meteorite admixture.

COHEN, E. (1905): Meteoritenkunde, Heft III, Schweizerbart, Stuttgart, 308-312.

DAVIAU, K.C., MAYNE, R.G., EHLMANN, A.J. (2012): 43<sup>rd</sup> Lunar and Planetary Conference, 1306.

KRACHER, A., WILLIS, J., WASSON, J.T. (1980): Geochim. Cosmochim. Acta, 44, 773-787.

NEČEMER, M., LAZAR, T., ŠMIT, Ž., KUMP, P., ŽUŽEK, P. (2013): Acta Chim. Slov., 60, 351-357.

## **AUTOMATED MINERAL ANALYZER: A NEW TOOL TO DISTINGUISH MAGMATIC AND METASOMATIC PROCESSES IN RARE-METAL GRANITES**

Breiter, K. & Hrstka, T.

Geological institute of the Czech Academy of Science, Rozvojová 269, CZ-16500 Praha 5, Czech Republic

An automated mineralogy approach was adopted for the detail study of mineral distribution and rock textures (Gottlieb et al., 2000; US patent No. 2013054153) The TESCAN Integrated Mineral Analyzer (TIMA) housed at the Institute of Geology of the Czech Academy of Sciences was used for this automated modal analysis. Modal analysis with 'High resolution mapping' includes collection of BSE and EDS data on a specified regular grid. The electron beam steps through a field in an equally spaced regular rectangular mesh (10µm in our case). At each point, the BSE level is determined. If the BSE level is above a certain threshold, the beam is kept directed on this spot until a specific number of counts (1,000 by default - 2500 in our case to improve the identification of phases with complex chemistry) from the spectrometer are collected. Then, the beam moves to the next point, from left to right. At the end of the line the beam moves rapidly one step down and to the left border. The procedure is repeated until the whole field is inspected. Each data point on a grid is compared against a classification scheme (which is a collection of rules based on element concentrations and/or their ratios, BSE brightness and other parameters) to produce mineral identification. The mineral map created by this approach is used to calculate the mineral distribution within the sample automatically.

To verify the applicability of the TIMA method for study of magmatic rocks which underwent intensive hydrothermal reworking, we collected distribution maps and data on rock-forming minerals in 15 samples representing all major varieties of granites and greisens in the classical Sn-W-Li deposit Cínovec/Zinnwald in the eastern Krušné hory/Erzgebirge. The Cínovec magmatic-hydrothermal system was chosen as the topic of study because the borehole CS-1 provides a unique cross-section through this highly differentiated magmatic system, saturated in water, probably repeatedly explosively opened and degassed. The first model assembled in the 1960s stressed intensive metasomatic albitization (ŠTEMPROK & ŠULCEK, 1969); more recent models prefer magmatic processes (RUB et al., 1998; JOHAN et al, 2012). Based on TIMA results, a new petrologic log of the CS-1 borehole was customized. In particular, a unit of mica-free granites and feldspathites at a depth of 259-368 m was defined. This unit is considered to be the restite after separation of F-Li-rich fluid that caused greisenization and silicification in the uppermost part of the cupola. Late to post-magmatic processes controlled by water-rich fluids influenced the Cínovec cupola to the depth of about 370 below the current surface. Deeper granites are preserved in primary magmatic conditions.

This work was supported by the Czech Science Foundation, project No. P210/14/13600S.

GOTTLIEB, P., WILKIE, G., SUTHERLAND, D., HO-TUN, E., SUTHERS, S., PERERA, K., JENKINS, B., SOENCER, S., BUTCHER, A., RAYNER, J. (2000): JOM 52, 24-25.

JOHAN, Z., STRNAD, L., JOHAN, V. (2012): Canadian Mineralogist 50, 1131-1148.

RUB, A.K., ŠTEMPROK, M., RUB, M.G. (1998): Mineralogy and Petrology 63, 199-222.

ŠTEMPROK, M., ŠULCEK, Z. (1969): Economic Geology 64, 392-404

**GEOCHEMICAL INVESTIGATION OF SELECTED LAVA FLOWS FROM  
MT. ETNA VOLCANO (ITALY)**

Brosch, E.<sup>1</sup> & Hauzenberger, C.<sup>1</sup>

<sup>1</sup>Institute of Earth Sciences, Department of Mineralogy and Petrology, University of Graz, Universitaetsplatz 2,  
8010 Graz, Austria  
ermanno.brosch@edu.uni-graz.at

This study deals with the analysis of 37 basaltic samples of selected lava flows from Mt. Etna volcano ranging from an early submarine fissure type to the present day summit eruptions. Mt. Etna's evolution is stratigraphically subdivided into four distinct phases: 1) Basal Tholeiitic, 2) Timpe, 3) Valle del Bove and 4) Stratovolcano (BRANCA et al., 2004). The eruptive history started almost 600 ka ago (BRANCA et al., 2004) and throughout the volcano's evolution there was a change in composition from subalkaline/Tholeiitic to alkaline. The volcano is nowadays predominantly composed of trachybasalts. Basal Tholeiitic phase samples represent the most primitive compositions of Mt. Etna's eruption products. They are subsequently followed by the more evolved alkalic compositions of the samples belonging to the other phases. However, the compositions of these alkali basalts change over time from chemically evolved to less evolved/more primitive ones and vice versa. This suggests that mainly fractional crystallisation and input of less evolved magma into the feeding system of Mt. Etna volcano played a huge role in the differentiation of the samples. From major and trace element whole-rock analyses it is evident that in general all samples display typical fractionation trends resulting from removal of the major rock forming minerals such as plagioclase, olivine and clinopyroxene and Fe-Ti oxides (such as spinel and ilmenite) and amphiboles. ICP-MS trace and REE element analyses of core and rim measurements of plagioclase, olivine and clinopyroxene phenocrysts reveal that rims of some plagioclase grains grew in the presence of less evolved and therefore more primitive liquids. As for the magma source of Mt. Etna, it has been regarded to derive from an already slightly depleted garnet lherzolite (CORSARO & CRISTOFOLINI, 1996). This would explain the depletion of HREE in the whole rock analyses as HREE are retained by a garnet lherzolite.

BRANCA, S., COLTELLI, M., GROPPPELLI, G. (2004): In BONCACCORSO, A., CALVARI, S., COLTELLI, M., DEL NEGRO, C., FALSAPERLA, S. (eds.): AGU Geophysical monograph series, 143, 49-63.  
CORSARO, R., A., CRISTOFOLINI, R. (1996): Mineral. Petrol., 57, 1-21.

# STRUCTURAL, SPECTROSCOPIC AND COMPUTATIONAL STUDIES ON $\text{Li}_2\text{Ca}_2\text{Si}_2\text{O}_7$

Brunello, E.<sup>1</sup>, Kahlenberg, V.<sup>1</sup>, Hejny, C.<sup>1</sup>, Krüger, H.<sup>1</sup>, Schmidmair, D.<sup>1</sup>, Tribus, M.<sup>1</sup> & Többs, D.M.<sup>2</sup>

<sup>1</sup>Institute of Mineralogy and Petrography, University of Innsbruck, Innrain 52, A-6020 Innsbruck

<sup>2</sup>Helmholtz-Zentrum Berlin für Materialien und Energie GmbH, Department of Crystallography, Hahn-Meitner-Platz 1, D-14109 Berlin

e-mail: volker.kahlenberg@uibk.ac.at

WEST (1978) was the first who published a comprehensive study on the phase relationships in the system  $\text{Li}_2\text{O}-\text{CaO}-\text{SiO}_2$ . According to his results the following four thermodynamically stable *ternary* phases have to be distinguished:  $\text{Li}_2\text{CaSiO}_4$ ,  $\text{Li}_2\text{Ca}_4\text{Si}_4\text{O}_{13}$ ,  $\text{Li}_2\text{Ca}_3\text{Si}_6\text{O}_{16}$  and  $\text{Li}_2\text{Ca}_2\text{Si}_2\text{O}_7$ . Up to now, only the latter phase has not been structurally characterized in detail. This is even more surprising because the incorporation of  $\text{Eu}^{2+}$  into  $\text{Li}_2\text{Ca}_2\text{Si}_2\text{O}_7$  has been investigated only recently in order to produce a green emitting phosphor when excited by UV light (KIM et al., 2012). In the present contribution we report the crystallographic description and a detailed spectroscopic characterization of this lithium calcium silicate.

Synthesis experiments from the melt resulted in the formation of single-crystals of  $\text{Li}_2\text{Ca}_2\text{Si}_2\text{O}_7$ . Structural investigations were based on single-crystal diffraction. At ambient conditions the compound has the following basic crystallographic data: hexagonal symmetry, space group  $P 6_1 2 2$ ,  $a=5.0961(2)\text{\AA}$ ,  $c=41.264(2)\text{\AA}$ ,  $V=928.07(6)\text{\AA}^3$ ,  $Z=6$ . Structure solution was performed using direct methods. The final least-squares refinement calculations converged at a residual of  $R(\text{IF})=0.0245$ . From a structural point the lithium calcium silicate belongs to the group of sorosilicates containing  $[\text{Si}_2\text{O}_7]$ -groups. Additional lithium and calcium cations are incorporated between the silicate dimers and are coordinated by four and six nearest oxygen neighbours, respectively. Each  $[\text{LiO}_4]$ -tetrahedron shares two common corners with directly neighboring tetrahedra forming *zweier* single-chains which are running parallel to  $\langle 100 \rangle$  in z-levels defined by the presence of the  $6_1^{[001]}$ -screw axes. From the corner-sharing  $[\text{LiO}_4]$ - and  $[\text{SiO}_4]$ -moieties a three dimensional framework can be constructed. An interesting feature of this framework is the presence of an  $\text{O}^{[3]}$ -type bridging oxygen linking *three* tetrahedra (one  $[\text{LiO}_4]$ - and two  $[\text{SiO}_4]$ -units). Structural similarities with other silicates will be discussed. The high-temperature behavior of the Si-O, Ca-O and Li-O bond distances in  $\text{Li}_2\text{Ca}_2\text{Si}_2\text{O}_7$  was investigated by *in-situ* single-crystal X-ray diffraction in the range between 65 and 700 °C. From the evolution of the lattice parameters, the thermal expansion tensor  $\alpha_{ij}$  has been determined. The structural characterization has been supplemented by micro-Raman spectroscopy. Interpretation of the spectroscopic data including the allocation of the bands to certain vibrational species has been aided by DFT-calculations.

WEST, A.R. (1978): J. Am. Ceram Soc., 61, 152-155.

KIM, J.S., SONG, H.J., ROH, H.S., YIM, D.K., NOH, J.H., HONG, K.S. (2012) Mater. Lett., 79, 112-115.

## ALUMINIUM PHOSPHATE-SULPHATE (APS) MINERALS IN THE GORNJA LIPA DEPOSIT, BOR DISTRICT, SERBIA

Buttinger-Kreuzhuber, T.<sup>1</sup>, Kolitsch, U.<sup>2</sup>, Pačevski, A.<sup>3</sup> & Đorđević, T.<sup>1</sup>

<sup>1</sup>Institut für Mineralogie und Kristallographie, Universität Wien, Althanstr. 14, A-1090 Wien, Austria

<sup>2</sup>Mineralogisch-Petrographische Abteilung, Naturhistorisches Museum, Burgring 7, A-1010 Wien, Austria

<sup>3</sup>Faculty of Mining and Geology, University of Belgrade, Đušina 7, 11000 Beograd, Serbia

e-mail: a0968787@unet.univie.ac.at

The Gornja Lipa high-sulphidation epithermal-porphyry copper deposit (DROVENIK, 1958) belongs to the Bor metallogenic zone. The deposit, mined until the mid-1960s, is a massive to disseminated mineralization in hydrothermally altered volcanic rocks. The ore body, which was pyritised, silicified, kaolinized and alunitized, consists mainly of pyrite, enargite and luzonite, and subordinate to trace arsenopyrite\*, bornite\*, chalcopyrite, chalcostibite, colusite\*, famatinite, galena, sphalerite and tennantite\* (DROVENIK, 1958; \*this work). The accompanying minerals comprise quartz, muscovite, kaolinite, diaspore, pyrophyllite\*, with accessory rutile, baryte\*, fluorapatite\* and titanite\*.

We have investigated ten ore-bearing waste rock samples by detailed SEM-EDX analyses and Raman spectroscopy. Our studies revealed the previously undetected presence of several different aluminium phosphate-sulphate (APS) minerals (DILL, 2001) of the alunite supergroup (BAYLISS et al., 2010) which form invariably zoned, euhedral to subhedral grains 5-100 µm in size. The central areas of the grains are composed of crandallite and/or woodhouseite (i.e. Ca-dominant), whereas a more or less discernible rim consists of svanbergite and/or goyazite (i.e. Sr-dominant). The deposit's mineralogy is similar to that of other transitional epithermal-porphyry copper systems (e.g., VOUDOURIS, 2014).

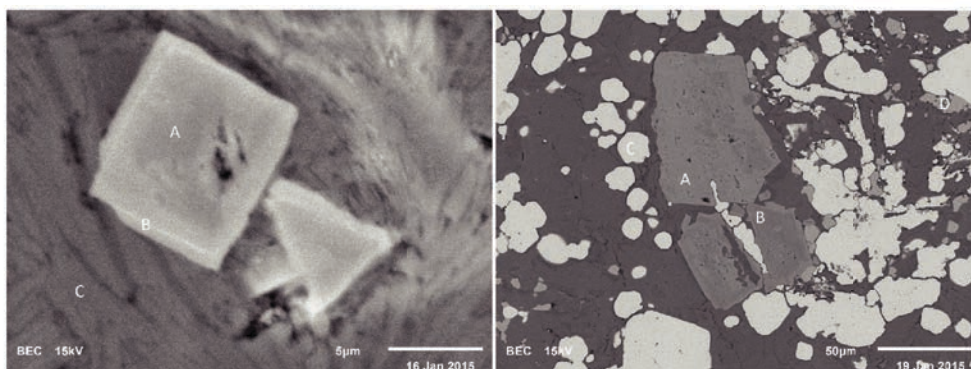


Figure 1: Crandallite (A), svanbergite (B), kaolinite (C) Figure 2: Svanbergite (A), crandallite (B), pyrite (C), rutile (D)

BAYLISS, P., KOLITSCH, U., NICKEL, E. H., PRING, A. (2010): Mineral. Mag., 75, 919-927.

DILL, G. (2001): Earth Sci. Rev., 53, 35-93.

DROVENIK, M. (1958): Geologija, 4, 63-78 (in Slovenian with English abstract).

VOUDOURIS, P. C. (2014): N. Jb. Mineral. Abh., 191, 117-136.



**Pb<sub>6</sub>Al(OH)<sub>8</sub>Cl<sub>2</sub>(NO<sub>3</sub>)<sub>5</sub>·3H<sub>2</sub>O from the Capillitas deposit, Argentina**

Effenberger, H.<sup>1</sup>, Lengauer, C.L.<sup>1</sup>, Libowitzky, E.<sup>1</sup>, Putz, H.<sup>2</sup>, & Topa, D.<sup>3</sup>

<sup>1</sup> Institut für Mineralogie und Kristallographie, Universität Wien, Althanstraße 14, 1090 Wien, Austria

<sup>2</sup> Friedl ZT GmbH Rohstoff- und Umweltconsulting, Karl-Lötsch-Straße 10, 4840 Vöcklabruck, Austria

<sup>3</sup> Naturhistorisches Museum-Wien, Burgring 7, 1010 Wien, Austria

e-mail: herta.silvia.effenberger@univie.ac.at

A new mineral with the composition Pb<sub>6</sub>Al(OH)<sub>8</sub>Cl<sub>2</sub>(NO<sub>3</sub>)<sub>5</sub>·3H<sub>2</sub>O was found at the Capillitas deposit, Argentina (Putz et al., 2009). Associated minerals are anglesite, cerussite and phosgenite. The colourless crystals are ~0.1 mm (up to 0.2 mm) in diameter. From spindle stage measurements, the averaged refractive index *n* is 1.852, 2*V*<sub>cal</sub> = 38(1)°, *n* > 1.79.

Electron-microprobe analyses were performed in the WDS mode (15 kV, 20 nA, beam diameter 30 µm, acquisition time 10 s for peaks and 5 s for backgrounds). The detected ranges (wt.-%) are Pb (69.87–71.25), Cl (4.25–4.47), Al (1.31–1.41), and Fe (0.00–0.21) with a negative correlation between Al and Fe. The presence of nitrate and hydroxyl groups as well as water molecules are in accordance with the empirical and simplified formulas

Pb<sub>6.22</sub>(Al,Fe)<sub>0.96</sub>(OH)<sub>8</sub>Cl<sub>2.25</sub>(NO<sub>3</sub>)<sub>5</sub>·3H<sub>2</sub>O and Pb<sub>6</sub>Al(OH)<sub>8</sub>Cl<sub>2</sub>(NO<sub>3</sub>)<sub>5</sub>·3H<sub>2</sub>O, respectively.

The crystal structure was solved and refined from single-crystal X-ray data (space group: *P*2<sub>1</sub>/*n*, *a* = 10.7834(6), *b* = 9.0584(5) Å, *c* = 13.6178(9) Å, β = 102.28(2)°, *Z* = 2; 222 variable parameters, *R*1(*F*) = 0.025 for 4968 reflections with *F**o* > 4σ(*F**o*), *wR*2(*F*<sup>2</sup>) = 0.063 for 5637 unique data). The one crystallographically unique Al atom has site symmetry  $\bar{1}$ . All other atoms are located at general positions. The Al atom is octahedrally six coordinated (1.899(3) ≤ Al—O<sub>h</sub> ≤ 1.908(3) Å). Three O<sub>h</sub> atoms are one-sided arranged around each of the three Pb atoms (2.323(3) Å ≤ Pb—O<sub>h</sub> ≤ 2.537(3) Å) as characteristic for divalent lead atoms with their stereochemically active lone-pair electrons. Also a Cl atom is included in the first coordination sphere (Pb3—Cl = 2.9043(13) Å). The three next-nearest neighbours are O<sub>n</sub>, O<sub>w</sub> and further O<sub>h</sub> atoms (Pb—O > 2.764(3) Å). Two crystallographically distinct nitrate groups are ordered, the third one shows a site disorder with a N···N splitting of 1.66(5) Å. The N—O<sub>n</sub> bond distances are 1.21(3) to 1.28(3) Å (average values ~1.25 Å). The H atoms of the hydroxyl groups were located experimentally. In contrast, the protons of the water molecules could not be located; the O<sub>w</sub> atoms are looser bonded (only in second coordination sphere of the Pb atoms). The hydrogen bonds of the water molecules are somewhat longer as compared to those of the hydroxyl groups.

The crystal structure is characterized by clusters forming a body centered *sub*lattice. The Al(O<sub>h</sub>)<sub>6</sub> octahedron is within their centres. Considering the three nearest neighbours of the Pb atom, all edges of two opposite faces of this Al(O<sub>h</sub>)<sub>6</sub> octahedron are connected with each one Pb(O<sub>h</sub>)<sub>3</sub> unit. The Pb atoms on their part are coordinated besides to two O<sub>h</sub> atoms in common with the Al(O<sub>h</sub>)<sub>6</sub> octahedron also to the O<sub>h</sub>4 atom. Thus the O<sub>h</sub>4 atom is coordinated to three Pb(O<sub>h</sub>)<sub>3</sub> units. Consequently the Pb(O<sub>h</sub>)<sub>3</sub> units share each two edges among each other. These {Pb<sub>3</sub>[Al(OH)<sub>6</sub>](OH)<sub>2</sub>Cl<sub>2</sub>}<sup>5+</sup> clusters are linked among each other by the nitrate groups and by the hydrogen bonds of the hydroxyl groups and the water molecules. The O<sub>n</sub> and O<sub>w</sub> atoms are involved in the second coordination sphere of the Pb atoms.

## NABESITE: DEHYDRATION BEHAVIOUR BETWEEN 100 AND 375 K

Feimuth, M.W.<sup>1</sup>, Kolitsch, U.<sup>2</sup> & Lengauer, C.L.<sup>1</sup>

<sup>1</sup>Institut für Mineralogie und Kristallographie, Universität Wien, Althanstraße 14, 1090 Wien, Austria

<sup>2</sup>Mineralogisch-Petrographische Abt., Naturhistorisches Museum, Burgring 7, 1010 Wien, Austria

e-mail: christian.lengauer@univie.ac.at

Nabesite,  $\text{Na}_2[\text{BeSi}_4\text{O}_{10}] \cdot 4\text{H}_2\text{O}$ , is a rare member of the zeolite-type framework beryllosilicates (GRICE, 2010), which is up to now only reported from the Ilímaussaq alkaline complex in south Greenland (PETERSEN et al., 2002), where it is associated with further zeolites. The microporous framework is classified with IZA topology code NAB. PETERSEN et al. (2002) also reported a significant response of this zeolite to dry conditions, however, sample quality prohibited further insights into the dehydration process. Co-type material from the collection of the NHM Wien allowed a more detailed study of framework and guest behaviour under non-ambient temperature and atmospheric conditions.

For the investigations single crystals were subjected to a temperature range from 100 to 375K under the dry  $\text{N}_2$  environment of an Oxford cryostream cooler attached to a Nonius KappaCCD diffractometer. Intensity data collections at  $293 \rightarrow 200 \rightarrow 100\text{K}$  for original, hydrated nabesite were followed by a measurement at 125K after partial dehydration at 330 K for 1 h. Complementary, short-term dT-scans with a 25K increment were performed over the selected temperature range. At 375 K the material started to disintegrate.

Nabesite exhibits a pseudo-tetragonal, orthorhombic cell ( $P2_12_12_1$ ) with  $a=9.75\text{\AA}$ ,  $b=10.13\text{\AA}$ ,  $c=11.95\text{\AA}$ ,  $V=1180.3\text{\AA}^3$ . The main features are orthogonal intersecting 9-ring channels along  $[110]$  and  $[1\bar{1}0]$ . The highest-symmetrical framework topology corresponds to an *I*-centered, tetragonal subcell with  $V \sim \frac{1}{2}V_{\text{nab}}$  ( $I\bar{4}m2$ ). Whereas nabesite remains almost unaltered at  $T < 298\text{ K}$ , the reversible partial dehydration process to  $\text{Na}_2[\text{BeSi}_4\text{O}_{10}] \cdot 2\text{H}_2\text{O}$  induces a reduction of the unit cell with  $a=9.70\text{\AA}$ ,  $b=10.03\text{\AA}$ ,  $c=11.98\text{\AA}$ ,  $V=1165.5\text{\AA}^3$ , and a significant rearrangement of the framework atoms, thus leading to a topology closer to the NAB aristotype. A further loss of guest water molecules at  $T > 350\text{ K}$  leads to the already mentioned collapse of the framework.

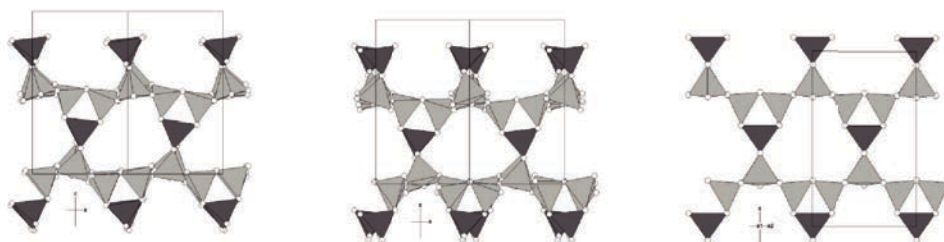


Figure 1: Framework view of untreated (left) and partially dehydrated nabesite //  $[110]$  (middle); NAB aristotype //  $[100]$  (right);  $\text{BeO}_4$  (dark gray) and  $\text{SiO}_4$  tetrahedra (light gray).

GRICE, J.D. (2010): Can. Mineral., 48, 1493-1518.

PETERSEN, O.V., GIESTER, G., BRANDSTÄTTER, F., NIEDERMAYR, G. (2002): Can. Min., 40, 173-181.



## MINERALOGICAL ASPECTS IN MINERAL PROCESSING

Flachberger, H.<sup>1</sup> & Böhm, A.<sup>1</sup>

<sup>1</sup> Chair of Mineral Processing, Department Mineral Resources Engineering, Montanuniversität Leoben,  
Franz-Josef-Straße 18, 8700 Leoben, Austria  
e-mail: helmut.flachberger@unileoben.ac.at

Finding the best processing method for each individual task should always be based on a systematic raw material characterization at laboratory scale. This will prepare for investigations at pilot plant scale in order to find processing techniques, which will keep labour and thus financial costs to the necessary minimum. Laboratory testing technology for raw material characterization can deliver more precise data than investigations at large scale simply because the amount of the product means it cannot be evaluated in detail, is liable to contamination and it cannot be measured as exactly. In the end of the characterization one has physically based characteristic values for the raw material, i.e. for the energy required for commutation, the degree of intergrowth or characteristic properties for separation. These, when combined with the parameters of the machines, will give early prognoses of results or at least deliver limits for sensible separation settings and the best possible separation results. This presentation is intended to explain the importance of investigation/testing methods for processing technologies, broadly sketch the investigation steps and explain these through examples of recent research projects.

One of these examples deals with the processing of LD slags (working group Böhm). From the mineral processor's point of view methods of liberation analysis are presented with an emphasis on the comparison of three dimensional – by means of property analysis evaluated by intergrowth spectra depicted in the Henry-/Reinhardt-chart – and two dimensional methods – by means of image analysis and automated phase mapping by QEMSCAN. Results of the traditional method of multi-dimensional property analysis are compared to those from automated phase and image analysis. The particle sets resulting from the property classes could be analyzed by means of QEMSCAN owing to cooperation with LKAB/ Sweden. The data were evaluated with respect to liberation by the software iDiscover 5.3.1 /FEI, which is available at the Chair of Mineral Processing.

Another example points out the importance of an extensive raw material characterisation - it contains chemical and mineralogical examinations, an intergrowth analysis and the analysis of specific separability characteristics - in order to evaluate the processability of magnesia-carbon (MgO-C) bricks (working group Flachberger), which represent a large part of currently accruing refractory scrap. The overriding target was to develop a processing method, which on the one hand separates graphite and on the other hand recovers magnesia as pure as possible.

## EVIDENCE FOR ARCHEAN CRUST IN THE PRE- PANAFRICAN HISTORY OF CENTRAL CAMEROON

Ganwa, A.A.<sup>1,2</sup> & Klötzli, U.<sup>2</sup>

<sup>1</sup>Department of Earth Sciences, University of Ngaoundere, P.O. Box 454, Ngaoundere, Cameroon

<sup>2</sup>Department für Lithosphärenforschung, Universität Wien, Althanstrasse 14, 1090 Wien, Austria

e-mail: alembert.alexandre.ganwa@univie.ac.at

The main geological feature of Central Cameroon is the wide spread occurrence of granitoids emplaced in close association with transcurent regional shear zones. The basement of this vast domain is a Paleoproterozoic ortho- and para-derivative formation, which had been intensely reworked, together with subsequent intrusions and sediments, during the Panafrikan orogenesis in the Neoproterozoic. As consequence, the area underwent pervasive metamorphism and intense deformation. This makes it difficult to distinguish between Panafrikan metasediments or syntectonic plutonites and their respective basement. Our study presents zircon feature (CL-BSE-SE) and U-Th-Pb LAM-ICPMS geochronology of a pyroxene-amphibole bearing gneiss of the Méiganga area in Central Cameroon. Typically zircons of the gneiss shows three main domains: 1) a core sometime with magmatic oscillatory zonation 2) a domain with oscillatory zonation, and 3) a narrow light rim not zoned or with only a very faint oscillatory zonation. These three domains suggest that the rock experienced at least three geological events. The U-Th-Pb data allow to decipher four ages: 2072±69Ma (upper intercept), consistent with ages from the Paleoproterozoic West Central African Belt (PENAYE et al., 2004); 2524±55Ma (upper intercept) which marks a late Neoarchean magmatic event; 2731±78Ma (upper intercept) related to a Neoarchean magmatic event in Central Cameroon, similar to the one describe in the Congo Craton (SHANG et al., 2007). A zircon core gives ages between 2900 and 2950 Ma which provides some evidence of the presence of the Mesoarchean basement prior to the Neoarchean magmatism. The lower intercept ages (975Ma, 491Ma and 411Ma) even though reflecting the successive Pb loss could be related to the magmatism known in Cameroon: Early Neoproterozoic for 975Ma and Late Neoproterozoic to Early Cambrian for 491Ma. The 411Ma may represent the Pb lost, or a tectonic event not yet identified in the study area. Geochemical data (GANWA et al., 2008) show that the REE, Y, Yb, Sr/Y of some samples are similar to the known Archean craton formations (depletion in REE, Y≤10 ppm, Yb≤1ppm, Sr/Y≥30). Further, samples of surrounding granitoids show a close similar chemical affinity that we interpret as imprints of the recycling Archean crustal material by metamorphism, melting or by incorporation in a juvenile magma. Our results show that the Pre-Panafrikan history of central Cameroon include Meso- to Neo-Archean crustal accretion and associated magmatism prior to the Paleoproterozoic event of the West Central African Belt. Respect to this new insight, any evolutionary reconstruction of the area should integrate the presence of the Archean crust.

GANWA, A.A., FRISCH, W., SIEBEL, W., EKOIDECK, G.E., SHANG, K.C., NGAOKO, V. (2008): *Comptes Rendus Geoscience*, 340, 211–222.

PENAYE, J., TOTEU, S.F., TCHAMENI, R., VAN SCHMUS, W.R., TCHAKOUNTE, J., GANWA, A., MIYEM, D., NSIFA, E.N., (2004): *J. Afr. Earth Sci.* 39, 159–164.

SHANG, K.C., SATIR, M., NSIFA E.N., LIEGEOIS, J.P., SIEBEL, W., TAUBALD, H. (2007): *Int. J. Earth Sci.*, 96, 817–841.

**SELTENE NI-CO-SULFIDE AUS DER MANGANLAGERSTÄTTE VEITSCH  
(GRAUWACKENZONE, STEIERMARK)**

Girtler, D. & Tropper P.

<sup>1</sup>Institut für Mineralogie und Petrographie, Universität Innsbruck, Innrain 52, 6020, Innsbruck, Österreich  
e-mail: Daniela.girtler@student.uibk.ac.at

In der Kleinveitsch sind am Friedelkogel und am Kaskogel Manganvererzungen bekannt, die zwischen 1880 und 1892 bergbaulich genutzt wurden. Die Manganvererzungen liegen im paläozoischen „Erzführenden Kalk“ innerhalb des Tirolisch-Norischen Deckensystems. Als Alter des „Erzführenden Kalkes“ wird Devon bis Unterkarbon angenommen. Die Vererzung selbst tritt in Form mehrerer schichtkonkordanten Linsen auf, die am Friedelkogel bis zu circa 3 Meter mächtig wurden, am Kaskogel jedoch eine Mächtigkeit bis zu 8 Meter erreicht haben dürften. Die Erzlinsen selbst bestehen hauptsächlich aus einem feinkörnigen Gemenge verschiedener Mangankarbonate und –silikate, unter anderem sind dies Rhodochrosit, Pyroxmangit, Tephroit und Spessartin (FRANCIS et. al. 2004). Akzessorisch treten innerhalb des feinkörnigen Haupterzes sowie in die Erzkörper durchschlagenden Mobilisaten eine Reihe von Co-, Ni-, Be-, B- und REE- führenden Mineralen auf, die Gegenstand jüngerer wissenschaftlicher Bearbeitungen waren (POSTL et. al. 2000, POSTL et. al. 1998, FRANCIS et. al. 2004, GIRTLER et. al. 2013).

Eine Gruppe der akzessorisch auftretenden Sulfide lässt sich als seltene Co- Ni- Sulfide zusammenfassen. Dazu gehören Cobaltit [Co As S], Co-Pentlandit [(Co,Ni,Fe)<sub>9</sub>S<sub>8</sub>], Jaipurit [CoS], sowie die Linnaeit-Gruppe mit dem Linnaeit [Co<sup>2+</sup>(Co<sup>3+</sup>)<sub>2</sub>S<sub>4</sub>], dem Carrolit [Cu (Co,Ni)<sub>2</sub>S<sub>4</sub>] und dem Ni-Carrolit [NiCo<sub>2</sub>S<sub>4</sub>]. Hierbei ist auffallend, dass Co-Pentlandit zumeist gemeinsam mit einem oder mehreren Vertretern der Linnaeit-Gruppe auftritt. Ni-Carrolit weist zum Teil isometrische Körner auf. Neben dieser Gruppe ist in den Proben außerdem noch Chalcopyrit [CuFeS<sub>2</sub>] verhältnismäßig häufig anzutreffen. Zudem kann man akzessorisch Sphalerit [(Zn,Fe)S], Pyrit [FeS<sub>2</sub>] und auch Galenit [PbS] beobachten. Sphalerit tritt hierbei meist in Verbindung mit Chalcopyrit auf, manchmal auch gemeinsam mit dem Ni-Carrolit, aber auch unabhängig.

FRANCIS, C.A. et al. (2004): *Joannea Mineralogie*, 2, S. 85-100.

GIRTLER, D. et al. (2013): Poster MinPet 2013, Graz, Austria September, 19th-23th.

POSTL, W., et al (2000): *Carinthia II*, 190/110, 214.

POSTL, W. et al. (1998): *Mitt. Abt. Miner. Landesmus. Joanneum*, 62/63, S. 59-64.

## HIGH-PRESSURE SYNTHESIS AND CRYSTAL STRUCTURES OF THE STRONTIUM OXOGALLATES $\text{Sr}_2\text{Ga}_2\text{O}_5$ AND $\text{Sr}_5\text{Ga}_6\text{O}_{14}$

Goettgens, V.<sup>1</sup>, Kahlenberg, V.<sup>1</sup>, Mair, P.<sup>1</sup> & Schmidmair, D.<sup>1</sup>

<sup>1</sup>Institute of Mineralogy and Petrography, University of Innsbruck, Innrain 52, A-6020 Innsbruck

In the literature,  $\text{Sr}_2\text{Ga}_2\text{O}_5$  has been mentioned as a “low melting point oxide” that can be used for the ease of sintering of ceria or stabilized ZrO<sub>2</sub> ceramics (LEE, 2006). However, a more detailed examination reveals that the authors reporting about  $\text{Sr}_2\text{Ga}_2\text{O}_5$  refer to the stoichiometric composition of the starting material and not to the chemical composition of a specific phase. Indeed, in all phase analytical studies performed so far no strontium gallate with a  $\text{SrO}:\text{Ga}_2\text{O}_3$  ratio of 2:1 has been reported and quite recent synthesis experiments aiming on the preparation of brownmillerite-type  $\text{Sr}_2\text{Ga}_2\text{O}_5$  at ambient pressure were also unsuccessful (ISTOMIN et al., 2014). On the other hand, brownmillerites based on main group II and III elements have been already obtained by introducing pressure as an additional synthesis parameter (KAHLENBERG et al., 2000). In the course of an ongoing project on brownmillerite-related compounds we tried to prepare the corresponding strontium-gallium equivalent at 1000°C and 1.5 GPa as well as 3.0 GPa using a piston–cylinder press. The present contribution reports the first results of these investigations including the structural characterization of two previously unknown quenchable high-pressure double oxides with composition  $\text{Sr}_2\text{Ga}_2\text{O}_5$  and  $\text{Sr}_5\text{Ga}_6\text{O}_{14}$ . The structures of both compounds have been solved from single-crystal diffraction data sets using direct methods. The first compound is orthorhombic with space group type *Pbca* ( $a=10.0021(4)\text{Å}$ ,  $b=9.601(4)\text{Å}$ ,  $c=10.6700(4)\text{Å}$ ,  $V=1024.6(4)\text{Å}^3$ ,  $Z=8$ ) and belongs to the group of single-layer gallates. Individual sheets are parallel to (001) and can be built from the condensation of unbranched vierer single-chains running along [010]. The layers are characterized by the presence of four- and strongly elliptical eight-membered rings of corner connected tetrahedra in UDD and UUUUDDDD conformation. Strontium atoms are sandwiched between the tetrahedral layers for charge compensation and are coordinated by six and seven oxygen ligands, respectively.  $\text{Sr}_2\text{Ga}_2\text{O}_5$  is isotypic with several other double sulfides and selenides. To the best of our knowledge, it is the first example of an oxide with this structure type, even though not related to the brownmillerite family of compounds. From a structural point of view,  $\text{Sr}_5\text{Ga}_6\text{O}_{14}$  is a phyllogallate as well. The crystal structure adopts the monoclinic space group *P21/c* ( $a=8.1426(3)\text{Å}$ ,  $b=8.1803(3)\text{Å}$ ,  $c=10.8755(4)\text{Å}$ ,  $\beta=91.970(4)^\circ$ ,  $V=723.98(5)\text{Å}^3$ ,  $Z=2$ ). Individual sheets extend along (001). Basic building units are unbranched dreier single-chains parallel to [100]. The layers contain tertiary (Q<sup>3</sup>) and quaternary (Q<sup>4</sup>) connected  $[\text{GaO}_4]$ -tetrahedra in the ratio 2:1 resulting in a Ga:O ratio of 3:7 and the formation of exclusively five-membered rings. Linkage between adjacent tetrahedral sheets is provided by three symmetrically independent strontium ions which are surrounded by six to eight oxygen atoms. The layers in  $\text{Sr}_5\text{Ga}_6\text{O}_{14}$  are similar to those observed in the melilite structure-type.

ISTOMIN, S.Y., ANTIPOV, E.V., FEDOTOV, Y.S., BREDIKHIN, S.I., LYSKOV, N.V., SHAFEEI, S., SVENSSON, G., LIU, Y., SHEN, Z. (2014): *J. Solid State Electrochem.* 18, 1415-1423.

KAHLENBERG, V., FISCHER, R.X., SHAW, C.S.J. (2000): *Am. Mineral.*, 85, 1061-1065.

LEE, J.S. (2006): *J. Electroceram. Soc.*, 152, H1-H5.

**FIRST REPORT ON THE OCCURRENCE OF SUBVOLCANIC RHYODACITES  
AND THEIR ASSOCIATED ALTERATION PHENOMENA - BOHEMIAN MASSIF,  
AUSTRIA**

Göd, R.<sup>1</sup>, Kurzweil, H.<sup>2</sup> & Klötzli, U.<sup>1</sup>

<sup>1</sup>Department of Lithospheric Research, University of Vienna, Faculty of Earth Sciences, Geography and  
Astronomy, A-1090 Vienna

<sup>2</sup>Department of Geodynamics and Sedimentology, University of Vienna, Faculty of Earth Sciences, Geography  
and Astronomy, Althanstrasse 14, A-1090 Vienna

During a gold exploration campaign focusing on the Bohemian Massif, a so far unknown rhyodacitic lithology was discovered within a quarry ca. 7km NW of Waidhofen/Thaya, close to the village Arnolz in Niederösterreich. The dyke-like subvolcanic rocks of approximately 30m thickness intruded into a fine-grained biotite-granite described as "Mauthausen type granite" (WALDMANN, 1950) which itself intruded into cordierite-bearing gneisses of the "Monotonous Series". Boulder mapping proved those porphyritic rocks to occur over a distance of at least 7km, following the regional NNE striking direction of 10° to 15°. Preliminary U/Pb zircon ages are 311±2Ma and 290±4Ma for the biotite-granite and the rhyodacite, respectively. The rhyodacites generally display a textbook-like volcanic texture with plagioclase phenocrysts up to 1cm in size and idiomorphic quartz phenocrysts up to 5mm in size showing corrosive embayments. Subordinated, totally chloritized amphibole and biotite individuals averaging ca. 5mm in size (both together comprise ca. 5vol%) are locally visible. Extremely fine grained orthoclase - ranging between 5vol% and 10vol% - has been verified by XRD only. Chemical composition of plagioclase and orthoclase within the matrix is close to their end-member compositions. Two types of rhyodacites can be distinguished, a reddish to brownish (Type I) and a greenish, strongly chloritized (Type II) variety. However, both types include several phenotypes in terms of colours, grain sizes and textures. Type I is interpreted to be the initial variety which has been hydrothermally altered subsequently giving rise to the formation of the chloritized Type II. The chloritization is associated with a penetrative disseminated pyrite mineralization. The pyrite crystals - their content does not exceed 1–2vol% - form idiomorphic cubes up to ca. 0.5mm but most of them are significantly smaller. Chloritization and pyrite mineralization seem to be cogenetic. Equally, the pyrite mineralization infiltrates the adjacent granites up to 5 to 10m away from the contacts with the volcanics. No sulfides other than pyrite have been observed so far. The hydrothermal alteration is also associated with the formation of kaolinite and montmorillonite. In terms of their bulk composition, Type I and Type II plot closely to the rhyolite-dacite trachydacite boundaries using the descriptive TAS classification. The trace element spectrum (24 elements analysed, including gold) does not show any enrichments in one of these elements. Bulk and trace element chemistries of Type I and Type II, including their different phenotypes, are almost identical. The only exception is the sulfur content, which increases with chloritization reaching a maximum of 0.6wt%. The alteration phenomena as observed, i.e. the chloritization as well as the formation of clay minerals, are not associated with any change in elemental distribution within the volcanics.

WALDMANN, L. (1950): Geologische Spezialkarte der Republik Österreich, 1:75000, Blatt Litschau-Gmünd (4454), Geol. B-A., Wien.

## THE USE OF THE TIMA AUTOMATED MINERAL ANALYZER FOR THE CHARACTERIZATION OF ORE DEPOSITS AND OPTIMIZATION OF PROCESS OPERATIONS

Gottlieb, P.<sup>1</sup>, Motl, D.<sup>2</sup>, Dosbaba, M.<sup>1</sup> & Kopřiva, A.<sup>2</sup>

<sup>1</sup>TESCAN ORSAY HOLDING Libušina třída 21, 623 00 Brno, Czech Republic

<sup>2</sup>TESCAN BRNO Libušina třída 1, 623 00 Brno, Czech Republic  
paul.gottlieb@tescan.cz

Detailed knowledge of mineral distribution and mineral texture are essential for feasibility studies, mine planning, feed ore characterization and the optimization of mineral processing operations. This knowledge can now be acquired through Automated Mineralogy (AM). AM refers to a range of analytical solutions based on Scanning Electron Microscopy (SEM) and Energy Dispersive X-ray Spectroscopy (EDX). Minerals are identified from their Electron Induced X-ray Emission (EIXE) spectra at each measurement point to create two dimensional mineral maps. The mineral maps are analyzed off-line to extract application dependent mineral and elemental distributions and mineral texture information.

TIMA is a new generation of automated mineral analyzer that incorporates many novel features to increase the capabilities and flexibility of the technology. The technology has been applied to a large number of commodities and industries such as base & precious metals, heavy minerals, coal, cement and oil & gas. It is used by mining companies at central and on-site laboratories, by service providers of mineralogical and metallurgical testing, by plant equipment and consumable suppliers and by earth science academic & research institutions.

A study by BREITER & HRSTKA (2015) describes how TIMA was used by the Czech Geological Survey to discriminate magmatic and metasomatic processes in granites.

This paper describes TIMA and presents the results of two other process mineralogy applications. The metallurgical use of TIMA answers questions regarding the processing of ores. Each commodity and each mineral association brings different metallurgical issues and different measurement and interpretation requirements. In the first example, TIMA was successfully used to quantify gold losses during ore beneficiation. TIMA located very rare gold grains in the tailings using its bright phase search algorithm. Textural information on gold association and liberation was automatically obtained and showed that the gold losses were due to insufficient liberation during grinding resulting in fine gold locked in gangue minerals. The cost of recovering the fine losses by further grinding can then be determined.

In the second example, a different issue of high titanium losses was observed in ilmenite rich beach sands from India. In this case the focus was on the deportment of titanium between the various titanium bearing minerals. It was found that a significant proportion was hosted by ilmenite that was partially or completely converted into leucoxene by the process of iron removal from the structure from the mineralogical point of view. The resulting low iron content of the leucoxene and strongly leucoxenized ilmenite particles could not be recovered efficiently using magnetic separation and a different process was needed.

BREITER, K. & HRSTKA, T. (2015): Automated mineral analyzer: A new tool to distinguish the magmatic and metasomatic processes in rare-metal granites. Mitt. Österr. Miner. Ges., 161, in press.



## PARTIAL MELTING OF PYROXENITIC CLASTS OF THE YURTUC METEORITE

Gravogl, G.<sup>1</sup>, Habler, G.<sup>1</sup>, Khisina, N.<sup>2</sup>, Lorenz, C.<sup>2</sup>, Ntaflos, T.<sup>1</sup> & Abart, R.<sup>1</sup>

<sup>1</sup>Dept. of Lithospheric Research, Univ. of Vienna, Althanstrasse 14, 1090, Vienna, Austria

<sup>2</sup>Vernadsky Institute of Geochemistry and Analytical Chemistry, Kosygin St. 19, Moscow Russia, 119991

e-mail: rainer.abart@univie.ac.at

Achondritic meteorites represent samples of differentiated bodies and bear important information on planetary evolution. In this contribution we present petrographic, mineral chemical and crystal orientation data from the Yurtuc meteorite. This achondrite has been classified as Howardite pertaining to the HED meteorites, and it probably represents metamorphosed regolith breccia from 4 Vesta the supposed HED parent body. Most of the investigated sample consists of a polymict breccia containing fragments of olivine, ortho- and clinopyroxene, plagioclase, spinel and quartz. A smaller fraction of the sample is represented by “lithic” pyroxenite clasts, which are comprised of several 100 micrometers sized orthopyroxene and less abundant olivine grains. In addition, fine-grained domains featuring graphic intergrowth of orthopyroxene, clinopyroxene, and Cr-rich spinel embedded in a matrix of calcic plagioclase are present, which are interpreted as former melt pockets. These melt pockets occupy interstitial positions and probably replaced primary interstitial augite, as indicated by the integrated composition of the melt pockets.

Primary orthopyroxene shows a gradual increase of its Fe-, Al-, Ca-, and Ti-contents towards the contacts with melt pockets and approaches the composition of the secondary orthopyroxene of the graphic intergrowth, which typically grows epitaxially on primary orthopyroxene. This is interpreted as secondary chemical zoning indicating chemical alteration of primary orthopyroxene at the contacts with the melt. When in contact with the melt, primary olivine was resorbed by the melt. Orthopyroxene - Cr-spinel symplectites replacing olivine along contacts between primary orthopyroxene and olivine produce similar chemical alteration in primary orthopyroxene as observed towards the melt pockets indicating that they are related to melt infiltration along grain and phase boundaries. Primary olivine shows a systematic increase in Cr content towards the interface with the orthopyroxene - Cr-spinel symplectite reaching up to 3800ppm Cr, indicating that the chromium was supplied by the infiltrating melt. Conventional geothermometry based on the Ca-content in orthopyroxene coexisting with clinopyroxene yields temperatures in the range of 900-1000°C for the graphic intergrowth of the melt pockets. Diffusion of chromium into olivine took place under silica activity buffered by the presence of orthopyroxene. Inverse diffusion modeling of the secondary chemical zoning in primary orthopyroxene yields time periods for alteration in the order of years. This combined evidence is compatible with a short-lived probably impact related thermal event leading to melting of augite in a pyroxenite of Vestas mantle.

## THE ORIGIN OF INCLUSIONS IN A METAPEGMATITE GARNET: PETROLOGICAL INFORMATION AND CHALLENGES

Griffiths, T.A.<sup>1</sup>, Habler, G.<sup>1</sup>, Rhede, D.<sup>2</sup> & Abart R.<sup>1</sup>

<sup>1</sup>Department of Lithospheric Research, University of Vienna, Althanstraße 14, 1080 Wien, Austria

<sup>2</sup>GFZ German Research Center for Geosciences, Telegrafenberg, 14473 Potsdam, Germany

e-mail: th.griffiths@univie.ac.at

Peraluminous metapegmatites of Permian origin from the Saualpe-Koralpe complex, Austria (locality Wirtbartl) contain cm-sized almandine-spessartine garnets with extremely abundant submicrometer to micrometer sized inclusions of corundum, ilmenite, rutile, xenotime, zircon, apatite and an Fe-Mn phosphate (wylleite group). Variations in inclusion abundance, phase assemblage, habit and grain size define concentric and sector zoning in the garnets. Attempting to determine the origins of these inclusions is the first step towards using them to understand the crystallization of the pegmatites, but also allows critical evaluation of the current state of research into inclusion origin determination.

Observed zoning is related to cm-scale or larger variations in the pegmatite system during magmatic crystallization. Sector zoning reflects differences between crystal facets with different miller indices. In the rarely developed outermost zone, rutile needles are oriented parallel to garnet <111> directions but do not favour all 4 directions equally, suggesting at least these inclusions may have crystallized simultaneously with garnet at its interface. The 3 inclusion phases studied with electron backscatter diffraction (EBSD) each show multiple crystallographic orientation relationships to garnet.

The inclusion phase assemblage and individual compositions are characteristic of pegmatite phases. Microprobe measurements of the integrated composition of garnet and inclusions show small deviations from perfect garnet stoichiometry. Variations in integrated element concentrations correlate with optically visible zoning. Correlations are present between different elements to varying degrees, but are difficult to interpret. The strongest correlation is negative, between Si and Al + P + Ti ( $r^2=0.99$ ). The weak positive correlation between Al and Ti cannot be explained by known crystal chemical mechanisms of Ti incorporation in garnet.

The only scenario that can be reasonably excluded by the current measurements is inclusion formation by overgrowth of independent, pre-existing crystals. The methods which provided the most useful information were a combination of microstructural observations and EBSD. Formation of the inclusions from exsolution or from oriented nucleation at the garnet surface and subsequent overgrowth cannot be differentiated between. The reason for this difficulty is the lack of studies of host-inclusion systems with known origins against which competing theories can be evaluated. Interpreting inclusions as exsolution products based on their crystallographic orientation relationships and shape-preferred orientations alone is not justifiable.



## MINERAL COMPOSITION MAPPING OF FINE-GRAINED ROCKS AT SUB-MICRON RESOLUTION

Haberlah, D.<sup>1</sup>, Butcher, A.R.<sup>2</sup>, Dobbe, R.<sup>2</sup> & Vesseur, E.J.<sup>2</sup>

<sup>1</sup>FEI Australia, 73 Northbourne Ave, Canberra 2600 ACT, Australia

<sup>2</sup>FEI Europe, 5 Achtseweg Noord, Eindhoven 5651GG, The Netherlands

e-mail: rene.dobbe@fei.com

SEM-EDS-based Automated Mineralogy has been employed for decades to map the mineralogy and textures of rocks and ore material at the micron scale. Although spectral analysis engines have generally been successful to classify the EDX spectra at each acquisition point into discrete mineral phases, the approach being used displays fundamental limitations when applied to fine-grained rocks, because of the size of the x-ray excitation volume being larger than the mineral constituents involved (HABERLAH et al., 2014; Fig. 1). A next generation spectral analysis engine has been developed with the objective to accurately quantify multiple mineral components within an electron-beam-interaction volume. In this new approach, measured EDX spectra are deconvolved into best matches of multiple minerals, by applying patented algorithms that rapidly produce unique best-match solutions taking into account contextual intelligence.

The theory, potential and physical limitations of high-resolution x-ray mineral mapping at sub-micron resolution applied to the analysis of fine-grained sedimentary rocks are explained in this contribution and demonstrated on a variety of samples. Results will show that this method provides accurate, quantitative, and spatially relevant data on the distribution of sub-micron mineral constituents in fine-grained rocks.

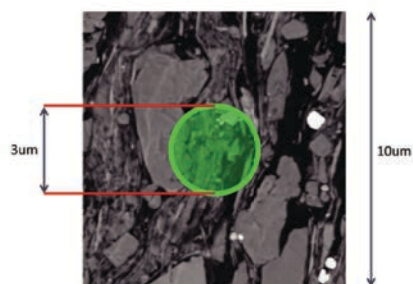


Figure 1. High-resolution BSE image with a green circle indicating the approximate excitation volume for EDX generation at 15 kV (in 2D).

HABERLAH, D.E., GOERGEN, G., HOWELL, M., OWEN, H., KRUSEMANN, D., PIRRIE, G., ROLLINSON, P., GOTTLIEB, BUTCHER, A.R. (2014): AAPG Article #90189, 2014 AAPG Annual Convention and Exhibition, Houston, Texas, USA.

## X-RAY IRRADIATION OF WATERMELON TOURMALINE FROM RWANDA

Haeger, T.<sup>1</sup>, Karlowski, P.<sup>1</sup>, Henn, U.<sup>2</sup> & Schmitz, F.<sup>2</sup>

<sup>1</sup>Centre for gemstone research; FB 09 Institute for geosciences; Johannes Gutenberg-University of Mainz, Germany (J.-J. Becherweg 21, 5099, Mainz, Germany)

<sup>2</sup>German gemmological association (DeGemG) (Prof.-Schlossmacher-Str. 1; 55743; Idar-Oberstein; Germany)  
e-mail: Tobias.Haeger@Uni-Mainz.de

The investigated watermelon tourmalines originate from the M'buye mine in Rwanda. Plane parallel slices were cut and polished in such a way, that the c axis was parallel to the surface. The chemical composition of the samples were determined with EPMA (acc. voltage 20kV with 12 nA, B<sub>2</sub>O<sub>3</sub> was fixed to 10.5 weight% and the values were ZAF corrected). Based on these results the tourmalines were determined as elbaïtes (55-60% of the x-position is occupied with Na) with clear rossmanite (35-40 % of the x position is unoccupied) and small amount of liddicoatite component (0-10 % of the x-position is occupied with Ca) (see also HENN & SCHMITZ (2014)). Additional to that, trace elements were determined by ICP-MS coupled with Laser ablation (Si-contents of the EPMA-results were used as the internal standard). Before irradiation the red core showed clear spin-allowed Mn<sup>3+</sup>-transitions (MANNING 1973). Due to irradiation with X-rays (acceleration Voltage 60keV with 60mA, duration 1h) the spin-allowed transitions intensified in the red core (see Figure 1), while the green rim remained unchanged.

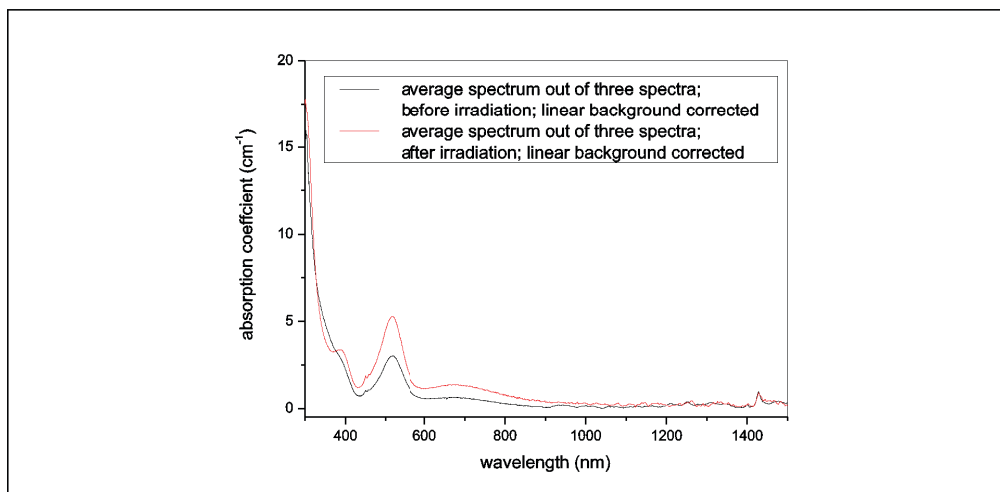


Figure 1: UV-Vis-NIR spectra of a red core of the watermelon tourmaline with E perpendicular to c. Black line before and red after irradiation with x-rays.

HENN, U. & SCHMITZ, F. (2014): The Journal of Gemmology, 34,  
MANNING, P.G. (1973): Canadian Mineralogist, 11, 971-977.

**MINERALOGICAL STUDY OF THE AWAK MAS DEPOSIT: A CONTRIBUTION  
TO THE ORE GENESIS OF DISSEMINATED GOLD DEPOSITS IN SOUTH  
CELEBES, INDONESIA**

Hakim, A.Y.A.<sup>1</sup> & Melcher, F.<sup>1</sup>

<sup>1</sup>Departement of Applied Geosciences and Geophysics,  
Montanuniversität Leoben, Peter-Tunner-Straße 5; A-8700 Leoben, Austria  
e-mail: andy-yahya.al-hakim@stud.unileoben.ac.at

The tectonic activities in the Indonesian arc system have led to the development of a significant number of metal prospects that have variable characteristics in each metallogenic province within the islands. Awak Mas in South Celebes is one of the most prospective gold deposits in Indonesia with current mineral resources of approximately 60,000 kg gold. The area is located in the south of the Central Celebes Metamorphic Belt. The deposit is hosted by the Late Cretaceous Latimojong Formation which consists of meta-sediments, basic to intermediate volcanics that intruded the Mesozoic Lamasi Complex Ophiolite, including basic-intermediate intrusives, pyroclastics and volcanogenic sediments. QUERUBIN & WALTERS (2011) postulate that the deposit is classified as a sediment-hosted deposit, characterized by broad shallow-dipping mineralized zones, stockwork quartz veins, and breccias associated with high angle faults and/or shear zones. These steeply dipping mineralized structures are inferred as main feeder zones to mineralization.

The gold deposits of Awak Mas show interesting mineralogical characteristics similar to Carlin-type deposits although they are hosted by volcanic rocks. The Mesel deposit in North Celebes (TURNER et al., 1994) and the Bau deposit in Sarawak are examples of volcanic-hosted disseminated gold deposits which are not restricted to a continental setting. The discoveries of these two deposits demonstrate the possible presence of Carlin-type deposits in Tertiary island-arc environments. The objectives of the study are to characterize the ore deposits and establish a tectonic framework for the occurrences. Various methods will be applied including mineralogical and mineral chemical observations, geochemical analysis, fluid inclusion, and stable isotope analysis.

From the preliminary mineralogical observations the deposits contain low amounts of fine-grained disseminated sulphide with drill core intersections grading up to 8.94 ppm of gold. Gold is usually associated with pyrite, chalcopyrite and arsenopyrite. Accessory minerals include magnetite, hematite, luzonite, tetrahedrite, carrollite, covellite and bornite, which are associated with quartz veins, silicification, carbonatization and brecciation zones. The alteration assemblage is characterised by the presence of albite, quartz, calcite, dolomite-ankerite, siderite, chlorite, epidote, zoisite and sericite.

TURNER, S.J., FLINDELL, P.A., HENDRI, D., HARDJANA, I., LAURICELLA, P.F., LINDSAY R. P., MARPAUNG B., WHITE, G.P. (1994): *Journal of Geochemical Exploration*. Vol.50, Issue 2, p.317-336  
QUERUBIN, C.D., WALTERS, S. (2011): *Proceedings of The Sulawesi Mineral Resources 2011*. Manado, North Sulawesi, Indonesia.

## MINERALOGY, HYDRO- AND ISOTOPE CHEMISTRY OF THERMAL WATER AND SCALINGS IN HYDROGEOTHERMAL PLANTS

Haslinger, E.<sup>1</sup>, Wyhlidal, S.<sup>1</sup>, Boch, R.<sup>2</sup>, Fröschl, H.<sup>3</sup>, Dietzel, M.<sup>2</sup>, Leis, A.<sup>4</sup>, Knaus, R.<sup>4</sup>,  
Goldbrunner, J.<sup>5</sup>, Shirbaz, A.<sup>5</sup> & Plank, O.<sup>1</sup>

<sup>1</sup>AIT Austrian Institute of Technology, Health & Environment Department,  
Konrad-Lorenz-Strasse 24, A-3430 Tulln, Austria

<sup>2</sup>Graz University of Technology, Institute of Applied Geosciences, Rechbauerstrasse 12, A-8010 Graz, Austria

<sup>3</sup>Seibersdorf Labor GmbH, Chemical Analytics, A-2444 Seibersdorf

<sup>4</sup>Joanneum Research, Resources – Institute for Water, Energy and Sustainability,  
Elisabethstrasse 18/II, A-8010 Graz

<sup>5</sup>Geoteam – Technical Office for Hydrogeology, Geothermal Energy and Environment  
Bahnhofgürtel 77, A-8020 Graz  
e-mail: edith.haslinger@ait.ac.at

The aim of the research project NoScale is to assess the risk of precipitation (scaling) and corrosion in the use of deep thermal groundwater. On the basis of comprehensive and complex chemical and mineralogical experiments and building upon detailed hydrochemical modeling the potential impact of the use of the thermal waters on the technical components of hydrogeothermal systems are to be shown. 15 hydrogeothermal plants were sampled in Austria as well as in Bavaria. At six plants, scalings could be sampled and analysed. The sampled plants are located in different (hydro)geological settings; the purpose of the geothermal plants (thermal, electricity, balneological) and therefore the exploitation depths varied to a great extent, therefore the isotope and hydrochemistry as well as the encountered scalings were different in each plant. The scalings were mostly carbonate scalings in pipes and on heat exchangers, but also precipitation of elemental sulphur occurred. In two plants, the scalings were so massive that they completely blocked the groundwater pump and the heat exchanger which subsequently led to a temporary shut-down of the plants after only one year of operation (Fig. 1). In ongoing laboratory experiments accompanied by thermodynamic-kinetic modelling, the nature and kinetics of the scaling processes shall be clarified. The investigated scaling processes in the different plants will result in recommendations for plant operators how to avoid scaling with the best suitable operating conditions.

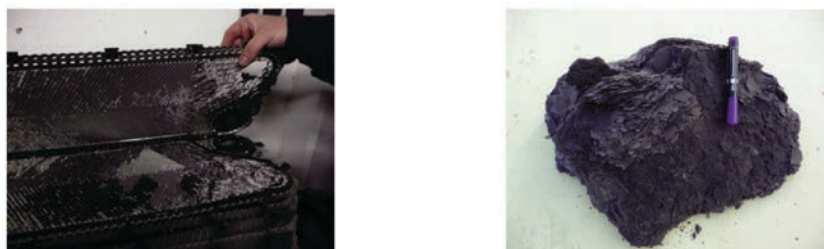


Figure 1: Precipitation of elemental sulphur on plate heat exchangers (left). Massive scalings of Mg-calcite at a heat exchanger (right).

## GENESIS OF RUBY AND SAPPHIRE DEPOSITS IN VIETNAM

Hauzenberger, C.A.<sup>1</sup>, Nguyen, N.K.<sup>3</sup>, Häger, T.<sup>2</sup>, Sutthirat, C.<sup>4</sup>, Wathankul, P.<sup>5</sup> & Le Thi-Thu Huong<sup>3</sup>

<sup>1</sup>Institute of Earth Sciences, University of Graz (Universitaetsplatz 2, 8010 Graz, Austria)

<sup>2</sup>Faculty of Geology, Hanoi University of Science (Hanoi, Vietnam)

<sup>3</sup>Centre of Gemstone Research, Johannes Gutenberg- University, D55099, Mainz, Germany

<sup>4</sup>Department of Geology, Faculty of Science, Chulalongkorn University, Bangkok 10330, Thailand

<sup>5</sup>GIT, Silom Road, Suriyawong, Bangrak, Bangkok 10500, Thailand

e-mail: christoph.hauzenberger@uni-graz.at

Only a few geological/mineralogical settings are favorable for the primary formation of corundum. Principally four different types of *in-situ* gem corundum deposits are known. These are: (1) Corundum mineralization associated with metasomatic/metamorphic processes in high grade rocks (2) Corundum from marbles (3) Corundum (sapphire) from volcanic rocks (4) Corundum from pegmatite-like rocks in a feldspathic matrix.

Northern Vietnam is an important ruby and sapphire producing area in Southeast Asia. Especially the areas around Yen Bai, Province Yen Bai and Quy Chau, Province Nghe An, are important gem stone deposits (alluvial deposits). To the north of Yen Bai, close to the city of Luc Yen, marble hosted primary corundum deposits have been reported. The typical mineral assemblage of the ruby bearing marbles are ruby - amphibole - phlogopite - sphene - calcite. Associated spinel bearing marbles are also known from this area comprising the mineral assemblage spinel - clinohumite - forsterite - amphibole - chlorite - phlogopite - dolomite - calcite. The rubies from the mined placer deposits around Luc Yen and Yen Bai crystallized originally in marbles as can be seen by stable isotope composition (HAUZENBERGER et al., 2001). The deposits around Quy Chau are less well documented but based on inclusions and stable isotope composition a similar setting as in Luc Yen and Yen Bai can be assumed (HAUZENBERGER et al., 2001). The variation in colour is directly linked to a wide spread in chemical composition. Cr is always present in high concentrations in pink sapphire and ruby, whereas Ti and Fe are concentrated in bluish, colourless and also in pinkish sapphires. V is usually higher in pink/red coloured corundum.

The sapphire deposits in southern Vietnam belong to the basalt hosted type. The alkali basalts are part of widespread Neogene volcanism found in southern China and Indochina regions. Samples from different localities between the cities of Ban Me Thuot and Saigon were recovered. Sapphire is typically associated with zircon which are mined from deep weathered red soil covering the alkali basalts. The basaltic sapphire is typically blue to dark blue in colour with high concentration of iron. Oxygen isotopes are similar to the hosting basalts which is in the range of average mantle composition.

HAUZENBERGER, C.A., HÄGER, T., BAUMGARTNER, L.P., HOFMEISTER, W. (2001): Proceed. Intern. Workshop on gems and minerals of Vietnam, Hanoi, 2001, pp. 124-138.

## PETROLOGICAL AND STRUCTURAL CHARACTERISTICS OF THE AUSTRO-ALPINE HIGH PRESSURE BELT IN THE SOUTHERN ÖTZTAL ALPS, TYROL

Heinisch, M.<sup>1</sup>, Hoinkes, G.<sup>1</sup>, Krenn, K.<sup>1</sup> & Tropper, P.<sup>2</sup>

<sup>1</sup>Institute of Earth Sciences, University of Graz, Universitätsplatz 2, 8010 Graz, Austria

<sup>2</sup>Institute of Mineralogy and Petrography, University of Innsbruck, Innrain 52, 6020 Innsbruck, Austria  
e-mail: georg.hoinkes@uni-graz.at

The investigated area is located in the southern Ötztal Alps at the transition from the Ötztal Complex (ÖC) in the north, part of the Ötztal-Bundschuh Nappe System and the Texel Complex (TC) in the south, part of the Koralpe-Wölz high pressure nappe system (SCHMID et al., 2004). Both reflect a polymetamorphic evolution which is documented by discontinuous chemical zonation of garnets due to a pre-Alpine core overgrown by an eo-Alpine rim. The metamorphic pattern of the southern Ötztal Alps is characterized by a continuously increasing eo-Alpine metamorphic grade towards the south from greenschist-amphibolite transition facies (ÖC) to eclogite facies (TC). The pre-Alpine imprint in this area is different: a high P/T Variscan in the ÖC and a Variscan and/or low P/T Permian in the TC (SCHUSTER & STÜWE, 2008).

It is generally accepted to classify the ÖC and TC as different tectonic units (SCHMID et al., 2004; SÖLVA et al., 2005) probably because of the occurrence of eclogites in the TC in contrast to the ÖC but by ignoring the metamorphic field gradient and the typical large scale structure characterized by vertical fold axes (“Schlingentektonik”). This large scale structure is well documented in the geological map of SCHMIDEGG (1932) showing that distinct lithologies can be traced from the TC into the ÖC.

This work is a petrological approach using garnet zoning patterns, geothermobarometry based on pseudo-sections and EMPA-monazite-dating to distinguish between lithologies of the TC and the ÖC by considering their different metamorphic history. Applying these methods to a distinct micaschist layer in the ÖC which continues into the TC, results in garnet zoning patterns typical for the TC. Additionally PT-conditions for garnet core formation show significant differences between the micaschist layer (ca. 6-7kbar) and the surrounding ÖC (8-9kbar). This is interpreted as hint for Permian vs. Variscan garnet core formation in the micaschist layer and the ÖC respectively. Moreover monazite of the ÖC is clearly of Variscan age but in the micaschist layer Permian additionally to Variscan ages were measured.

We conclude that lithologies of different metamorphic history are tectonically interlayered in the southern ÖC which probably belong to the eo-Alpine HP wedge (TC). This mingling of parts of the wedge enclosed within the upper plate (ÖC) result from SE-directed subduction and subsequent exhumation of the TC below the ÖC.

SCHMID, S., FÜGENSCHUH, B., KISSLING, E. & SCHUSTER, R. (2004): *Eclogae geologicae Helveticae*, 97, 39-117.

SCHMIDEGG, O. (1932): *Geologische Karte Sölden – St.Leonhard*. Geologische Bundesanstalt, Wien.

SCHUSTER, R. & STÜWE, K. (2008): *Geology*, 36, 963-966.

SÖLVA, H., GRASEMANN, B., THÖNI, M., THIEDE, R., HABLER, G. (2005): *Tectonophysics*, 401, 143-166.



# (3 + 1)-DIMENSIONAL MODULATED CRYSTAL STRUCTURE OF Cs<sub>3</sub>ScSi<sub>6</sub>O<sub>15</sub>

Hejny, C.<sup>1</sup>, Kahlenberg, V.<sup>1</sup> & Dabić, P.<sup>2</sup>

<sup>1</sup>University of Innsbruck, Institute of Mineralogy and Petrography, Innrain 52, A-6020 Innsbruck, Austria

<sup>2</sup>University of Belgrade, Laboratory of Crystallography, Djusina 7, 11000 Belgrade, Serbia

e-mail: Clivia.hejny@uibk.ac.at

Single crystal X-ray diffraction experiments of Cs<sub>3</sub>ScSi<sub>6</sub>O<sub>15</sub> show intense Bragg reflections, indexed on an *R*-centred hexagonal cell with *a*=13.861(1)Å, *c*=6.992(1)Å. Inspection of the distribution histograms of the remaining unindexed reflections reveal them to be satellite reflections of up to the third order in *c*\*-direction; the satellite reflections are present for *h* – *k* – *l* + *m* = 3*n*. The modulation wave vector was subsequently defined and refined to **q**=0.14153(2)**c**\*. This is close to, but distinctly different from 1/7. The crystal structure of Cs<sub>3</sub>ScSi<sub>6</sub>O<sub>15</sub> was solved in (3+1) dimensional superspace group *X*3̄*m*1(00*g*)0*s*0 from 1838 observed reflections by charge flipping with the program Superflip (PALATINUS & CHAPUIS, 2007) and refined with the program JANA2006 (PETRICEK et al., 2014). Refinement of three modulation waves for positional and ADP values for all atoms converged to *R**o* values for all, main, and satellite reflections of first, second and third order of 0.0200, 0.0166, 0.0181, 0.0214 and 0.0303, respectively.

Cs<sub>3</sub>ScSi<sub>6</sub>O<sub>15</sub> has a mixed octahedral-tetrahedral framework structure with six-membered rings of [SiO<sub>4</sub>]-tetrahedra and regular [ScO<sub>6</sub>]-octahedra forming infinite chains along the [0001] direction. According to bond valence calculations interatomic distances up to 3.5Å have to be considered as bonding for Cs. All atoms apart from Sc show very large positional modulations with maximum atomic displacements of up to 0.93Å. [ScO<sub>6</sub>]-octahedra and [SiO<sub>4</sub>]-tetrahedra remain rigid with minor variation of interatomic distances. However, as a function of *t* the [ScO<sub>6</sub>]-octahedra and [Si<sub>6</sub>O<sub>18</sub>]-rings rotate around the 3̄-axis by over 38° and inter-tetrahedral angles within the Si<sub>6</sub>O<sub>18</sub> ring diversify greatly. The coordination environment of Cs is irregular with oxygen atoms moving in and out of the Cs coordination in order to maintain the bond valence sum around Cs at a constant level of ca. 1.075 v.u..

The only another Cs-Sc-silicate known to date, Cs<sub>3</sub>ScSi<sub>8</sub>O<sub>19</sub> (KOLITSCH & TILLMANN, 2004), has a microporous framework structure different from Cs<sub>3</sub>ScSi<sub>6</sub>O<sub>15</sub>. However, similar topological features as found in Cs<sub>3</sub>ScSi<sub>6</sub>O<sub>15</sub> have also been reported for Cs<sub>3</sub>EuSi<sub>6</sub>O<sub>18</sub> (HUANG et al. 2005), Cs<sub>3</sub>DySi<sub>6</sub>O<sub>15</sub> (ZHAO et al., 2010), and Cs<sub>1.86</sub>K<sub>1.14</sub>DySi<sub>6</sub>O<sub>15</sub>, (WIERZBICKA-WIECZOREK et al., 2015).

HUANG, M.Y., CHEN, Y.H., CHANG, B.C., LII, K.H. (2005): Chem. Mater., 17, 5743-5747.

KOLITSCH, U., TILLMANN, E. (2004): Mineral. Mag., 68, 677-686.

PALATINUS, L., CHAPUIS, G. (2007): J. Appl. Cryst., 40, 786-790.

PETRICEK, V., DUSEK, M., PALATINUS, L. (2014): Z. Kristallogr., 229, 345-352.

WIERZBICKA-WIECZOREK, M., GÖCKERITZ, M., KOLITSCH, U., LENZ, C., GIESTER, G. (2015): Eur. J. Inorg. Chem. 2015, 2426-2436.

ZHAO, X., LI, J., CHEN, P., LI, Y., CHU, Q., LIU, X., YU, J., XU, R. (2010): Inorg. Chem., 49, 9833-9838.

**FORMATIONAL MECHANISMS OF EARLY CAMBRIAN SEPTARIAN  
CARBONATE CONCRETIONS (YANGTZE PLATFORM, SW CHINA)**

Hippler, D.<sup>1</sup>, Mamczek, M.<sup>2</sup>, Struck, U.<sup>3</sup> & Franz, G.<sup>4</sup>

<sup>1</sup>Technische Universität Graz, Inst. Applied Geosciences, Rechbauerstraße 12, 8010 Graz, Austria

<sup>2</sup>Universität Tübingen, Department of Petrology, Wilhelmstraße 56, 72076 Tübingen, Germany

<sup>3</sup>Museum für Naturkunde, Invalidenstraße 43, 10115 Berlin, Germany

<sup>4</sup>Technische Universität Berlin, Inst. Applied Geosciences, Ackerstraße 76, 13355 Berlin, Germany

Corresponding author's e-mail: dorothee.hippler@tugraz.at

Carbonate concretions are widespread and well known from the Neoproterozoic to Phanerozoic geological record, and mostly result from complex physicochemical processes during diagenesis. To date however, no modern depositional analogue has been found in near-surface sediments, in order to identify mechanisms responsible for concretionary growth. Carbonate concretions develop variable shapes; with their cement textures often indicate concentric or pervasive growth. Different growth models therefore exist, which relate concretionary growth to the necessary carbonate supersaturation (i) throughout the porewater, (ii) generated in situ by organic matter decay or (iii) through mixing with external fluids. Crack formation in septarian concretions can either occur through localized over pressuring due to compaction, gas expansion, chemical dehydration and/or synsedimentary seismicity. Here, we present structural, mineralogical and (isotope-) geochemical data of an early Cambrian septarian carbonate concretion from the Kunyang phosphate mine at Meishucun (Yunnan Province, SW China), in order to examine the growth and formational mechanisms as well as signs for crack formation. The sampled concretion is ellipsoidal and exhibits deformed laminae and multi-branched septarian structures. It consists mainly of dolomite and minor portions of quartz, feldspar, mica and pyrite. We observe a clear mineralogical zoning with dolomite and pyrite content decreasing from the centre towards the margins. Crack-filling cement is made up of early dolomite and late calcite. Cathodoluminescence and scanning electron microscopy indicate also zoning of the dolomite cements. Stable isotope records within the matrix yield small variations from the centre towards the margins, with  $\delta^{13}\text{C}$  values ranging from -6.2 to -5.4 ‰ (VPDB) and  $\delta^{18}\text{O}$  values from -11.8 to -11.1 ‰ (VPDB), respectively. Stable isotope compositions of the septarian infills reveal higher variability and slightly stronger fractionation. Our findings indicate a synsedimentary to early diagenetic origin and pervasive to concentric growth of the carbonate concretions within the zone of bacterial sulfate reduction and methanogenesis, respectively. Septarian crack formation is possibly related to synsedimentary seismicity, and thus septarian concretions might contribute promising hints about basin seismicity. However, this is ambiguous and cracking could also be related to gas expansion.

Financial support of the research project by DFG-FG 736, NAWI Graz and EFRI – Land Steiermark is kindly acknowledged. Thanks also to K. Born (MfN Berlin) for assistance with CL and SEM analyses.



## CHEMISTRY AND MINERALOGY OF FILTER CAKES FROM WASTE WATER TREATMENT BY ZERO-VALENT IRON FOR CRITICAL METAL RECOVERY

Höllen, D.<sup>1</sup>, Krois, L.-M.<sup>1</sup>, Binder, H.<sup>1</sup>, Müller, P.<sup>2</sup>, Mischitz, R.<sup>2</sup> & Olbrich, T.<sup>3</sup>

<sup>1</sup> Chair of Waste Processing Technology and Waste Management, Montanuniversität Leoben,  
Franz-Josef-Str. 18, 8700 Leoben, Austria

<sup>2</sup>ferroDECONT GmbH, Peter-Tunner-Str. 19, 8700 Leoben, Austria

<sup>3</sup>AVR GmbH, Dr.-Otto-Neurath-Gasse 7, 1220 Wien, Austria

e-mail: daniel.hoellen@unileoben.ac.at

Within the project “RECOMET–Recovery of Metals”, which is funded by the Austrian Research Promotion Agency (FFG), it is investigated which (potentially) critical raw materials (Be, Mg, Mn, Ni, Co, Zn, Cr, Al, Ga, In, rare earth elements (REE), Ge, Sb, Nb, Ta, W, V, Mo, platinum group elements (PGE)) can be reduced and/or adsorbed onto iron granules by fluid-bed processes from low-concentration industrial waste waters.

A fluidized-bed technology (ferroDECONT process), which is approved for the remediation of contaminated sites, i.e. the reduction of chromate, and the know-how in the field of waste water cleaning (AVR) are adapted to the new field of critical metal recovery considering the transition from the “disposal society” to the “recycling society” to lay the foundation of future R&D projects for metal recovery from rinsing waters.

For this purpose synthetic and real waste waters were treated with zero-valent iron (ZVI) in laboratory and pilot scale experiments where pH, reaction time and liquid:solid ratio were varied. After the experiment, the solutions were separated from the solids by a three step sieving and filtration approach using mesh widths of 2mm, 2 $\mu$ m and 0,45 $\mu$ m. Selected fine fractions were investigated for chemistry by ICP-MS and for mineralogy by X-ray diffraction and Raman spectroscopy.

It has been demonstrated that for most elements more than 90% of (potentially) critical metals can be removed from waste water by ZVI. After the treatment of the waste water these elements are fixed in a filter cake which consists of fine-grained particles in the range of few  $\mu$ m. X-ray diffraction patterns and Raman spectra of these filter cakes indicate that they consist of magnetite with minor amounts of goethite, lepidocrocite and a graphite-like phase of lower crystallinity. Specific mineral phases which contain the fixed (potentially) critical metals could not be found which can be explained by the low content of the fixed critical metal in the filter cake of about 1 wt-%. It has to be discussed how (potentially) critical metals are bound in those phases or adsorbed on their surfaces in order to find out how they can be extracted for further metallurgical treatment. For this purpose advanced mineralogical methods like electron microprobe analyses and transmission electron microscopy shall be applied and both hydro- and pyrometallurgical recovery options shall be discussed.

HÖLLEN, D., KROIS, L.-M., MÜLLER, P., MISCHITZ, R., OLBRICH, T., OLBRICH, R. (2014): DepoTech 2014, 357-360.

## SLAGS AND ASHES AS SECONDARY RESOURCES FOR CO<sub>2</sub> CAPTURE AND UTILIZATION

Höllen, D.<sup>1</sup>, Niesenbacher, I.<sup>2</sup>, Treimer, R.<sup>3</sup>, Stöllner, M.<sup>1</sup>, Melcher, F.<sup>4</sup> & Lehner, M.<sup>2</sup>

<sup>1</sup>Chair of Waste Processing Technology and Waste Management, Montanuniversität Leoben, Austria

<sup>2</sup>Chair of Process Technology and Industrial Environmental Protection, Montanuniversität Leoben, Austria

<sup>3</sup>Chair of Mining Engineering and Mineral Economics, Montanuniversität Leoben, Austria

<sup>4</sup>Chair of Geology and Economic Geology, Montanuniversität Leoben, Austria

e-mail: daniel.hoellen@unileoben.ac.at

Carbon dioxide emissions are the main driving force of global warming, whereas mineral waste constitutes the largest waste stream in the world. Consequently, Carbon Capture and Utilization (CCU) which is investigated within the Research Studio Austria (RSA) “CarboResources” is a powerful tool to protect the climate and geogenic carbonate deposits simultaneously following the waste hierarchy for both solid and gaseous waste. CCU is based on the reaction of carbon dioxide with Ca and Mg oxides or silicates to form the corresponding carbonates which can be applied as industrial minerals and construction materials. An EAF stainless steel slag, two MSWI bottom ashes and one fly and bottom ash each from biomass incineration were selected for characterization and carbonation experiments. These Ca and Mg rich materials are dissolved in different acids, impurities are removed and Ca and Mg carbonates are produced by reaction with CO<sub>2</sub>. The suitability of slags and ashes for CCU as well as the applicability of (by-)products in the industry depends significantly on chemistry and mineralogy which are assessed by XRF/ICP-MS and optical/electron microscopy (incl. WDX), XRD and Raman spectroscopy, respectively. XRF analyses indicate that EAF slag and biomass ashes contain about 30wt% and MSWI bottom ash about 20wt% CaO, whereas MgO contents are generally only in the range of 5wt%. ICP-MS analyses show that the valuable metals Cr and Mn are present in steel slags with about 2wt% whereas Ti is present with up to 1wt% in MSWI bottom ash; both might be recovered during CCU. Optical and electron microscopy, XRD and Raman spectroscopy show that Ca in EAF slag is distributed predominantly among brownmillerite, alite, mayenite and melilite which are suitable for carbonation during CCU, whereas both ashes already contain carbonates formed during storage besides melilite and portlandite (Fig. 1).

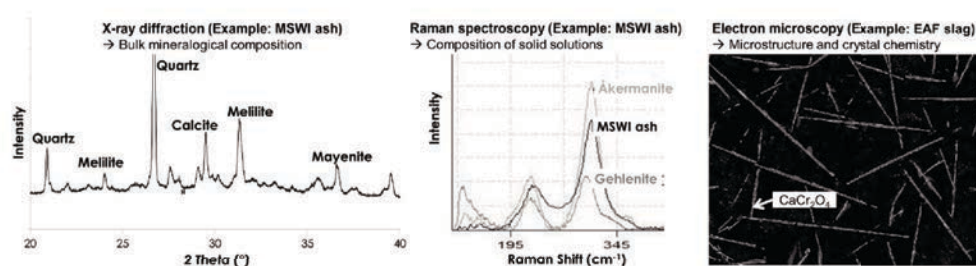


Figure 1. Mineralogical composition of slags and ashes for CCU.

## SILIKAT-SULFIDWECHSELWIRKUNGEN IN PB-ZN LAGERSTÄTTEN: ZN IM GRANAT AUS DER LAGERSTÄTTE SCHNEEBERG

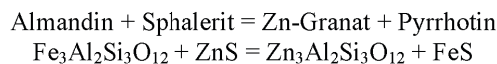
Holzmann, J.\* & Tropper, P.

<sup>1</sup>Institut für Mineralogie und Petrographie, Universität Innsbruck, Innrain 52, 6020, Innsbruck, Österreich

\*Verunglückt am 23.6.2013

e-mail: peter.tropper@uibk.ac.at

Zink ist ein sehr untypisches Element für Granat. Da in vielen erzführenden Gesteinen des Lazzacher- und Pflerschtals sowie des Schneeberges aus der Pb-Zn Lagerstätte Schneeberg Granate mit Zinkblende koexistieren, wurde Zink in den Granaten mitgemessen. Unter normalen Umständen ist Staurolith das klassische Zinkmineral in silikatischen amphibolitfaziellen Paragenesen. Ab dem Zusammenbruch von Staurolith wird Zink vermehrt in Biotit eingebaut. Erst ab der Granulitfazies, also ab dem Zusammenbruch von Biotit wird Zink normalerweise in Granat eingebaut. Hierbei bewegen sich die Zn- Gehalte jedoch maximal im 100er ppm-Bereich. Mit Zinkblende koexistierende Granate weisen einen maximalen Zinkgehalt von 1.25 Gew.% (durchschnittlicher ZnO-Gehalt von 0.76 Gew.%) auf. Aus allen Messungen koexistierender Granate ergab sich folgende durchschnittliche Granatformel:  $(\text{Fe}_{1.979}\text{Ca}_{0.388}\text{Mg}_{0.294}\text{Mn}_{0.259}\text{Zn}_{0.044})\text{Al}_{1.991}\text{Si}_{3.031}\text{O}_{12}$ . Zink nimmt dabei den Platz von Eisen auf der X-Position im Granat ein. Für den Zinkeinbau in Granat kann folgende Austauschreaktion zwischen Granat und Zinkblende definiert werden:



Das freigewordene Eisen wird in der Zinkblende eingebaut oder entmischt in Letzterer in Form von Pyrrhotin-Tröpfchen. Wie aus der obenstehenden Reaktion hervorgeht lässt sich ein theoretisches Zinkendglied von Granaten der Pyrrhotin-Gruppe mit der Formel  $\text{Zn}_3\text{Al}_2\text{Si}_3\text{O}_{12}$  ableiten. In der Granatformel erreicht Zink natürlich nur einen sehr kleinen stöchiometrischen Koeffizienten. Der durchschnittliche Molenbruch der Zinkkomponente beträgt dabei  $X_{\text{Zn}}=0.015$ . Im Zuge dieser Untersuchungen wurden auch das Volumen und die Standardentropie ( $S_{298}$ ) dieses Endglieds berechnet. Anhand von Schreinemakers-Analysen im System  $\text{ZnO-Al}_2\text{O}_3\text{-SiO}_2\text{-FeO-O}_2\text{-S}_2$  wurde aufgezeigt, dass dieses  $\text{Zn}_3\text{Al}_2\text{Si}_3\text{O}_{12}$  Endglied zu hohen Temperaturen, hohen Sauerstoffpotenzialen und niedrigen Schwefelpotenzialen hin stabil ist.

**MAGMATIC FORMATION/INTRUSION AGE OF MONZOGRAHITE FROM  
ŠANDROVAC QUARRY, NW PAPUK MT., CROATIA**

Horvat, M.<sup>1</sup>, Klötzli, U.<sup>2</sup>, Klötzli, E.<sup>2</sup>, Jamičić, D.<sup>3</sup> & Buda, GY.<sup>4</sup>

<sup>1</sup> Croatian Geological Survey, Sachsova 2, 10000 Zagreb, Croatia

<sup>2</sup> University of Vienna, Department of Lithospheric Research, Althanstraße 14, A-1090 Vienna, Austria

<sup>3</sup> Svetojanska 21, 10000 Zagreb, Croatia

<sup>4</sup> Eötvös Lóránd University, Institute of Geology, Department of Mineralogy,

Pázmány Péter sétány 1/c, H-1117 Budapest, Hungary

e-mail: mhorvat@hgi-cgs.hr

Papuk Mt. is one of the Slavonian Mts. in the southern part of the Pannonian Basin in Croatia. In north-western part of the Mountain smaller extrusive bodies intersect rocks of the Palaeozoic granite-metamorphic complex which, superficially, are mostly represented by various metamorphic rocks ranging from the chlorite to amphibolite facies in association with various/varieties granite rocks. The studied granitoid sample 2PPG-32 is from Šandrovac Quarry (NW Papuk Mt). The main mineral phases are: grey quartz grains, white or greenish feldspar grains, black biotite leaves and shine mica leaves. The texture is fine to medium-grained and the structure is homogeneous. Feldspars are K-feldspar (proved to be max microcline on the basis of their XRD pattern; HORVAT et al., 2011) and plagioclase (oligoclase  $Or_{2-3}Ab_{73-90}An_{17-24}$ ). Muscovite is developed in allotriomorphic leaves. It can be found in plagioclase as inclusion but also as rock constituent. Biotite is fully chloritized. The  $K_2O$  content of biotite fluctuates between 3.43 and 9.13 wt% and  $TiO_2$  content is low (1.25–2.95 wt%). Accessory minerals are zircon, monazite, REE-carbonates, Fe-oxides and garnet. According to modal and chemical composition the 2PPG-32 sample is classified as muscovite-biotite monzogranite (HORVAT & BUDA, 2004). The sample has a  $Na_2O/K_2O$  molar ratio approximately equal to 1.0 with 3.92wt%  $Na_2O$ . Accordingly to the alumina saturation index and the A/NK molar ratio peraluminous character of magma are indicating. AFM ternary diagram confirm affinity to calc-alkaline series and 2PPG-32 sample plots in alkaline corner. This classification is in accordance with the petrographic observations of investigated sample as a two-mica monzogranite. The sample has a relatively high total REE concentration (120 ppm) with strong negative Eu, Ti, Sr and Nb anomalies. Elevated  $\Sigma REE$  and a negative Eu anomaly indicate typical magmatic fractional crystallisation of this monzogranite. The alteration-independent Yb-Ta discriminant speaks for a syn-collision (SYN-COLG) tectonic setting, while Rb, Hf, Ta systematics favour a late (LATE-COLG) to post-collision (POST-COLG) tectonic setting. CL images of zircons reveal a typical oscillatory zonation, interpreted as being characteristic for magmatic growth plus different alteration zones. Within the oscillatory zonation: one, two or even three CL-dark zones can be distinguished. Also some crystals have a CL-dark outer alteration zone. Characteristic is a CL-bright rim inwards the altered zone. U-Pb isotopic data obtained by LA-MC-ICP-MS analysis of seven zircons yield a concordia age of  $381.6(7) \pm 1.6(7)$  Ma which is interpreted as the best estimate for the intrusion age of the monzogranite from Šandrovac Quarry.

HORVAT, M., BUDA, GY. (2004): Acta Mineralogica-Petrographica, 45/1, 93-100.

HORVAT, M., TIBLAŠ, D., BUDA, GY., LOVAS, GY. (2011): Geologia Croatica, 64/2, 153-162.

**PHASE RELATIONS OF REE MINERALS FLORENCITE, ALLANITE AND  
MONAZITE IN QUARTZITIC GARNET KYANITE SCHIST OF ECLOGITE ZONE,  
TAUERN WINDOW, AUSTRIA**

Hoschek, G.<sup>1</sup>

<sup>1</sup>Institute of Mineralogy and Petrography, University of Innsbruck, Innrain 52f, A-6020 Innsbruck, Austria  
e-mail: Gert.Hoschek@uibk.ac.at

All three REE phases are present in quartzitic garnet kyanite schist of the Eclogite Zone, Tauern Window with peak conditions around 570-600°C, 20-25kbar. Florencite  $(\text{REE})\text{Al}_3(\text{PO}_4)_2(\text{OH})_6$  inclusions are mostly in garnet rim region and kyanite but also in the muscovite-quartz matrix breaking down to monazite symplectite. Allanite  $(\text{REE},\text{Ca})(\text{Fe},\text{Mg})\text{Al}_2(\text{SiO}_4)_3(\text{OH})$  is mostly present in garnet core but not in kyanite and matrix. This suggests florencite stability at higher P-T values than allanite. Pseudo-sections with bulk composition including Ce and La reveal florencite stability from low to higher P-T, however the present stability relations are only an estimate due to insufficient thermodynamic data for florencite and allanite. Higher Ca in bulk composition remarkable extends allanite and decrease florencite stability at higher T, but changes of Fe and Al are of minor resp. neglectable effect. Fractional garnet crystallization with more complex changes in bulk composition has a strong influence and extends florencite stability to path dependent lower P-T positions. The retrograde P-T path was calculated with a bulk composition dominated by matrix. Despite the large difference in bulk composition, e.g. Fe and Ca, the pseudo-section is partly similar than the prograde result. Compared with florencite, stability of allanite is remarkable reduced at retrograde conditions. Results of calculations with formation of allanite and later florencite growth at higher P-T followed by florencite breakdown at retrograde conditions are in accord with petrographic observations. For the present sample florencite stability is mainly due to the low Ca-content in bulk composition.

## LOOK BEFORE YOU LEAP: MAJOR AND TRACE ELEMENT DIFFUSION (AND CONFUSION) IN OLIVINE

Jollands, M.<sup>1</sup>

<sup>1</sup>Research School of Earth Sciences, Australian National University, Canberra, ACT0200, Australia

Solid state diffusion in minerals is a fundamental, yet still relatively poorly-understood process.

The validity of radiogenic isotope decay schemes, as well as stable isotope tracers, requires knowledge of the relevant elements' diffusion rates, and hence closure temperatures, to be known. Measurement of the trace and major element composition of melt inclusions is only reasonable if the melt inclusion and host mineral have not diffusively exchanged. The same is true when using rapidly emplaced mantle xenocrysts to infer, for example, the 'water' content of the lithosphere; have the xenocrysts diffusively lost or gained water during entrainment and ascent? Frozen trace and major element diffusion profiles in xenocrysts dropped into magma chambers may provide information regarding residence times, but these duration estimates require high quality experimental data to be meaningful.

Whilst diffusion in olivine has been studied for several decades, it is only with recent advances in micro-analytical techniques that it has been feasible to generate large datasets in which the impact of different variables on diffusion can be investigated in turn. Traditional studies often investigated the effect of temperature, crystal orientation and occasionally oxygen fugacity, and analysed their experimental products using electron probes, early ion probes or nuclear methods. Rarely was the effect of chemical activity considered.

In this talk, the effect of several variables (e.g. temperature, chemical activity, crystal orientation, presence of water, diffusant concentration) on the diffusion of some major and trace elements in olivine will be presented. Constraining chemical activities is fundamental according to the phase rule, and, indeed, can have a considerable effect on the rate of diffusion. In addition, by constraining this and other variables, a full thermodynamic treatment of the diffusion interface (where the diffusant source meets the target mineral) is possible. Many previous studies have not given consideration to equilibrium thermodynamics when studying diffusion kinetics; this talk will show that the two cannot, and should not be separated.

Finally, the application of new, fully thermodynamically-constrained diffusion data to natural olivine xenocrysts will be presented. With good understanding of the relevant variables and high-quality diffusion data, it is possible to extract robust timescales and shed light on the duration of geologically rapid processes regardless of their absolute age.



**PLATINUM-GROUP ELEMENTS IN PRISTINE AND NEAR-SURFACE ORES  
FROM THE PLATREEF, BUSHVELD COMPLEX, SOUTH AFRICA**

Junge, M.<sup>1</sup>, Oberthür, T.<sup>1</sup>, Kraemer, D.<sup>2</sup>, Melcher, F.<sup>3</sup>, Kärner, K.<sup>1</sup> & Marbler, H.<sup>1</sup>

<sup>1</sup>Bundesanstalt für Geowissenschaften und Rohstoffe (Stilleweg 2, D-30655, Hannover, Germany)

<sup>2</sup>Earth and Environmental Sciences, Jacobs University Bremen (Campus Ring 1, D-28759, Bremen, Germany)

<sup>3</sup>Lehrstuhl für Geologie und Lagerstättenlehre, Montanuniversität Leoben (Peter Tunner Strasse 5, A-8700, Leoben, Austria),

e-mail: malte.junge@bgr.de

The Bushveld Complex of South Africa is the largest layered intrusion on Earth and hosts the world's largest resources of platinum-group elements (PGE) which occur in three major ore bodies: the Merensky Reef, the UG-2 chromitite, and the Platreef. The Platreef is located in the northern limb of the Bushveld Complex and is composed of mineralized pyroxenite with sulphide contents of about 3% and PGE contents between 1 to 4 g/t (VERMAAK 1995). The Platreef is mined in a number of open pits and currently, about 100 Mt of rock is moved annually to recover about 8 Mt of ore. Economic concentrations of PGE are mainly restricted to sulphide-bearing ores. Although, near-surface oxidized PGE ores have a huge potential, attempts to extract the PGE have proved to be uneconomic due to low PGE recoveries (<<50%) achieved by conventional metallurgical methods (EVANS 2002, LOCMEILIS et al., 2010). For the Bushveld Complex the PGE potential of the oxidized ores was estimated at around 26 Moz. Different processing methods are needed to increase recovery rates and to make the oxidized PGE-ores from the Bushveld Complex economic. For the oxidized ores of the Great Dyke in Zimbabwe it was shown that a mild hydrochloric acid leach combined with a subsequent leach with biogenic siderophores in an aqueous solution can effectively extract Pt and Pd from the oxidized ores (KRAEMER et al. (2015)).

Three boreholes covering a sequence of oxidized and pristine Platreef ore are studied. In the pristine Platreef ore, PGE occur as discrete platinum-group minerals (PGM) usually associated with sulfides (mainly pyrrhotite, pentlandite, chalcopyrite and minor pyrite), or within sulfides. The PGM in these ores are (Pt,Pd)-bismuthotellurides, cooperite-braggite and sperrylite, whereas in the oxidized ore only relict PGM are present, most commonly sperrylite and cooperite-braggite. The variation in the PGM assemblage indicates different stabilities of PGM during the weathering process. PGE contents in sulfides of pristine Platreef ores were analysed by electron microprobe (EPMA). The results indicate that pentlandite (n=69) contains Pd concentrations ranging from <146 ppm to 681 ppm. Rhodium was below the detection limit of 117 ppm Rh. Concentrations of Pd and Rh in chalcopyrite (n=25), pyrrhotite (n=31) and pyrite (n=21) were all below the detection limits of Pd (146 ppm) and Rh (117 ppm). EPMA studies of the oxidized ores showed that Fe- and Mn-oxides/hydroxides and secondary silicates contain several 100s of ppm of Rh, Pt and Pd. From pristine to oxidized ore, the Pt/Pd ratio increases due to the greater mobility of Pd.

EVANS, D.M. (2002): *Appl. Earth Science*, 111, B81-86.

KRAEMER, D., JUNGE, M., OBERTHÜR, T., BAU, M. (2015): *Hydrometallurgy*, 152, 169-177.

LOCMEILIS, M., MELCHER, F., OBERTHÜR, T. (2010): *Min.Dep.*, 45, 93-109.

VERMAAK, C. (1995): *The Platinum-Group Metals - A global perspective*. Mintek, Johannesburg.

## INVESTIGATIONS ON ALUNOGEN UNDER MARS-RELEVANT TEMPERATURE CONDITIONS

Kahlenberg, V.<sup>1</sup>, Braun, D.E.<sup>2</sup> & Orlova, M.<sup>1</sup>

<sup>1</sup>Institute of Mineralogy and Petrography, University of Innsbruck, Innrain 52, A-6020 Innsbruck

<sup>2</sup>Institute of Pharmacy, Pharmaceutical Technology, University of Innsbruck, Innrain 52c, A-6020 Innsbruck  
e-mail: volker.kahlenberg@uibk.ac.at

Since alunogen has been postulated to occur in martian soils (GOLDEN et al., 2005) the low-temperature (LT) dependent behavior of a synthetic alunogen sample with composition  $\text{Al}_2(\text{SO}_4)_3 \cdot 16.61\text{H}_2\text{O}$  has been studied in the overall temperature range from -100 to 23 °C by DSC measurements, *in-situ* powder and single-crystal X-ray diffraction as well as Raman spectroscopy. Cooling/heating experiments using the different techniques prove that alunogen undergoes a reversible, sluggish phase transition somewhere between -30 and -50 °C from the triclinic room-temperature (RT) form (MENCHETTI & SABELLI, 1974) to a previously unknown LT-polymorph. A significant hysteresis for the transition was observed with all three methods and the transition temperatures were found to depend on the employed cooling/heating rates. The crystal structure of the LT-modification has been studied at -100 °C using single crystals which have been grown from an aqueous solution. Basic crystallographic data are as follows: monoclinic symmetry, space group type  $P2_1$ ,  $a = 7.4125(3)\text{Å}$ ,  $b = 26.8337(16)\text{Å}$ ,  $c = 6.0775(3)\text{Å}$ ,  $\beta = 97.312(4)^\circ$ ,  $V = 1199.01(10)\text{Å}^3$  and  $Z = 2$ . Structure analysis revealed that LT-alunogen corresponds to a non-stoichiometric hydrate. Notably, the first-order transition results in a single-crystal-to-single-crystal transformation. In the asymmetric unit there are two Al-atoms, three  $[\text{SO}_4]$ -tetrahedra, and seventeen crystallographically independent sites for water molecules, whose hydrogen positions could be all located by difference-Fourier calculations. According to site-population refinements only one water position (Ow5) shows a partial occupancy. A comfortable way to rationalize the crystal structure of the LT-modification of alunogen is based on a subdivision of the whole structure into two different slabs parallel to (010). The first type of slab (type A) is about nine Å thick and located at  $y \approx 0$  and  $y \approx \frac{1}{2}$ , respectively. It contains the  $\text{Al}(\text{H}_2\text{O})_6$ -octahedra as well as the sulfate groups centered by S1 and S2. Type B at  $y \approx \frac{1}{4}$  and  $y \approx \frac{3}{4}$  comprises the remaining tetrahedra about S3 and a total of five additional “zeolitic” water sites (Ow1-Ow5) which are not a part of a coordination polyhedron. Within slab-type A alternating chains of (unconnected) octahedra and tetrahedra can be identified which are running parallel to [100]. In addition to electrostatic interactions between the  $\text{Al}(\text{H}_2\text{O})_6^{3+}$ - and the  $(\text{SO}_4)^{2-}$ -units, hydrogen bonds are also essential for the stability of these slabs. A detailed comparison between both modifications including a derivation from a hypothetical aristotype based on group-theoretical concepts will be presented.

Our new findings may help in the identification of the LT-form by X-ray diffraction using the Curiosity Rover’s ChemMin instrument or by Raman spectroscopy.

GOLDEN, D.C., MING, D.W., MORRIS, R.V., MERTZMAN, S.A. (2005) J. Geophys. Res., 110, E12S07, 1-15.  
MENCHETTI, S., SABELLI, C. (1974) Tsch. Mineral. Petrogr. Mitt., 21, 164-178.

## HERSTELLUNG VON POLYEDERMODELLEN FÜR DIE LEHRE

Kahlenberg V.<sup>1</sup>, Tessadri R.<sup>1</sup>  
Artho R.<sup>2</sup>, Jank A.<sup>2</sup>, Falschlunger H.<sup>2</sup>, & Schmidt-Baldassari M.<sup>2</sup>

<sup>1</sup>Institut für Mineralogie & Petrographie, Universität Innsbruck, Innrain 52, 6020 Innsbruck, Austria

<sup>2</sup>HTL-Höhere Technische Bundeslehranstalt Fulpmes, Waldrasterstr. 21, 6166 Fulpmes, Austria

e-mail1: volker.kahlenberg@uibk.ac.at, e-mail2: htl-fulpmes@tsn.at

Am Institut für Mineralogie und Petrographie der Universität Innsbruck (IMP) existiert eine historische Sammlung von Kristallpolyedern aus dem 19. Jahrhundert, die insgesamt 909 Holzmodelle umfasst (Kaltenhauser & Tessadri, 2001). Teile dieser Kollektion wurden bis jetzt im Rahmen der mineralogisch-kristallographischen Ausbildung eingesetzt. Um diese in mehrfacher Hinsicht wertvolle Sammlung zu schonen und im Bereich der Lehre zu ersetzen, wurden im Rahmen eines Diplomarbeitprojektes mit der HTL-Fulpmes (Tirol) Polyederformen als Aluminiumkörper hergestellt.

Die Auswahl der Polyeder erfolgte nach didaktischen Kriterien bezüglich der Symmetriekerennung. Ferner sollte jede der 32 Punktgruppen zumindest einmal realisiert werden. Der entsprechende Entwurf jedes Polyeders wurde mit dem Programm JCrystal© am IMP erstellt. Die daraus resultierenden Dateiformate mussten dann von den Studenten mehrfach konvertiert und bearbeitet werden (z.B. MeshLap© – Software für die Bearbeitung von Polygon-Oberflächennetzen von 3D-Modellen, HyperMill©, HyperCad©), um die komplexe Maschinenprogrammierung unter Berücksichtigung der Kristalldimensionen, der optimalen Verfahrenswege, der Befestigungs-/Einspannstrategien der Fräse, sowie anschließender Frässimulation durchzuführen.

Die Produktion der Aluminiummodelle (insgesamt acht Sets mit je 52 Polyedern) erfolgte mit einer 5-Achsen-Universalfräse der Firma DMU MORI (Winterthur/Schweiz). Zur Verbesserung der haptischen Eigenschaften wurden die Körper anschließend einer Oberflächenbehandlung mit Sandstrahltechnik unterzogen. Für die sichere Aufbewahrung wurden aufwändig konstruierte Behälter hergestellt.



Abbildung 1: Polyedersatz aus oberflächenbehandeltem Aluminium (insgesamt 52 Modelle).

KALTENHAUSER, G. & TESSADRI, R. (2001): Die Kristallmodellsammlung aus dem 19. Jahrhundert des Instituts für Mineralogie und Petrographie der Universität Innsbruck. - Mitt. Österr. Miner. Ges., 146, 122.

## CHARAKTERISIERUNG VON EISENERZTRÄGERN MITTELS BILDVERARBEITUNG

Kain-Bückner, B.<sup>1</sup>, Hanel, M.<sup>2</sup> & Mali, H.<sup>1</sup>

<sup>1</sup>Lehrstuhl für Geologie und Lagerstättenlehre, Montanuniversität Leoben, Franz-Joseph- Straße 18,  
8700 Leoben, Österreich

<sup>2</sup>Lehrstuhl für Eisen- und Stahlmetallurgie, Montanuniversität Leoben, Franz-Joseph- Straße 18,  
8700 Leoben, Österreich

e-mail: birgit.kain-bueckner@unileoben.ac.at

Mit der Bildverarbeitungssoftware VisuMet (entwickelt am Lehrstuhl für Geologie und Lagerstättenlehre) ist eine Abschätzung des Reduktionsverhaltens von Eisenträgern möglich. Anhand von mikroskopischen Aufnahmen an polierten Anschliffen werden bei Eisenerzen die Anteile an Limonit, Hämatit und Magnetit und bei Eisenerzpellets die Anteile Eisenoxid, Glas und Poren bestimmt (Abb. 1). Für die Vorhersage der Reduktionsgeschwindigkeit des Materials bei Standardreduktionsbedingungen fließt das Gefüge der Eisenerze in die Beurteilung mit ein. Bei Pellets hat sich gezeigt, dass die Porengrößenverteilungen mit der Reduzierbarkeit zusammenhängen. Vor der eigentlichen Verarbeitung der Bilder werden diese auf Unschärfe geprüft und farbkorrigiert, um Kanteneffekte an Mineralgrenzen zu minimieren. Für die einzelnen Phasen werden die optimalen Schwellenwerte von Rot/Grün/Blau (RGB) und Farbwert/Farbsättigung/Helligkeit (HSL) festgelegt. Bei Pellets werden die Werte Helligkeit, Kontrast und Gamma (BCG) verändert, um die Unterscheidung von Glas zu harzgefüllter Pore zu verbessern. Diese Art der Bewertung setzt eine gründliche Probenvorbereitung (Politur) und gleichbleibende Einstellungen bei der Bilderstellung voraus. In Zukunft soll dieses Verfahren eine kostengünstige Alternative zu Standardreduktionstests darstellen.

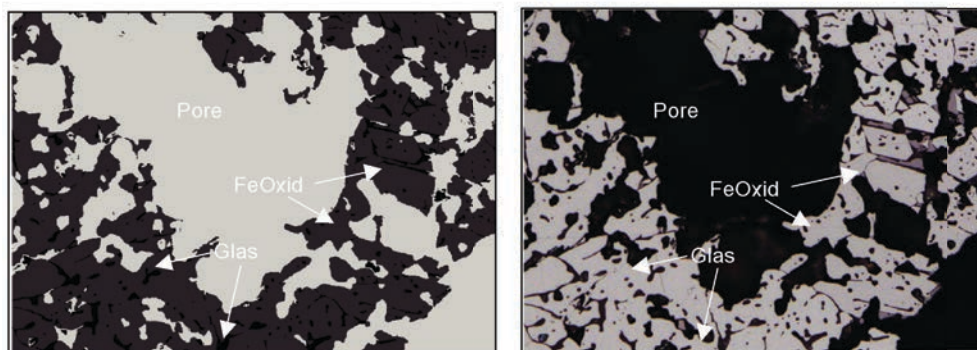


Abbildung 1: Phasenidentifizierung eines Eisenerzpellets, links VisuMet, rechts Original, Bildbreite 0,354 mm



## HIGH TEMPERATURE MICROSCOPIC INVESTIGATIONS IN THE FIELD OF CERAMICS – AN OVERVIEW

Kircher, V.<sup>1</sup>, Kölbl, N.<sup>1</sup>, Marschall, I.<sup>1</sup> & Harmuth, H.<sup>1</sup>

<sup>1</sup>Montanuniversität Leoben, Chair of Ceramic, Peter Tunner Straße 5, 8700 Leoben, Austria  
e-mail: volkmar.kircher@unileoben.ac.at

The possibility to investigate high temperature processes microscopically opens a wide spread field for applications in research and development. Several microscopic examinations have been carried out to observe in situ solid – liquid transitions. The Hot Stage Microscope (HSM) is implemented successfully for the characterization of mould powders during heating (KÖLBL et al., 2008). It comprises a reflected light microscope and an electrically heated corundum furnace in a gas-tight furnace chamber on a tilting table. Fig. 1 (a) shows a polished section of an analyzed (SEM and EDX) mold powder including identified mineral phases and Fig. 1 (b) shows structural changes of these phases and advanced carbon burnout due to heat treatment. Further interesting measurements were performed to investigate the expansion of perlite in dependence of temperature by means of a HSM. Furthermore HSM and Double Hot Thermocouple Technique (DHTT) are used for the observation of the crystallization behaviour of slags. The crystal growth – especially of mold slags for the steel industry – is a key property for heat transfer in the mold. The setup of the DHTT allows to simulate the temperature gradient between steel strand and mold. It consists of a heatable furnace chamber with two additional heating units inside, a tripod with camera and lens, a controller and a computer for image recording. A pressed sample is molten between the heating units and stretched to a thin slag layer wherein the crystallization starts during cooling. The superior feature of the High Temperature Laser Scanning Confocal Microscope (HT-LSCM) is the very good image resolution at elevated temperatures. A sample inside a Pt-crucible is heated by the radiation of a halogen bulb and a blue laser beam scans the surface of the sample. Besides crystallization experiments, this device is able to measure dissolution rates of ceramic refractory particles in slags due to the high experimental temperature of up to 1700°C. That leads to an understanding about dissolution mechanisms and offers the opportunity for calculating effective diffusivities.

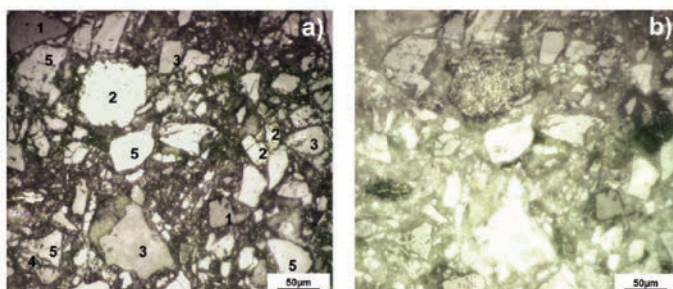


Figure 1. HSM representation of advanced carbon burnout a) Original structure, b) advanced carbon burnout. Phases: (1) fluorite, (2) graphite, (3) phosphorus slag, (4) albite, (5) glassy phase.

KÖLBL, N., HARMUTH, H. (2008): In 3rd Intern. Conf. Proc. Develop. Iron and Steelmaking, 73-81.

## NEW GEOCHEMICAL DATA FROM THE "ÜBERGANGSPORPHYROID" AT THE STYRIAN ERZBERG

Klammer, D.<sup>1</sup>, Anelli-Monti, I.<sup>1</sup> & Scholger, R.<sup>2</sup>

<sup>1</sup>Institute of Applied Geosciences, Graz University of Technology, Rechbauerstrasse 12, 8010 Graz, Austria

<sup>2</sup>Department Applied Geosciences and Geophysics, Montanuniversität, Peter-Tunner-Strasse 25,  
8700 Leoben, Austria  
e-mail: dietmar.klammer@tugraz.at

This study deals with rock samples of the so-called „Übergangsporphyr“ from a drill hole which was drilled in the Pressler Stöckl at the height of the Dreikönigs floor at the Styrian Erzberg as well as with typical rock samples of the Porphyroide complex (ANELLI-MONTI et al., 2014). The aim of this investigation was a geochemical study with the aim to obtain a more detailed knowledge of the rock matrix of the „Übergangsporphyr“.

The geochemical data of the „Übergangsporphyr“ show significant differences compared to those of the Porphyroide complex. Uniform geochemical profiles with respect to the main, minor, trace and rare earth elements are the characteristic of the studied Porphyroide samples. In contrast the geochemical data of the analysed samples of the „Übergangsporphyr“ are characterized by strongly divergent values. Among other things it shows based on Zr/Ti to Nb/Y ratios, which were used due to the strong alteration of these rocks for the characterisation and classification to a volcanic type (WINCHESTER & FLOYD, 1977) an extreme chemical differentiation. While the Zr/Ti to Nb/Y ratio of the Porphyroide samples show a uniformly rhyodacitic/dacitic composition however the values of the „Übergangsporphyr“ scatter from a rhyodacitic/dacitic to a rhyolitic to a trachyandesitic composition. A unique assignment to a distinct volcanic type is therefore not possible. Commonly the K/Rb ratio is an indicator of the degree of crystallization differentiation of a magma. In this case it is suitable as a proxy for representation the different rock chemistry and the strong differentiation within the rocks of the „Übergangsporphyr“. The K/Rb ratio in the Porphyroide samples reaches up to about 100 in the samples of the „Übergangsporphyr“, it is however on average at  $309 \pm 36$ . Moreover the presence of newly formed sericite as a result of a K-metasomatism is another characteristic of these rocks. This differentiation is superimposed by a clearly mapped and differently strong Ca-metasomatism which is reflected in a more or less intensive formation of calcite. In addition, an increasing transformation of the alkali feldspar crystals into microcline can be detected. The Na/K ratio confirmed this observation. The Na/K ratio of the Porphyroid is 0.4 while those of the „Übergangsporphyr“ are characterized by values of  $0.06 \pm 0.02$ . This phenomenon is due to the result of a metasomatic alteration under slightly elevated PT-conditions. Initial analyses of rare earth elements confirm at least partially the previous geochemical findings.

The geochemical investigation results indicates that the rock matrix of the „Übergangsporphyr“ in the area of the Styrian Erzberg is not only the result of retrogression of Porphyroid rocks but also external sources must be considered. Striking geochemical similarities to the series of the „Polsterquarz“ confirm this assumption.

ANELLI-MONTI, I., KLAMMER, D., SCHOLGER, R. (2014): Pangeo Austria 2014.

WINCHESTER, J.A., FLOYD, P.A. (1977): Chemical Geology, 20, 325-343.



**PETROLOGY AND MINERALIZATION OF THE SERPENTINE DEPOSIT,  
DULUTH COMPLEX MINNESOTA, USA**

Kleindienst, A.<sup>1</sup>, Mogessie, A.<sup>1</sup>, Raic, S.<sup>1</sup> & Zsolt, B.<sup>2</sup>

<sup>1</sup> Institute of Earth Sciences, University of Graz, Universitaetsplatz 2, 8010 Graz, Austria

<sup>2</sup> Hungarian Academy of Sciences, Institute for Nuclear Research, Bem tér 18/c, 4026 Debrecen, Hungary  
e-mail: alina.kleindienst@edu.uni-graz.at

The Serpentine Cu-Ni Deposit (South Kawishiwi Intrusion, SKI) is located at the western edge of the Duluth Complex (1.1 Ga) in northeastern Minnesota. The Duluth Complex is among the largest layered mafic intrusions of the world and extends over 5 700 km<sup>2</sup>. Reactivation of Archean structures during development of the North American Mid-continent Rift appears to control the emplacement and the regional distribution of the mafic intrusions.

The basal units at the Serpentine deposit are mainly troctolites, gabbros, norites and are underlain by the Virginia Formation, a metasedimentary hornfelsic unit with horizons of bedded pyrrhotite. These are again underlain by the Biwabik Iron Formation. Due to deformation all lithological units interfinger and inclusions of hornfelsic sections within the troctolites are common.

Sulfide mineralization appears to concentrate at the basal contact zones from troctolites to Virginia formation. Appearance of secondary sulfides is restricted to alteration zones of troctolites containing chlorite, serpentine and altered plagioclase. The dominant primary sulfide minerals found within the serpentine deposit are pyrrhotite, chalcopyrite, cubanite and pentlandite. Magnetite and ilmenite are common.

Detailed petrographic investigations (transmitted and reflected light microscopy) and electron microprobe analyses of sulfide phases as well as silicates and oxides from representative samples of the Serpentine drill core have been conducted along a stratigraphic profile. These preliminary investigations revealed the occurrence of arsenic-rich phases in the footwall hornfelsic Virginia Formation. These phases appear along rims of primary magmatic sulfide assemblages and are classified as di-arsenides in the system CoAs<sub>2</sub> – NiAs<sub>2</sub> – FeAs<sub>2</sub> and sulfarsenides of the cobaltite-gersdorffite solid solution series. Such textural relationships indicate the later formation of the Ni-Co-Fe-rich phases, and may suggest the involvement of a late stage hydrothermal fluid which reacted with the Virginia Formation, that is considered to be the source for the arsenic enrichment and the final formation of the arsenides and sulfarsenides.

**DURATION OF IGNEOUS ACTIVITY IN THE SESIA MAGMATIC SYSTEM AND IMPLICATIONS FOR HIGH-TEMPERATURE METAMORPHISM IN THE IVREA-VERBANO DEEP CRUST**

Klötzli, U.<sup>1</sup>, Sinigoi, S.<sup>2</sup>, Quick, J.<sup>3</sup>, Demarchi, G.<sup>2</sup>, Tassinari, C.<sup>4</sup>, Sato, K.<sup>4</sup> & Günes, Z.<sup>1</sup>

<sup>1</sup>Department for Lithospheric Research, University of Vienna, Althanstrasse 14, A-1090 Vienna, Austria

<sup>2</sup>Dipartimento di Matematica e Geoscienze, Università di Trieste, via Weiss 8, 34127 Trieste, Italy

<sup>3</sup>Southern Methodist University, Box 750240, Dallas, TX 75275-0240, USA

<sup>4</sup>Centro de Pesquisas Geocronológicas, Universidade de São Paulo, R. Lago 562, São Paulo 05508-080, Brazil  
e-mail: urs.kloetzli@univie.ac.at

Advection of heat by the intrusion of mantle-derived magma is frequently invoked as the driving force of high-temperature metamorphism in the deep crust. One of the best places worldwide to study and evaluate this process is the deep crustal section of the Ivrea-Verbania Zone of northwest Italy.

The Ivrea-Verbania Zone and the adjacent Serie dei Laghi constitute a virtually complete cross section of the Adriatic continental crust, which was intruded at different levels by coeval magmas of Permo-Carboniferous age, collectively referred to as the “Sesia Magmatic System”. At the deepest levels of the section, the relationship between magmatic underplating and granulite-facies metamorphism in the Ivrea-Verbania Zone can be studied.

The relationship between magmatism and granulite-facies metamorphism in this area has been addressed by a number of investigators, some of whom inferred that the Permo-Carboniferous intrusions provided the heat for partial melting of deep crustal rocks and their granulite-facies metamorphism, while others questioned this interpretation, noting the largest mafic intrusion cross cuts the regional structural and metamorphic gradient and is mantled by only a relatively thin metamorphic aureole.

We present new in-situ zircon U-Pb age data, which significantly extend the record of igneous activity in this crustal section, and which demonstrate that igneous pulses began intruding the deep and middle crust no later than 314Ma, an age corresponding to that inferred for regional granulite-facies metamorphism and predating by more than 20Ma the well-documented, main magmatic pulse at about 292 to 282Ma. A gap in age information from 316±3Ma to 276±4Ma, observed in the deep-crustal granulite-facies paragneisses overlaps a gap from ca. 314 to 283Ma between igneous and reset zircons in a closely associated mafic-ultramafic sill. On the other hand, the U/Pb zircon ages demonstrate an intrusive activity section upwards in the middle and upper crust during this time gap. We thus infer that prolonged maintenance of temperatures above the zircon stability field or zircon open-system behaviour in the granulite-facies paragneisses could explain the gap in zircon ages in those rocks. Viewed in this light, a gap in the geochronological record of high-grade terranes does not necessarily mean an absence of events, but instead may record the occurrence and prolonged duration of a thermal peak.

## PETROLOGY OF THE HEMATITE ORE ZONE, WALDENSTEIN, CARINTHIA

Knebl, U. G.<sup>1</sup>, Mogessie, A.<sup>1</sup> & Krenn, K.<sup>1</sup>

<sup>1</sup>Institute of Mineralogy and Petrology, University of Graz, Universitaetsplatz 2, A-8010 Austria  
e-mail: urs.knebl@edu.uni-graz.at

The hematite deposit at Waldenstein is located in the footwall of the Saualpe-Koralpe complex as part of the Eo-Alpine high pressure wedge (SCHMID et al., 2004). It is characterized as epigenetic hydrothermal vein-type ore mineralization (PROCHASKA et al., 1995), which occurs almost entirely in the embedded marble lenses and within layers of metapelites. These host rocks, which strike almost E-W and dip to the N, reflect a Paleozoic origin. In addition concordant and discordant late Variscan (Permian?) pegmatites occur. Petrographic and mineral chemical investigations indicate that alteration is associated with ore mineralisation. This alteration is defined by chloritisation and partial dolomitisation in the mineralized calcite marbles as well as pseudomorphosis of chlorite after biotite and garnet in the metapelites. Investigations on primary fluid inclusions (H<sub>2</sub>O-NaCl-CaCl<sub>2</sub> with ~ 24 wt. % salinity) in quartz, which is associated with hematite precipitation, display homogenisation temperatures from about 180 to 270 °C. On the basis of isochores, combined with oxygen isotopic composition temperatures of hematite, chlorite and quartz at about 300°C after (PROCHASKA et al., 1995), pressures of up to 2.4 kbar at maximum depths of ~7.5 km are proposed.

Secondary fluid inclusions (FIs) in the system CO<sub>2</sub>-H<sub>2</sub>O-NaCl are interpreted as fluid activity of the Lavantal Shear Zone and yield together with the primary aqueous FIs an isothermal decompressional path for the hematite mineralized area at Waldenstein.

PROCHASKA, W., POHL, W., BELOCKY, R., KUCHA, H. (1995): *Geologische Rundschau*, 84, 831-842.

SCHMID, S. M., FÜGENSCHUH, B., KISSLING, E., SCHUSTER, R. (2004): *Eclogae geologicae Helvetiae*, 97, 93-117.

## IN SITU OBSERVATION OF SLAG CRYSTALLIZATION

Kölbl, N.<sup>1</sup>, Harmuth, H.<sup>1</sup> & Kircher, V.<sup>1</sup>

<sup>1</sup>Montanuniversitaet Leoben, Chair of Ceramics (Peter Tunner Straße 5, 8700 Leoben, Austria)  
e-mail: nathalie.koelbl@unileoben.ac.at

In the field of metallurgy and ceramics, slags play an important role considering product quality and reliability during service. Therefore, an extensive characterization of their properties – in some cases especially the crystallization behavior – is necessary. Nevertheless, standardized investigation methods like the microscopic investigation of quenched samples after heat treatment with SEM/EDX do often not yield sufficient results concerning the crystallization behavior. Thus in situ observation methods have been implemented in order to enable the direct observation of slags during crystallization in dependence on the temperature profile according to operating conditions. Both the Hot Stage Microscope (HSM) and the Single Hot Thermocouple Technique (SHTT) are used for the in situ characterization of transparent or translucent slags. With the HSM the samples are heated within a platinum crucible in contact to an additionally inserted, loop shaped thermocouple to a maximum temperature and afterwards cooled with defined cooling rates. The crystallization is evaluated concerning location of the first crystals, their shape and growth direction (Fig. 1a). Using a Confocal Laser Scanning Microscope with a mirror furnace also the crystal growth rate or the dissolution rate of particles in the slag can be determined. If the slag composition changes during service due to reactions with the refractory material or the product, operation relevant additives are added to the original slag to estimate their impact on the crystallization behavior. Contrary to this type of investigation method, the SHTT allows the observation of a many times larger slag film area. Within a loop shaped electrically heated platinum wire a slag is stretched to a very thin layer at the maximum temperature. Then it is either cooled with defined cooling rates or otherwise quenched to a selected temperature, which is then kept constant until the end of the test. Here also roughly the shape of the crystals (dendrites, columnar, star like) are detected (Fig. 1b), but rather the crystallized area and the viable perimeter are evaluated in dependence on time in order to calculate the crystal growth rate. Both the HSM and the SHTT provide important information for the characterization, comparison and further development of slags.

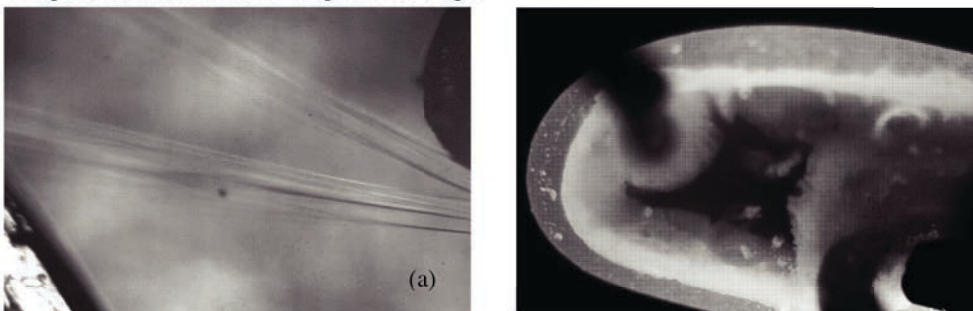


Figure 1. Images of a mould slag during crystallization received with (a) HSM and (b) SHTT.

CRYSTAL STRUCTURE OF  $\text{KSc}(\text{SO}_4)_2$ , ISOTYPIC WITH YAVAPAIITE  $[\text{KFe}(\text{SO}_4)_2]$ Kolitsch, U.<sup>1,2</sup><sup>1</sup>Mineralogisch-Petrographische Abteilung, Naturhistorisches Museum, Burgring 7, A-1010 Wien, Austria<sup>2</sup>Institut für Mineralogie und Kristallographie, Universität Wien, Althanstr. 14, A-1090 Wien, Austria

e-mail: uwe.kolitsch@nhm-wien.ac.at

$\text{KSc}(\text{SO}_4)_2$  was first synthesised by Perret and coworkers (PERRET & ROSSO, 1968; PERRET, 1970; COUCHOT et al, 1971) who suggested, based on an indexed powder XRD pattern and IR spectrum, that the compound probably crystallises in the structure type of yavapaiite  $[\text{KFe}(\text{SO}_4)_2]$ . As possible space groups,  $C2/m$ ,  $C2$  and  $Cm$  were given.

The previously unknown crystal structure of  $\text{KSc}(\text{SO}_4)_2$  was solved using crystals grown from an sulfuric acid aqueous solution of  $\text{K}_2\text{CO}_3$  and  $\text{Sc}_2\text{O}_3$ , and single-crystal X-ray intensity data (Nonius Kappa CCD, Mo- $K\alpha$ ,  $T \sim 20^\circ\text{C}$ ,  $2\theta_{\text{max}} = 65^\circ$ , crystal size  $0.03 \times 0.03 \times 0.05$  mm). The structure was refined in space group  $C2/m$ ,  $a = 8.501(2)\text{\AA}$ ,  $b = 5.266(1)\text{\AA}$ ,  $c = 7.960(2)\text{\AA}$ ,  $\beta = 93.47(3)^\circ$ ,  $V = 355.69(14)\text{\AA}^3$ , to  $R1(F) = 2.30\%$  (SHELX-97) for 37 parameters. The unit-cell parameters agree well with those reported earlier. Atomic coordinates and displacement parameters are given below. The structure contains sheets composed of corner-linked  $\text{ScO}_6$  octahedra ( $\langle \text{Sc}-\text{O} \rangle = 2.078\text{\AA}$ ) and  $\text{SO}_4$  tetrahedra ( $\langle \text{S}-\text{O} \rangle = 1.468\text{\AA}$ ), which are based on the kröhnkite-type chain motif (FLECK & KOLITSCH, 2003). These sheets are separated by  $^{100}\text{K}$  atoms [ $\text{K}-\text{O} = 2.8757(18) - 3.1904(12)\text{\AA}$ ].  $\text{KSc}(\text{SO}_4)_2$  is isotypic with yavapaiite  $[\text{KFe}(\text{SO}_4)_2]$  and  $\text{KV}(\text{SO}_4)_2$ , as well as eldfellite  $[\text{NaFe}(\text{SO}_4)_2]$  and other synthetic Na-compounds. In contrast,  $\text{KLu}(\text{SO}_4)_2$  and  $\text{KYb}(\text{SO}_4)_2$  have a different structure.

| Atom | <i>x</i>    | <i>y</i>  | <i>z</i>    | <i>U</i> <sub>eq</sub> |
|------|-------------|-----------|-------------|------------------------|
| K    | 0.0         | 0.0       | 0.5         | 0.02866(19)            |
| Sc   | 0.0         | 0.0       | 0.0         | 0.01112(13)            |
| S    | 0.36412(5)  | 0.0000    | 0.21251(6)  | 0.01119(13)            |
| O(1) | 0.23259(17) | 0.0000    | 0.0831(2)   | 0.0201(3)              |
| O(2) | 0.3128(2)   | 0.0000    | 0.3811(2)   | 0.0287(4)              |
| O(3) | 0.46172(13) | 0.2274(2) | 0.18469(13) | 0.0203(2)              |

| Atom | <i>U</i> <sub>11</sub> | <i>U</i> <sub>22</sub> | <i>U</i> <sub>33</sub> | <i>U</i> <sub>23</sub> | <i>U</i> <sub>13</sub> | <i>U</i> <sub>12</sub> |
|------|------------------------|------------------------|------------------------|------------------------|------------------------|------------------------|
| K    | 0.0362(4)              | 0.0333(4)              | 0.0167(3)              | 0.000                  | 0.0033(3)              | 0.000                  |
| Sc   | 0.0102(2)              | 0.0086(2)              | 0.0143(2)              | 0.000                  | -0.00150(16)           | 0.000                  |
| S    | 0.0116(2)              | 0.0092(2)              | 0.0129(2)              | 0.000                  | 0.00137(15)            | 0.000                  |
| O(1) | 0.0123(6)              | 0.0180(7)              | 0.0289(8)              | 0.000                  | -0.0067(6)             | 0.000                  |
| O(2) | 0.0324(9)              | 0.0376(10)             | 0.0173(7)              | 0.000                  | 0.0126(7)              | 0.000                  |
| O(3) | 0.0220(5)              | 0.0149(5)              | 0.0230(5)              | 0.0053(4)              | -0.0053(4)             | -0.0080(4)             |

COUCHOT, P., NGUYEN MINH HOANG, F. &amp; PERRET, R. (1971): Bull. Soc. Chim. Fr., 1971, 360-362.

FLECK, M. &amp; KOLITSCH, U. (2003): Z. Kristallogr., 218, 553-567.

PERRET, R. (1970): Bull. Soc. Fr. Minéral. Cristallogr., 93, 493-494.

PERRET, R. &amp; ROSSO, B. (1968): C. R. Acad. Sci., Paris, Sér. C, 266, 1038-1040.

## MINERALOGY AND GENESIS OF THE LAVRION ORE DEPOSIT: NEW INSIGHTS FROM THE STUDY OF ORE AND ACCESSORY MINERALS

Kolitsch, U.<sup>1,2</sup>, Rieck, B.<sup>3</sup> & Voudouris, P.<sup>4</sup>

<sup>1</sup>Mineralogisch-Petrographische Abteilung, Naturhistorisches Museum, Burgring 7, A-1010 Wien, Austria

<sup>2</sup>Institut für Mineralogie und Kristallographie, Universität Wien, Althanstr. 14, A-1090 Wien, Austria

<sup>3</sup>Schwenkgasse 12/4, 1120 Wien, Austria

<sup>4</sup>National and Kapodistrian University of Athens, Faculty of Geology & Geoenvironment, Dept. of Mineralogy and Petrology, Panepistimioupolis-Ano Ilisia, 15784 Athens, Greece  
e-mail: uwe.kolitsch@nhm-wien.ac.at

Ore samples collected underground and from surface outcrops and dumps in the Plaka, Kamariza and “porphyry hill” areas of the famous Lavrion polymetallic ore district (SKARPELIS, 2007; VOUDOURIS et al., 2008a,b, KOLITSCH et al. 2014) were studied by SEM-EDS, EPMA, XRD and optical methods, with a focus on skarn-sulphide mineralisations and vein-type ores. A large number of previously unreported species (including Te, REE, U and Th ones) were detected, mainly in polished sections. The results confirm the multistage, intrusion-related character of Lavrion (porphyry- and breccia-type mineralisations, Fe-rich skarn, carbonate-replacement Pb-Zn-Ag±Au ores, hydrothermal vein-type Pb-Zn-As-Sb-Ag ores). Several Te-minerals (altaite, rickardite and tellurobismuthite(?) or tsumoite(?)) occur as tiny (< 5 µm) pyrrhotite-hosted grains in skarn from the Adami 2 adit. Tetradymite, originally reported in the 1970s, was also confirmed. Cobaltite (up to 0,2 mm) is revealed to be the Co source for the erythrite at Plaka (145 and Adami 2 adits). The following Ni and Co minerals were observed at Plaka (145 adit): Cattierite, pentlandite(?), polydymite\*, siegenite, ullmannite\* and violarite\* (\*also at km 3). Vaesite was detected at km 3 and in Jean Baptiste. Anhedral, tiny freieslebenite occurs in the Adami 80 vein, and euhedral plagionite on galena crystals in a fluorite-dolomite-galena-sphalerite vein (Plaka 145).

The following accessory and rock-forming minerals were identified as well (from Adami 2 adit if not noted otherwise): Allanite-(Ce) (also Hilarion), andradite, brannerite (first primary U mineral; Hilarion), chamosite, ferroactinolite, laumontite, marialite (Adami 80), monazite-(Ce) (porphyry hill, in molybdenite sample), paragonite (Clemence), (primary) stolzite (Adami 80), strontianite (from baryte vein, Adami 80), synchysite-(Ce) (Hilarion), thorite (first Th mineral; Hilarion), vesuvianite (Adami 80), wollastonite (Hilarion), xenotime-(Y) (porphyry hill, in molybdenite sample). Secondary(?) zavaritskite (BiOF) was detected as rims around native bismuth in the Hilarion Bi-Au-Sb mineralisation studied by SOLOMOS et al. (2004). Numerous newly determined secondary species will be reported elsewhere.

KOLITSCH, U., RIECK, B., BRANDSTÄTTER, F., SCHREIBER, F., FABRITZ, K. H., BLAß, G. & GRÖBNER, J. (2014): Mineralien-Welt 25 (1), 60-75.

SKARPELIS, N. (2007): N. Jb. Mineral. Abh., 183, 227-249.

SOLOMOS, C., VOUDOURIS, P. & KATERINOPOULOS, A. (2004): Bull. Geol. Soc. Greece 34, 387-396.

VOUDOURIS, P., MELFOS, V., SPRY, P. G., BONSALE, T., TARKIAN, M. & ECONOMOU-ELIOPOULOS, M. (2008a): Mineral. Petrol., 93, 79-110.

VOUDOURIS, P., MELFOS, V., SPRY, P.G., BONSALE, T.A., TARKIAN, M. & SOLOMON, Ch. (2008b): Mineral. Petrol., 94, 85-106.



**ARDENNITE-(AS), ARDENNITE-(V), GASPARITE-(CE) AND CHERNOVITE-(Y):  
FIRST RESULTS OF A MINERALOGICAL STUDY OF THE  
METARADIOLARITE-HOSTED MANGANESE ORE MINERALISATIONS IN THE  
FUCHSSEE AREA, RADSTADT TAUERN, SALZBURG, AUSTRIA**

Kolitsch, U.<sup>1,2</sup>, Schachinger, T.<sup>3</sup> & Bernhard, F.<sup>4</sup>

<sup>1</sup>Mineralogisch-Petrographische Abteilung, Naturhistorisches Museum, Burgring 7, A-1010 Wien, Austria

<sup>2</sup>Institut für Mineralogie und Kristallographie, Universität Wien, Althanstr. 14, A-1090 Wien, Austria

<sup>3</sup>Akkonplatz 5/20-21, 1150 Wien, Austria

<sup>4</sup>Institut für Erdwissenschaften, Bereich Mineralogie und Petrologie, Karl-Franzens-Universität Graz,  
Universitätsplatz 2, A-8010 Graz

e-mail: uwe.kolitsch@nhm-wien.ac.at

In the Fuchssee area (WNW of Tweng im Lungau, Radstadt Tauern) manganese ore mineralisations are hosted by folded Jurassic metaradiolarites (Hochfeind Nappe, Lower Austroalpine unit; TOLLMANN, 1964; HÄUSLER, 1988). The following minerals were reported previously: "alurgite", apatite, braunite, jacobsonite, piemontite, rhodonite, roméite and spessartine (MEIXNER, 1935, 1951). A detailed, ongoing re-investigation of the layered, lenticular to nodular mineralisations by SEM-EDS and single-crystal X-ray methods led to the identification of three arsenate minerals new for Austria: ardennite-(As), ardennite-(V) and gasparite-(Ce). (We note that ardennite-(As) was also recently identified by us from the Navis creek, Navis valley, North Tyrol.) The following other species were confirmed as well (in alphabetical order): albite, baryte, braunite, calcite, celestine, cerianite-(Ce), chernovite-(Y), clinocllore, coronadite, cryptomelane-group minerals (often Ca-dominant), dravite (Cu-bearing), fluorapatite, hematite, kretznichite(?), kutnohorite, magnesioriebeckite(?), manganocummingtonite, monazite-(Ce) (As-rich), muscovite, piemontite (in part REE-bearing), pyrolusite, pyrophanite, pyroxmangite(?), rhodochrosite, rhodonite, senaite(?) (Mn-rich), spessartine, a stilpnomelane-group mineral, tephroite, titanite, quartz. Many mineral components show distinct zoning which reflects at least two tectonometamorphic episodes involving fluid activity. For example, fluorapatite has large As-enriched cores. It is worthy noting that baryte and celestine, both with strongly variable Ba:Sr ratios, were found as tiny grains within braunite aggregates or quartz, attesting to the hydrothermal origin of the ore. Cerianite-(Ce) also occurs as tiny inclusions within braunite.

Selected details on these mineralisations, which are similar to some of the As-rich manganese ore mineralisations in Liguria, Italy (CABELLA et al., 1999; MARCHESINI & PAGANO, 2001), will be presented and discussed.

CABELLA, R., LUCCHETTI, G. & MARESCOTTI, P. (1999): *Can. Mineral.*, 37, 961-972.

GÜNTHER, W. & TICHY, G. (1979): *Mitt. Ges. Salz. Landeskunde*, 119, 351-373.

HÄUSLER, H. (1988): *Jb. Geol. B.-A.*, 131, 21-125.

MARCHESINI, M. & PAGANO, R. (2001): *Mineral. Record*, 32, 349-379; 415.

MEIXNER, H. (1935): *N. Jb. Mineral., Beil. Bd.*, 69, A, 500-514.

MEIXNER, H. (1951): *N. Jb. Mineral., Mh.*, 8, 174-178.

TOLLMANN, A. (1964): *Mitteilungen der Geologischen Gesellschaft in Wien*, 57, 49-56.

**PETROLOGY AND GEOCHEMISTRY OF THE LITHOSPHERIC MANTLE  
BENEATH GOBERNADOR GREGORES, SOUTHERN PATAGONIA, ARGENTINA.  
EVIDENCE OF MODAL METASOMATISM**

Kolosova-Satlberger, O.<sup>1</sup>, Ntaflou, Th.<sup>1</sup> & Bjerg E.<sup>2</sup>

<sup>1</sup>University of Vienna, Austria

<sup>2</sup>Universidad Nacional del Sur, Bahía Blanca, Argentina  
e-mail: kolosova@gmx.net

Mantle xenoliths from Gobernador Gregores, southern Patagonia are spinel- lherzolites, harzburgites and wehrlites. Composite xenoliths consisting of websterites, olivine-websterites and spinel-lherzolites or harzburgites are present as well.

The lithospheric mantle beneath Gobernador Gregores region was affected by multiple modal metasomatic events as can be inferred from the presence of amphibole, phlogopite and apatite. The existence of amphibole as inclusion in clinopyroxene suggests dehydration reaction of peridotites, which previously experienced modal metasomatism. This textural evidence records the earliest detectable metasomatic event.

A second distinct modal metasomatic event consists of disseminated up to 6mm in diameter coarse grained amphiboles (100\*mg#=89.9) which show breakdown reactions and pseudomorphic replacement by glass and fine grained second generation of olivine, clinopyroxene and spinel. The intensity of the breakdown reaction is variable. In most cases amphibole occurs as a relict within these pseudomorphs. However, melt pockets of up to 10mm in diameter are abundant and are irregular in shape. They contain the same minerals as the pseudomorph clearly indicating amphibole breakdown because remnants of it were found enclosed by second generation clinopyroxene. Phlogopite, where present, experienced similar breakdown reactions.

Some harzburgites and composite xenoliths reveal a further metasomatic event: peridotite, enriched in orthopyroxene (mainly orthopyroxenite veinlets, rare websterite), suggests interaction with a silica-saturated melt. Veinlets up to 1 mm thick consisting mainly of second generation fine grained orthopyroxene (200-700 microns in diameter) propagate intergranularly along coarse grained matrix of olivine and orthopyroxene. Other minerals found in the veinlets are amphibole, phlogopite and clinopyroxene. The primary phases (ol, opx) exhibit light to moderate intracrystalline deformation, such as undulose extinction, kink bands etc., whereas the second generation orthopyroxenes are strain-free, indicating that the metasomatic event took place after the deformation. Absence of glass suggests that the metasomatic event took place long before their entrainment in the ascending magma.

Textural evidences that show dissolution of orthopyroxene and formation of second generation olivine, clinopyroxene, spinel and glass, exhibit a third evident metasomatic event. This is the result of interaction with a silica undersaturated melt. Since this metasomatic event affected both, primary and secondary opx it should be considered as the very last event.

Both dissolution of orthopyroxene and breakdown of amphibole and phlogopite took place en route since glass could not survive for long time in the lithosphere and would react with the matrix minerals.

## EXPERIMENTAL STUDY ON THE ARAGONITE-STRONTIANITE SOLID SOLUTION SERIES AT AMBIENT TEMPERATURE

Konrad, F.<sup>1</sup>, Mavromatis, V.<sup>1</sup>, Baldermann, A.<sup>1</sup> & Dietzel, M.<sup>1</sup>

<sup>1</sup>Institute of Applied Geosciences, Graz University of Technology, Rechbauerstrasse 12, 8010 Graz, Austria  
e-mail: florian.konrad@tugraz.at

The incorporation of Sr as trace element into naturally occurring aragonites, e.g. in corals and travertine, is used as a proxy for determining paleo temperatures and environmental changes. Owing to the isostructural framework of aragonite and strontianite, the incorporation of Sr ions into aragonite is characterized by a partitioning coefficient ( $D_{Sr}$ ) close to 1. However, the mechanisms of temperature-dependent foreign cation incorporation and whether biological/vital effects are influencing the Sr uptake and consequently modifying the elemental partitioning behaviour are not yet clear. Despite the fact that aragonite and strontianite form a solid solution to date only a few experimental studies exist, where the complete aragonite-strontianite solid solution series and subsequently the partitioning of Sr into aragonite have been investigated systematically at ambient temperatures.

Here, we present a new set of precipitation experiments encompassing the complete  $Ca_xSr_{(1-x)}CO_3$  solid solution performed at 25°C and 1atm  $CO_2$  using a mixed flow reactor modified after MAVROMATIS et al. (2013) where precipitation occurs at steady-state conditions. Contradictory to previous studies, which found miscibility gaps, our results indicate the formation of a complete solid solution series, as evidenced by the continuous peak shift over the compositional range of the solids derived from single phase XRD-patterns. The unit-cell parameters of the precipitated  $Ca_xSr_{(1-x)}CO_3$  minerals, based on Le Bail fitting, are increasing linearly as a function of  $(Sr/Ca)_{solid}$  ratios determined by ICP-OES and therefore fulfilling Vegard's law.

The obtained results shed light on the formation of strontianites-aragonites and bidirectional cation incorporation in natural settings, as well as on the thermodynamic behaviour of this binary system during diagenetic alteration. Further work on stable isotopes (O, Ca, Sr) is going to verify the mechanisms controlling isotope fractionation between solid and aqueous medium.

MAVROMATIS, V. GAUTIER, Q. BOSCH, O. SCHOTT, J. (2013): *Geochim. Cosmochim. Acta*, 114, 188-203.

**PETROLOGY AND GEOCHEMISTRY OF APATITE±WHITLOCKITE-BEARING  
PERIDOTITE MANTLE XENOLITHS FROM SOUTHERN LAOS**

Konzett, J.<sup>1</sup>, Hauzenberger, C. A.<sup>2</sup>, Krenn, K.<sup>2</sup>, Stalder, R.<sup>1</sup>, Gröbner K.<sup>1</sup>, Sieberer A.-K.<sup>1</sup>,  
Hoang, N.<sup>3</sup> & Khoi, N.N.<sup>4</sup>

<sup>1</sup>Institute of Mineralogy and Petrography, University of Innsbruck, Innrain 52, A-6020 Innsbruck, Austria

<sup>2</sup>Institute of Earth Sciences, Karl-Franzens-University Graz, Universitätsplatz 2, 8010, Graz, Austria

<sup>3</sup>Institute of Geological Sciences, Vietnam Academy of Science & Technology

84 Chua Lang, Dong Da, Hanoi, Vietnam

<sup>4</sup>Department of Geology, Hanoi University of Science, 334 Nguyen Trai, Thanh Xuan, Hanoi, Vietnam

e-mail: juergen.konzett@uibk.ac.at

Cenozoic basalts are widespread throughout Southeast Asia and form what is called a “diffuse igneous province” consisting of tholeiites and late-stage, small-volume alkali basalts. We report the results of a petrological and geochemical study of a suite of spinel-lherzolites and ortho/clino-pyroxenites sampled by nepheline±leucite-bearing alkali basalts of the Bolaven Plateau/southern Laos. Lherzolites (ol+opx+cpx+sp+FeNi-sulfide) and pyroxenites (opx+cpx+FeNi-sulfide) show evidence for cryptic or modal metasomatism characterized by a strong enrichment of Li in cpx and opx with respect to ol (cryptic) and by the appearance of apatite rarely associated with minor phlogopite ± pargasite. The pargasites are in part unusually P-rich with up to 0.13wt% P<sub>2</sub>O<sub>5</sub>. Two compositional types of apatite are present: (1) apatite characterized by low P<sub>2</sub>O<sub>5</sub> (37.9-41.0wt%) and low analytical totals (93.8-97.4wt%) combined with high Na<sub>2</sub>O (0.9-1.6wt%) indicative of a significant type-A carbonate-apatite component and (2) apatite with high P<sub>2</sub>O<sub>5</sub> (40.5-42.4wt%) and high analytical totals (97.7-100.9wt%) combined with low Na<sub>2</sub>O (0.3-0.7wt%). Low-P<sub>2</sub>O<sub>5</sub> apatites show a restricted range in F and Cl (0.2-0.9wt% F, 0.6-1.6wt% Cl) compared to high-P<sub>2</sub>O<sub>5</sub> apatites (0.3-3.1wt% F, 0.3-4.1wt% Cl). One apatite-bearing sp-lherzolite sample (VJ40-5-2) contains whitlockite-merrillite [Ca<sub>18</sub>Mg<sub>2</sub>(PO<sub>4</sub>)<sub>12</sub>[PO<sub>3</sub>(OH)]<sub>2</sub>-Ca<sub>18</sub>Na<sub>2</sub>Mg<sub>2</sub>(PO<sub>4</sub>)<sub>14</sub>] intergrown with apatite together with phlogopite+pargasite. Whitlockite-merrillite is extremely rare in mantle rocks and has been known so far from only one locality in Siberia where its formation was ascribed to a distinct type of ±anhydrous REE-metasomatism (IONOV et al., 2006). In the sample from Laos, whitlockite-merrillite is always intergrown with apatite and was unambiguously identified using EMPA and micro-Raman spectroscopy. It contains 3.5-3.9wt% MgO and 2.4-3.1wt% Na<sub>2</sub>O, respectively. Thermometry of this sample yields 900-950°C for 1.5GPa. Sample VJ40-5-2 contains abundant pure CO<sub>2</sub> fluid inclusions trapped in pyroxenes and olivine. Maximum fluid densities of pyroxene-inclusions of 1.21-1.30g/cm<sup>3</sup> indicate upper mantle trapping pressures of ~1.8-2.0GPa. Fluid densities measured for inclusions in olivine are in the range 0.8-1.2g/cm<sup>3</sup>. In addition to pure CO<sub>2</sub>, pure H<sub>2</sub>O with a density of 0.88g/cm<sup>3</sup> was found in a single fluid inclusion trapped in pyroxene. H<sub>2</sub>O contents of ~250ppm and ~170ppm in clino- and orthopyroxene measured with FTIR provide independent evidence for interaction of the VJ40-5-2 assemblage with a H<sub>2</sub>O-bearing fluid.

IONOV, D.A., HOFMANN, A.W., MERLET, C., GURENKO, A.A., HELLEBRAND, E., MONTAGNAC, G., GILLET, P., PRIKHODKO, V.S. (2006) Earth. Planet. Sci. Lett. 244, 201-217.

## CRYSTAL-PLASTIC DEFORMATION OF ZIRCON AND ITS EFFECT ON MICROCHEMISTRY AND GEOCHRONOLOGY

Kovaleva, E.<sup>1,2</sup>, Klötzli, U.<sup>1</sup> & Habler, G.<sup>1</sup>

<sup>1</sup>Department of Lithospheric Research, University of Vienna, Althanstrasse 14, UZA II, 1090, Vienna, Austria

<sup>2</sup>Department of Geology, University of the Free State, Nelson Mandela Drive 205, 9300, Bloemfontein, South Africa

The research is focused on zircon grains derived from high-temperature ductile shear zones from the western Tauern Window (Eastern Alps), the Ivrea-Verbano zone (Southern Alps) and the Ötztal-Stubai crystalline complex (Eastern Alps). Zircon from the shear zones has been affected by crystal-plastic deformation. We have investigated plastically deformed zircon grains in-situ with secondary electron (SE) imaging, forward-scatter electron (FSE) imaging, electron backscatter diffraction (EBSD), field emission gun electron microprobe analyzer (FEG-EMPA) and nano-scale secondary ion mass spectrometry (NanoSIMS).

We demonstrate that trace elements in zircon are being re-distributed in most of the crystals showing deformation microstructures. Low angle boundaries and distorted lattice domains are usually depleted in Y, Yb (HREE), U, Pb and enriched in Ce and Nd (LREE). Thus we conclude that the behaviour of trace elements in crystal-plastically strained crystal lattice is mainly controlled by the respective atomic radii. For Ti, Hf and P the re-distribution seemingly is more erratic and may primarily depend on the availability of these elements in the host matrix.

Measured age of zircons may be greatly affected by crystal-plastic deformation. Lattice distortion can cause lead isotope re-distribution and, therefore, relative rejuvenation or ageing of zircon domains:

a) Relative ageing of the zircon U-Pb system was observed in highly deformed rim domains, where a dense network of low- and high-angle boundaries is developed. The aging effect can be explained by contamination of the crystal lattice by common lead from grain exterior sources.

b) Relative rejuvenation of the U-Pb system is attributed to weakly deformed zircon domains in the grain interior. Invoked processes can either be an internal re-distribution of U and Pb or the simple loss of radiogenic Pb from the crystal lattice.

In both cases the degree of age shift is proportional to the dislocation density. The knowledge of the deformation state of a zircon crystal lattice and the understanding of the underlying deformation processes is thus essential to interpret measured U-Pb systematics from strained zircon. This on the other hand allows linking U-Pb ages in crystal-plastically deformed zircon to high-temperature ductile shear zone activity and thus may provide a potential to directly date high-temperature deformation events.

**NEW ISOTOPE (U-Pb, Lu-Hf,  $^{87}\text{Sr}/^{86}\text{Sr}$ ) AND TRACE ELEMENT DATA FROM  
FELBERTAL SCHEELITE DEPOSIT: CONSTRAINTS ON EARLY  
CARBONIFEROUS TUNGSTEN MINERALIZATION**

Kozlik, M.<sup>1</sup>, Raith, J.G.<sup>1</sup> & Gerdes, A.<sup>2</sup>

<sup>1</sup> Montanuniversität Leoben, Chair of Resource Mineralogy, Peter Tunner Straße 5, 8700, Leoben, Austria

<sup>2</sup> University of Frankfurt, Institute of Geosciences, Mineralogy, Altenhöferallee 1, 60438 Frankfurt, Germany  
e-mail: michael.kozlik@unileoben.ac.at

Combined in-situ U-Pb, Lu-Hf and trace element data on zircons from the W-mineralized K1-K3 orthogneiss in the Felbertal scheelite deposit provide new constraints on the genetic link between the Early Carboniferous K1-K3 orthogneiss and scheelite mineralization at Felbertal. The isotopic record of zircon from the mineralized K1-K3 orthogneiss is compared to that from the barren Felbertauern augengneiss. In addition, the Sr isotope systematics of scheelite were studied and compared with  $^{87}\text{Sr}/^{86}\text{Sr}$  ratios of magmatic and metamorphic apatite from the K1-K3 orthogneiss. The new U-Pb concordia ages of zircons from four samples of the K1-K3 orthogneiss and one sample of a related aplitic gneiss confine the emplacement period of the highly fractionated granitic melt between 341.0 Ma and 336.6 Ma. The corresponding apparent  $\epsilon\text{Hf}_i$  are constantly below the chondritic values and range from -7.6 to -4.9, indicating a crustal source. Both the U-Pb and the Lu-Hf data of zircon are comparable to those from the Felbertauern augengneiss; the latter yielding a U-Pb concordia age of  $338.5 \pm 1.3$  Ma and apparent  $\epsilon\text{Hf}_i$  values between -6.8 and -5.3. In addition to geochemical whole rock data, the U-Pb and Lu-Hf zircon data support a common petrogenetic evolution of the W-mineralized K1-K3 orthogneiss and the barren Felbertauern augengneiss. Based on cathodoluminescence images and trace element compositions, magmatic and hydrothermal zircon can be distinguished in the K1-K3 orthogneiss. Characteristic for magmatic zircons are systematically decreasing Zr/Hf ratios and increasing trace element concentrations (U, W, Nb, Ta, Hf) from core to rim. In contrast, hydrothermal zircons feature anomalous high B concentrations and the highest level of trace element enrichment, indicative for crystallization in the presence of a metal- and volatile-rich magmatic-hydrothermal fluid/vapour phase related to the crystallization of the K1-K3 orthogneiss protolith. These fluids also caused an incongruent release of  $^{87}\text{Sr}$  from Rb-rich minerals (e.g. biotite, muscovite) during interaction of the mineralizing fluid with the various Early Palaeozoic host rocks of the Habach Complex. Magmatic apatite from the K1-K3 orthogneiss re-equilibrated with  $^{87}\text{Sr}$ -rich fluids, what is reflected in highly radiogenic and considerable scattering  $^{87}\text{Sr}/^{86}\text{Sr}$  ratios of apatite (0.7204-0.7451). The inhomogeneous Sr isotope composition is already typical for the early magmatic-hydrothermal scheelite generations (Scheelite 1 and 2) with  $^{87}\text{Sr}/^{86}\text{Sr}$  ratios ranging from 0.7208 to 0.7642 and from 0.7072 to 0.7683, respectively. Metamorphic Scheelite 3, formed by recrystallization and local mobilization of older scheelite, is characterized by even more radiogenic  $^{87}\text{Sr}/^{86}\text{Sr}$  ratios between 0.74331 and 0.80689, matching the  $^{87}\text{Sr}/^{86}\text{Sr}$  ratios of the metamorphic apatite generation (0.7456-0.7794). The further increase in  $^{87}\text{Sr}/^{86}\text{Sr}$  ratios in Scheelite 3 and apatite rims is attributed to Young Alpine (?) metamorphic recrystallization and redistribution of  $^{87}\text{Sr}$  in metamorphic fluids.



**INVESTIGATING NEW APPROACHES FOR (BIO-) GEOCHEMICAL  
EXPLORATION OF CONCEALED METAL DEPOSITS:  
ENHANCED MOBILIZATION AND FRACTIONATION OF ‘IMMOBILE’ HIGH  
FIELD STRENGTH ELEMENTS (REY; Zr, Hf, Th, U) BY LEACHING IN  
PRESENCE OF BIOGENIC LIGANDS (SIDEROPHORES)**

Kraemer, D.<sup>1</sup> & Bau, M.<sup>1</sup>

<sup>1</sup> Earth and Environmental Sciences, Jacobs University Bremen, Campus Ring 1, 28759 Bremen, Germany  
e-mail: d.kraemer@jacobs-university.de

We present results of batch leaching experiments conducted with different rocks and ores in the presence of the biogenic reagent desferrioxamine B (DFOB). DFOB belongs to a group of organic molecules known as siderophores (or metallophores) which are exuded by a range of microorganisms, plants and fungi to cope with the scarcity of bioavailable iron in their habitat and which constitute one of the most important groups of biogenic ligands in many natural environments. In oxidized systems, Fe is trivalent and thus is immediately bound to insoluble oxyhydroxide structures and hence removed from the dissolved pool. Hence, under modern atmospheric conditions Fe is not available as a trace nutrient for organisms, although almost all living organisms and plants need Fe as an essential micronutrient. Therefore, specific compounds such as siderophores are synthesized and excreted to the environment by plants, microbes and fungi alike to facilitate the dissolution of specific minerals and to complex liberated trace metals. It was shown that DFOB not only forms highly stable complexes with Fe<sup>3+</sup>, but they also significantly complex other metal ions, some of which are considered as toxic at higher concentrations, but at the same time are needed in trace concentrations as essential nutrients.

Thus, besides a high affinity for Fe<sup>3+</sup>, DFOB is also very efficient in binding metal ions with high ionic potentials, i.e. high field strength elements (HFSE). HFSE such as the rare earths and yttrium (REY), the geochemical twins Zr and Hf and the element pair Th and U are considered rather immobile during low-temperature water rock interaction. We investigated the impact of DFOB on the mobilization of these HFSE in low-temperature environments and show that DFOB significantly enhances the mobility of REY, Mo, Zr, Hf, Th and U. We also show that Ce is decoupled from its light REY neighbors and that U is strongly fractionated from Th. The REY patterns obtained in the leachates are apparently characteristic for leaching in presence of siderophores.

Our data show that biogenic compounds such as siderophores are actively promoting the mobilization of these ‘immobile’ trace elements. Metal-siderophore complexes are enzymatically reduced at the cell membranes and the metal (signature) may be incorporated into the organism and/or plant. Due to the misbelief of strictly ‘immobile’ HFSE, many studies on geochemical exploration involving plants and fungi as indicator plants/organisms lack the consideration of HFSE. However, “biology” is apparently able to bind and mobilize such elements – even from igneous rocks which have rather low HFSE concentrations. This gives rise to the possibility that the HFSE signature of plants and fungi may be able to indicate the occurrence of concealed ore deposits like those of REY, Sc, Zr, Hf, Mo, U and others.

**(BIO-) LEACHING OF OXIDIZED PGE ORES: ENHANCING PLATINUM AND PALLADIUM EXTRACTION USING BIOGENIC AND INORGANIC LIXIVIANTS**

Kraemer, D.<sup>1</sup>, Junge, M.<sup>2</sup>, Bau, M.<sup>1</sup> & Oberthür, T.<sup>2</sup>

<sup>1</sup>Earth and Environmental Sciences, Jacobs University Bremen, Campus Ring 1, 28759 Bremen, Germany

<sup>2</sup>Federal Institute for Geosciences and Natural Resources, Stilleweg 2, 30655 Hannover, Germany

e-mail: d.kraemer@jacobs-university.de

We present data on the mobilization of platinum (Pt) and palladium (Pd) from oxidized platinum-group element (PGE) ores of the Main Sulphide Zone (MSZ) of the Great Dyke, Zimbabwe, and of the Platreef, Bushveld Complex, South Africa.

The *pristine* ('fresh', unweathered) material mined at those sites is treated following conventional metallurgical practice by – inter alia – froth flotation and subsequent matte smelting. Recoveries of Pt and Pd of >85% are common.

However, the Great Dyke in Zimbabwe also hosts about 160-250 Mt of *oxidized* MSZ material with average grades of 3 to 5 ppm Pt+Pd. The resources of oxidized material available in the South African Bushveld may even exceed those of the Great Dyke oxidized ores. The complex mineralogical composition of the oxidized PGE ores is challenging and thus, processing of the surficial, intensely weathered ('oxidized') ores is uneconomic at present (recoveries mostly <<50%, mainly caused by naturally floating gangue). Currently no (hydro)\_metallurgical technology is available that yields sufficiently high (hence economic) recovery rates for oxidized PGE ores. Therefore, in spite of the considerable resources available, oxidized PGE ores are currently not mined and processed.

In order to tackle the processing issue, leaching experiments with organic and inorganic lixivants were conducted and two organic leaches that selectively mobilize either Pt or Pd from the bulk oxidized ore material with only minimal amounts of base metals co-mobilized were developed. One of the tested lixivants is produced by a wide range of organisms and plants, enabling the option of potential bioleaching efforts, whilst the other is a non-toxic organic food additive, easily available and rather inexpensive. Additionally, leach processes based on inorganic lixivants were tested and it was found that these mobilize almost all of the Pt and Pd in one leaching step whilst base metal liberation including Ni is restricted.

Our results show that leaching with either inorganic or organic chemical reagents is a highly efficient option in making these extremely valuable PGE deposits profitable for the mining industry. Bioleaching and heap leaching of vast amounts of easily accessible and to some parts already stockpiled ore represent promising future techniques in the processing chain of (oxidized) PGE deposits.

Our research efforts also indicate that Pt and Pd can be extracted from the bulk oxidized ore separately in two subsequent leaching stages using biogenic reagents. Currently, our studies aim at the optimization of the leaching stages, potential up-scaling, simulation of heap leaching situations, and the recovery of platinum-group metals from multi-element solutions containing inorganic and/or organic reagents.

## MINERALOGICAL INVESTIGATIONS OF GRAPHITE AT THE MICRO- AND NANO-SCALE

Lämmerer, W.<sup>1</sup>, Rantitsch, G.<sup>2</sup>, Melcher, F.<sup>2</sup>, Fisslthaler, E.<sup>3</sup>, Mitsche, St.<sup>3</sup>, Twrdy, G.<sup>4</sup> & Flachberger, H.<sup>1</sup>

<sup>1</sup> Chair of Mineral Processing, Department Mineral Resources Engineering, Montanuniversität Leoben, Franz-Josef-Straße 18, 8700 Leoben, Austria

<sup>2</sup> Chair of Geology and Economic Geology, Department Applied Geosciences and Geophysics, Montanuniversität Leoben, Franz-Josef-Straße 18, 8700 Leoben, Austria

<sup>3</sup> Graz Centre for Electron Microscopy, Steyrergasse 17, 8010 Graz, Austria and Institute for Electron Microscopy and Nanoanalysis, Graz University of Technology, Steyrergasse 17, 8010 Graz, Austria

<sup>4</sup> Grafitbergbau Kaisersberg GmbH, Bergmannstraße 39, 8713 St. Stefan bei Leoben  
e-mail: wolfgang.laemmerer@unileoben.ac.at

The use of natural graphite as high quality product is controlled by raw material parameters such as morphology, grain size distribution, crystallite size, surface area, ash content etc. The structural properties of graphite influence both, the processing technique of the raw materials, as well as the industrial use due to the properties of refined products. The knowledge of the relevant raw material properties is therefore of great interest.

Graphite results from organic metamorphism of carbonaceous materials (CM), improving the structural ordering of the carbon lattice in three dimensions. Due to the gradual nature of the controlling coalification and graphitization processes, different transitional products (anthracite, meta-anthracite, semi-graphite, and graphite) are discriminated (KWIECINSKA & PETERSEN, 2004). The significant heterogeneity of natural graphitic matter on the micro- and nano-scale, however, complicates the clear diagnosis of the implicated CM. To explore the structural change of natural CM, graphite samples from several deposits around the world were investigated by a multi-methodological approach, including Raman Spectroscopy, X-ray Diffraction, Scanning Electron Microscopy, and High-Resolution Transmission Electron Microscopy. The results demonstrate clear differences between the semi-graphite of Kaisersberg (Austria, RANTITSCH et al., 2004) to low-ordered graphites from Huan Lutang (China) and Korea and to well-ordered graphites from the Bohemian Massif (Austria), Mozambique, Norway, Brazil, Ukraine, Russia, China, Mongolia, Sri Lanka and Madagascar. The differences are explained by a different metamorphic rank of the host rocks and by the different type of metamorphism (regional metamorphism, fluid deposition, contact metamorphism). As a result, we propose the application of Raman Spectroscopy as a quick and easy-to-use tool to objectively discriminate the different types of CM.

This work is part of the research project "Innovative Graphite", which is a research-cooperation between the chair of Mineral Processing and the chair of Geology and Economic Geology of the Montanuniversität Leoben and Grafitbergbau Kaisersberg GmbH, funded by the Forschungsförderungsgesellschaft (FFG).

KWIECINSKA, A B., PETERSEN, H.I. (2004): *Int. J. Coal Geol.*, 57, 99-116.

RANTITSCH, G., GROGGER, W., TEICHERT, Ch., EBNER, F., HOFER, Ch., MAURER, E.-M., SCHAFFER, B., TOTH, M. (2004): *Int. J. Earth Sci.*, 93, 959-973.

# INVESTIGATING CORUNDUM/SPINEL/PERICLASE INTERFACE MIGRATION IN THE ATOMIC SCALE VIA SCANNING TRANSMISSION ELECTRON MICROSCOPY

Li, C.<sup>1</sup>, Jerabek, P.<sup>2</sup>, Götze, L. C.<sup>3</sup>, Pennycook, T. J.<sup>4</sup>, Mangler, C.<sup>4</sup>, Habler, G.<sup>1</sup> & Abart, R.<sup>1</sup>

<sup>1</sup>Department of Lithospheric Research, University of Vienna, Althanstrasse 14, 1090 Vienna, Austria

<sup>2</sup>Faculty of Science, Charles University in Prague, Albertov 6, 12843 Prague, Czech Republic

<sup>3</sup>Institute of Geological Sciences, Freie Universität Berlin, Malteserstr. 74-100, 12249 Berlin, Germany

<sup>4</sup>Faculty of Physics, University of Vienna, Boltzmannngasse 5, 1090 Vienna, Austria

e-mail: chen.li@univie.ac.at

One common pathway of mineral formations is the growth of a new mineral at the interface between two reactant minerals, so called reaction rim growth. In order to understand how the two original minerals react, form a new phase, and spread the reaction interfaces further, it is essential to know the atomic structure of the interfaces. In this research, spinel has been grown between periclase and corundum, using both uniaxial stress (JERABEK et al., 2014) and pulsed laser deposition methods (GÖTZE et al., 2014). Electron Backscatter Diffraction has been used to probe the interfacial orientation relationship on  $\mu\text{m}$  scale, then Focused Ion Beam plus Ar-milling have been applied to prepare specimens for examination in a sub-Å resolution Scanning Transmission Electron Microscopy. Fig. 1 (a) shows topotaxial growth of spinel on periclase along the same [001] cubic axis. The interface has a wavy shape: one “valley” for every  $\sim 23$  spinel (010) planes, accommodating one extra spinel plane per “valley”, which is due to the 4.33% lattice mismatch. Fig. 1 (b) reveals that spinel with  $[\bar{1}\bar{1}1]$  axis grows along the corundum [001] direction. The interface is located where the (001) lattice plane of corundum and the (111) lattice plane of spinel coincide, whereby both are occupied by Al atoms exclusively.

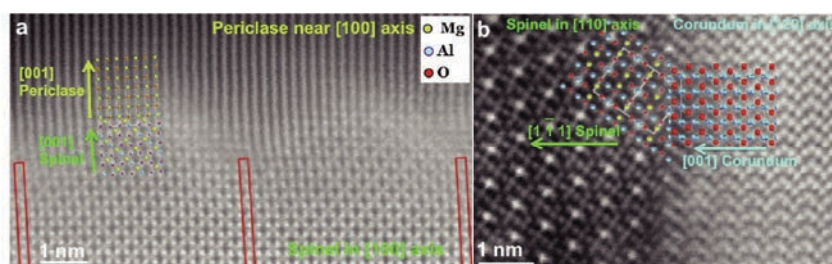


Figure 1. Atomic resolution STEM images showing the interface structure of (a) periclase/spinel and (b) spinel/corundum interfaces. Atomic models have been overlapped on the corresponding structure, where yellow, blue and red circles indicate Mg, Al, and O atomic columns, respectively. The red boxes in (a) show extra spinel planes.

JERABEK, P., ABART, R., RYBACKI, E., HABLER, G. (2014): American Journal of Science, 314, 940-965.

GÖTZE, L. C., ABART, R., MILKE, R., SCHORR, S., ZIZAK, I., DOHMEN, R., WIRTH, R. (2014): Phys. Chem. Minerals, 41, 681-693.

## DIE PRÄKAMBRISCHEN ORTHOGNEISE DES WALDVIERTELS UND IHRE GEOCHEMIE

Lindner, M.<sup>1</sup> & Finger, F.<sup>1</sup>

<sup>1</sup>FB Materialforschung und Physik, Universität Salzburg, Hellbrunnerstr. 34, 5020 Salzburg, Österreich  
e-mail: Martin.Lindner@stud.sbg.ac.at

Im Waldviertel finden sich drei große Orthogneiszüge mit präkambrischem Protolithalter (FUCHS & MATURA, 1976; FRIEDL et al., 2004): der Dobra Gneis (DG) (Zirkonalter 1,38Ga, GEBAUER & FRIEDL, 1993), der Spitzer Gneis (SG) (610Ma) und der moravische Bittesche Gneis (BG) (ca. 580Ma). Die Vergneisung der Gesteine erfolgte i.W. während der variszischen Orogenese. Während der BG unbestritten Teil des Moravikums ist, befinden sich der SG und der DG nach klassischer Sichtweise im Moldanubikum. Trotzdem wird von etlichen Bearbeitern eine Zugehörigkeit der drei Gesteinskörper zu einem gemeinsamen präkambrischen Krustensegment (Avalonia) in Erwägung gezogen, wodurch die Bedeutung der moldanubischen Überschiebung im Hangenden des BG als plattentektonische Suture in Frage gestellt wird (MATURA, 2003). FINGER & FRASL (1990) stufen die drei Orthogneise anhand erster Stichproben als kalk-alkalische I-Typ Granitoide ein und betonen den deutlichen Unterschied zum moldanubischen Gföhler Gneis (S-Typ Granit mit altpaläozoischem Intrusionsalter). Weiterführende petrographisch-geochemische Untersuchungen an den drei Orthogneiskörpern sind derzeit an der Universität Salzburg im Laufen und haben bisher folgende Ergebnisse erbracht:

- 1) Die generelle I-Typ Charakteristik der drei Gneise hat sich bestätigt.
- 2) Alle drei Orthogneiskörper bilden eigenständige Felder in geochemischen Diagrammen mit nur relativ geringer Überlappung bei manchen Elementen.
- 3) Aufgrund der Hauptelementchemie ist der BG als Granit bis Leukogranodiorit zu interpretieren, der SG als Hbl-Bt Tonalit bis Bt-Granodiorit, und der DG als Bt±Hbl-Granodiorit bis Granit.
- 4) Während die geochemische Variationsbreite im BG und SG eher gering ist (jeweils nur eine Magmensuite), beinhaltet der Dobra Gneiskörper zumindest zwei verschiedene magmatische Suiten (Typ A und B). Der Typ A ist reicher an Kalium (3,5-5,6Gew%) und hat auch erhöhte Gehalte an Th (19-40 vs. <11ppm bei Typ B), Rb (100-215 vs. 45-99ppm), Zr (meist 150-250 vs. <130ppm) und den LSEE. Der DG Typ B kommt in seiner Geochemie dem BG nahe, ist aber tendenziell etwas weniger sauer (meist 70-73 vs. meist 72-75Gew% SiO<sub>2</sub>). Die Varietäten A und B bilden eigene Lamellen im Dobra Gneiskörper deren genaue Grenzen noch abzustecken sind. Die mit 1,38Ga datierte Probe gehört dem Typ A an. Ob der Typ B ebenfalls dieses hohe Alter besitzt, wäre zu überprüfen.

FINGER, F., FRASL, G. (1990): TSK Abstracts, 3, 58-60.

FRIEDL, G., FINGER, F., PAQUETTE, J.L., VON QUADT, A., McNAUGHTON, N., FLETCHER, I.R. (2004): Int. J. Earth Sci., 93, 802-823.

FUCHS, G., MATURA, A. (1976): Jahrb. Geol. Bundesanst., 119, 1-43.

GEBAUER, D., FRIEDL, G. (1993): Eur. J. Mineral., 5, 115.

MATURA, A. (2003): Jahrb. Geol. Bundesanst., 143, 221-225.



**SOLUBILITY OF F-CL-APATITES IN KCL-H<sub>2</sub>O BRINES AT 800°C AND 1GPa:  
IMPLICATIONS FOR REE TRANSPORT IN BRINES DURING HIGH-GRADE  
METAMORPHISM**

Mair, P.<sup>1</sup>, Tropper, P.<sup>1</sup>, Manning, C.E.<sup>2</sup> & Harlov, D.<sup>3</sup>

<sup>1</sup>Institute of Mineralogy and Petrography, University of Innsbruck, Innrain 52, 6020, Innsbruck, Austria

<sup>2</sup>Department of Earth, Planetary and Space Sciences, University of California, Los Angeles, CA, USA

<sup>3</sup>Helmholtz Zentrum Potsdam, GeoForschungsZentrum, Telegrafenberg, Potsdam, Germany

e-mail: philipp.mair@uibk.ac.at

Chloride-rich brines are increasingly recognized as playing an important role in high P-T metamorphic and magmatic systems (NEWTON et al., 2010). The origins of these saline, multi-component fluids are still debated, but experimental evidence suggests that regardless of their origin they are important agents of rock alteration and mass transfer wherever they occur. Apatite (Ca<sub>5</sub>(PO<sub>4</sub>)<sub>3</sub>(OH, F, Cl)) is a ubiquitous accessory mineral in many crustal rocks that is widely used to evaluate petrogenetic processes (SPEAR et al., 2002) and is also particularly suitable for assessing the role of fluids at high pressures and temperatures, where metasomatic activity is important but poorly understood. Apatite is an important host for LREE, F, and Cl and thus can be used to monitor elemental mass transfer in high P-T settings. Therefore the determination of its solubility in geologic fluids is of utmost geochemical importance. To this end, we have investigated the influence KCl-H<sub>2</sub>O aqueous fluids on the solubility behaviour of synthetic F-apatite, synthetic Cl-apatite, and natural Durango F-apatite at 800°C and 1.0GPa using 3mm diameter/1cm long Pt capsules arc welded shut and the piston-cylinder apparatus (NaCl setup, cylindrical graphite oven). The experimental results indicate a strong increase in apatite solubility for aqueous fluids with a moderate KCl mole fraction ( $X_{\text{KCl}}$ ). Synthetic F-apatite and synthetic Cl-apatite dissolve congruently. Their solubility increases from 19 and 37 ppm in pure H<sub>2</sub>O to 1917 and 2487ppm, respectively, at  $X_{\text{KCl}}=0.4$ . Natural Durango F-apatite dissolves incongruently at  $X_{\text{KCl}}<0.2$  to monazite + fluid and congruently at  $X_{\text{KCl}} > 0.2$ . The solubility behaviour of both apatites with increasing  $X_{\text{KCl}}$  indicates the participation of H<sub>2</sub>O in the dissolution reaction. In contrast to the NaCl-H<sub>2</sub>O system investigated by (ANTIGNANO & MANNING, 2008), apatite solubilities in the system KCl-H<sub>2</sub>O are considerably lower and at all conditions (700 to 900°C and 0.7 to 2.0GPa), apatite dissolves incongruently to monazite + fluid.

ANTIGNANO, A., MANNING, C. 2008: Chem. Geol., 251, 112-119.

NEWTON, R.C., MANNING, C. 2010: Geofluids, 10, 58-72.

SPEAR, F.S., PYLE, J.M. 2002: Rev. Mineral. Geoch., 48, 293-335.



## MONAZITE DATING OF FLUID-ROCK INTERACTION DURING PERMIAN CONTACT METAMORPHISM IN THE KLAUSEN CONTACT AUREOLE

Mair, P.<sup>1</sup>, Tropper P.<sup>1</sup> & Zöll K.<sup>1</sup>

<sup>1</sup>Institute of Mineralogy and Petrography, University of Innsbruck, Innrain 52, 6020, Innsbruck, Austria  
e-mail: philipp.mair@uibk.ac.at

The Klausen Diorite is part of the Permian calc-alkaline plutonic association consisting of Brixen Granodiorite, Ifinger Granite, Kreuzberg Granite and Cima d'Asta Granitoid as the most prominent members. They all intruded into the polymetamorphic basement of the Southalpine Brixen Quartzphyllite. The Klausen dioritcomplex – the common local name is Klausenite – is located to the south of the Brixen Granodiorite in the eastern part of the Southalpine. The main focus of the research conducted in the course of this work is the monastery-mountain Säben near to Klausen, a small town in South Tyrol (Italy). During the Permian the diorite intruded into the Brixen Quarzphyllites. The pressure conditions of this intrusion range from 0.3GPa to 0.55GPa, which corresponds to a depth of 8 to 17km. The intrusion formed a small, about 140 to 180m wide, contact aureole at the locality of Säben. The aureole can be divided into four different zones based upon mineralogical, mineral chemical and textural features. This study focuses on the petrology of a hornfels from the diorite contact aureole at the Kloster Säben, South Tyrol, Italy which contains the contact metamorphic mineral assemblage plagioclase + K-feldspar + biotite + quartz ± pyrite ± rutile ± titanite ± ilmenite. In addition to this assemblage abundant texturally and chemically zoned F-apatite showing two stages of apatite growth was found in the hornfels. EMPA analyses of the apatites indicate that the lightest zone is enriched in Y + LREE (0.23wt% Y<sub>2</sub>O<sub>3</sub>, 0.11wt% La<sub>2</sub>O<sub>3</sub>, 0.34wt% Ce<sub>2</sub>O<sub>3</sub> and 0.24wt% Nd<sub>2</sub>O<sub>3</sub>), whereas the darkest zone is depleted in Y + LREE (0.13wt% Y<sub>2</sub>O<sub>3</sub>, 0.00wt%La<sub>2</sub>O<sub>3</sub>, 0.07wt% Ce<sub>2</sub>O<sub>3</sub> and 0.08wt% Nd<sub>2</sub>O<sub>3</sub>). Monazite formed both as an inclusion within the second LREE-poor generation of apatite as well as on its rims. Electron microprobe U-Th-Pb dating of monazite inclusions in apatite yielded Permian ages ranging from 252.2Ma to 298.9Ma. These data also represent the first geochronological data from this contact aureole and based on these data the age of the contact metamorphic overprint is 278.4±12.1Ma. These textures can be explained by metasomatic activity involving apatite and an externally derived probably brine-rich fluid, which results in different solubility behaviour and recrystallization of LREE-poor apatite and subsequent enrichment of LREE in abundant monazite inclusions. This feature provides insights into the chemistry of the metasomatizing fluids since HARLOV & FÖRSTER (2003) have experimentally shown that these textures occur when KCl-H<sub>2</sub>O-rich fluids interact with F-apatites.

HARLOV, D.E., FÖRSTER, H.-J. (2003): Am. Mineral., 88, 1209-1229.

## MY FIFTY YEARS WITH SULFOSALTS

Makovicky, E.

Department for Geoscience and Natural Resources Management, University of Copenhagen

Sulfosalts are a large subgroup of complex sulfides (and selenides) characterized by the presence of As, Sb or Bi in a formally trivalent state. These elements almost always exhibit a typical one-sided coordination characterized by lone electron pair activity which determines crystal structures of this group of compounds. With elements of fitting atom radius, such as Pb, Sn, Ag, these As, Sb or Bi form modular structures which can be based on PbS (low LEP activity) or SnS (elevated LEP activity) archetype; these are present as rods, blocks or layers of various sizes and shapes. The structure of chovanite, one of the Pb-Sb oxy-sulfides, will be used to illustrate how minor presence of oxygen in the sulfosalt can create an entirely new structure motif. Modular character leads in several cases to homologous series (or geometrically less strict plesiotypic series) which are a basis of systematics of these compounds. Chemical substitutions of the type  $2\text{Pb} \square (\text{As}, \text{Sb}, \text{Bi}) + \text{Ag}$  or  $2\text{Pb} \square \text{Ti} + (\text{As}, \text{Sb})$  (more rarely those involving Cu and Fe) in a given homologue usually lead to two or more discrete (super)structures and minerals with different cation ordering, unit cell and symmetry while preserving the homologue order N. Differences between As and Sb in bond lengths and LEP activity lead often to spectacular differences between the structures of their sulfosalts and/or to their specific roles when these elements occur in the same structure. The size and bonding differences between As or Sb and Pb in the structures of lead sulfosalts respectively result in organization of short and long cation-anion distances into crankshaft chains with different lengths and orientations, and into separate distinct pairs or groups. The example of ‘andorite species’ and the examples from the sartorite homologous series, especially the pair dufrénoysite – rathite and the new ‘sartorite omission series’ of distinct phases will illustrate this phenomenon. The problem of separate As and Sb accommodation in this series leads to a threefold superstructure of polloneite which will be demonstrated. An inherent feature of sulfosalts based on the PbS and/or SnS archetype is the presence of finite-to-infinite interfaces with non-commensurability of the motifs facing one another. Many Pb-Sb sulfosalts have short, several polyhedra wide interfaces of this kind whereas cylindrite and franckeite have infinite interfaces with two-dimensional incommensurability – we shall show what solution Nature presents to this problem. The infinite interfaces of this kind in the Pb-Bi sulfosalt cannizzarite are modified in felbertalite and proudite, and in a synthetic Cu-Pb-Bi selenosalt to be shown.

A surprising number of sulfosalt structures are subject to OD (order-disorder) phenomena, in which the position or orientation of consecutive layers of the structure motif is subject to two-fold or higher ambiguity. I shall demonstrate the OD structure of the Ag-Pb-Sb sulfosalt owyheite, of the Ti-As sulfosalt imhofite, Ag-Pb-Bi sulfosalt gustavite, and mention some other examples.

This short and incomplete review of the sulfosalt family, based on a combination of the results of our group(s) with data of other important sulfosalt aficionados, tries to introduce you to a selection of interesting aspects of sulfosalt crystal chemistry which I met at some stages of my long engagement with these interesting minerals. The (co)authors, whose achievements and assistance I enjoyed along the way, will be quoted at individual structures.

**GARNETS FROM TANZANIAN KIMBERLITES (MWADUI, SINGIDA,  
NYANGWALE AND GALAMBA): EVIDENCE FOR MANTLE METASOMATISM  
BELOW THE TANZANIA CRATON**

Mandl, M.<sup>1</sup>, Hauzenberger, C.A.<sup>1</sup>, Konzett, J.<sup>2</sup>, Jumanne, R.<sup>3</sup>, Gobba, J.M.<sup>4</sup> & Hoang, N.<sup>5</sup>

<sup>1</sup>Department of Earth Sciences, University of Graz, Universitaetsplatz 2, 8010 Graz, Austria

<sup>2</sup>Institute of Mineralogy and Petrography, University of Innsbruck, Austria

<sup>3</sup>Williamson Diamond Mine, Petra Diamonds Ltd., Tanzania

<sup>4</sup>Gobbex Ltd., Tanzania

<sup>5</sup>Institute of Geological Sciences, Vietnam Academy of Science and Technology, Vietnam

e-mail: m.mandl@uni-graz.at

Kimberlites from Mwadui, Singida, Nyangwale and Galamba have been emplaced within the northern part of the Tanzania Craton during the Paleogene. These ultrapotassic and ultrabasic rocks have been derived from great depth and contain important information about the underlying lithospheric mantle by (1) their chemical composition and by (2) their xenolith and xenocryst content. Studied mantle derived garnets show chemical variations in their major- and trace element compositions and can be distinguished into five groups: low-Cr megacrysts (G1), eclogitic- (G3), pyroxenitic- (G4), lherzolitic- (G9) and harzburgitic (G10) garnets. Some garnets within group G4 and G10 can be associated with diamonds (G4D and G10D). Garnets from the Williamson diamond mine are cm sized megacrysts which belong to the low Cr megacrysts (G1). From the Singida kimberlite garnet grains of only a few mm could be recovered. Most of these garnet grains are eclogitic (G3) and low Cr megacrysts (G1), but there are also pyroxenitic (G4) and lherzolitic (G9) grains. From the Nyangwale kimberlite only few garnet samples from heavy mineral concentrates were obtained. They are classified as group 9 (lherzolitic). The Galamba kimberlite is situated to the south of the Mwadui kimberlite. The chemical composition of the garnet is slightly different from the garnet megacrysts from the Mwadui kimberlite. They are lherzolitic (G9) and low Cr megacrysts (G1).

The different originated garnets are strongly influenced by metasomatic mantle processes. An enrichment in light rare earth elements and a depletion in incompatible elements in the only harzburgitic garnet indicates the presence of carbonatitic melts, originated within the asthenospheric mantle. Lherzolitic garnets are derived from a less depleted to depleted mantle, which was influenced by phlogopite-type respectively basic/ultrabasic melt-type metasomatism. Low-Cr megacrysts mainly display a basic/ultrabasic melt-type metasomatism trend and pyroxenitic garnets probably have experienced several metasomatic events. Eclogitic garnets found only in the Singida kimberlite are interpreted to be derived from subducted oceanic crust.

This is a contribution to IGCP 557. The financial support from the Austrian Academy of Science is gratefully acknowledged.

# STRUCTURAL INVESTIGATIONS ON A SI-FREE Mg-CONTAINING SFCA-PHASE WITH COMPOSITION $\text{Ca}_3\text{MgFe}_{10}\text{Al}_6\text{O}_{28}$

Manninger, T. & Kahlenberg, V.

University of Innsbruck, Institute of Mineralogy & Petrography, Innrain 52, A-6020 Innsbruck, Austria  
e-mail: tanja.manninger@student.uibk.ac.at

Sinter ore used in the iron-making blast furnace process is usually composed of unreacted hematite and magnetite embedded in a porous matrix consisting of chemically complex so-called SFAC phases (silico-ferrite of calcium and aluminium) as well as a glassy phase.

In the course of a research project on the crystal chemistry of SFCA-related materials we obtained single crystals of a Si-free Mg-containing SFCA compound that were characterized using electron microprobe analysis (EMPA) and X-ray single-crystal diffraction. EMPA results collected on a polished specimen with a cross section of  $60\mu\text{m} \times 115\mu\text{m}$  indicated the following chemical composition:  $\text{Ca}_{2.90}\text{Mg}_{0.95}\text{Fe}_{10.11}\text{Al}_{5.99}\text{O}_{28}$  or  $\text{Ca}_3\text{MgFe}_{10}\text{Al}_6\text{O}_{28}$ . Notably, the crystals contain exclusively ferric iron. Single-crystal diffraction data were acquired at  $25^\circ\text{C}$  using the same sample. Basic crystallographic data are as follows: triclinic symmetry, space group P-1,  $a=10.2980(4)\text{\AA}$ ,  $b=10.4677(4)\text{\AA}$ ,  $c=11.6399(4)\text{\AA}$ ,  $\alpha=94.363(3)^\circ$ ,  $\beta=111.498(3)^\circ$ ,  $\gamma=109.744(3)^\circ$ ,  $V=1069.81(7)\text{\AA}^3$ ,  $Z=2$ . The cations are distributed among a total of 20 different cation sites. Site-population refinements were used to determine the cation distributions of the Fe and (Al+Mg) ions on the octahedral and tetrahedral positions. From a structural point of view the present compound is isotypic with the so-called SFCA-I phase that was first described by MUMME et al. (1998) for a sample with composition  $\text{Ca}_{3.18}\text{Fe}^{2+}_{0.82}\text{Fe}^{3+}_{14.66}\text{Al}_{1.34}\text{O}_{28}$ . It can be allocated as a homologue of the aenigmatite structure type.

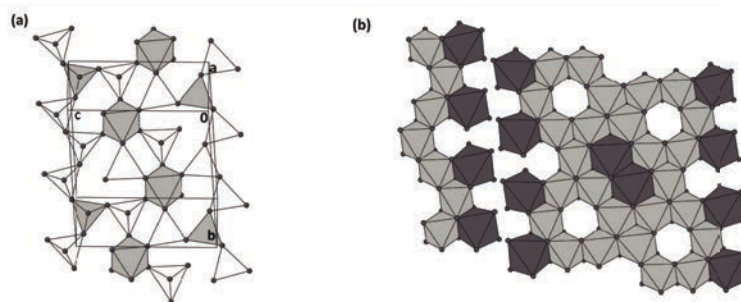


Figure 1. Two fundamental layers comprising the crystal structure of  $\text{Ca}_3\text{MgFe}_{10}\text{Al}_6\text{O}_{28}$  shown in projections perpendicular to the sheets: (a) layer of corner-sharing  $[\text{FeO}_4]$ -tetrahedra (white),  $[\text{AlO}_4]$ -tetrahedra (light grey) and  $[\text{FeO}_6]$ -octahedra and (b) layer containing bands of edge-sharing  $[\text{FeO}_6]$ -octahedra (light grey) as well as  $[\text{CaO}_6]$ -octahedra (dark grey).

MUMME, W., CLOUT, J. & GABLE, R. (1998): Neues Jahrbuch Mineralogie - Abhandlungen, 173, 93-117.

## PHASE FORMATION IN MOULD POWDERS AND MOULD SLAGS DURING SERVICE

Marschall, I.<sup>1</sup> & Harmuth, H.<sup>1</sup>

<sup>1</sup>Montanuniversität Leoben, Chair of Ceramics, Peter Tunner Straße 5, 8700 Leoben, Austria  
e-mail: irmtraud.marschall@unileoben.ac.at

In the continuous casting process mould powders are used as an additive, for insulation of the meniscus, absorption of non-metallic inclusions, lubrication of the strand and controlling of the heat flux. These powders are mixtures of natural and synthetic silicates, oxides, carbonates, fluorides and carbon. They are feed on top of the steel meniscus where they melt and infiltrate the gap between the strand and the water cooled copper mould. In contact with the mould the liquid slag solidifies to form a so called slag film.

During melting these raw materials react. In a temperature range of 500°C-750°C (Fig. 1) the carbonates dissociate in contact with the silicates. This leads on the one hand to the formation of combeite ( $\text{Na}_2\text{Ca}_2\text{Si}_3\text{O}_{10}$ ) due to solid state diffusion processes and on the other hand to the crystallisation of sodium-lime-silicates out of first liquid phases. Additionally, cuspidine ( $\text{Ca}_4\text{Si}_2\text{O}_7\text{F}_2$ ) will appear due to solid state diffusion of fluorine ions into sodium-lime-silicates. Between 750°C-900°C  $\text{Na}_2\text{O}$  diffuses into alumina and silicates with high  $\text{Al}_2\text{O}_3$  content. As a consequence sodium-alumina-silicates are formed. But the main solid phase will be cuspidine, which crystallises out of the melt (Fig.1). In dependence of the  $\text{CaO}/\text{SiO}_2$  ratio the liquidus temperature of the powders lie between 1100°C and 1200°C.

Within the slag films three distinctive layers can be determined. A so called glassy layer in contact with the mold, a crystalline layer and a layer which has been liquid during casting and solidified afterward. Cuspidine ( $\text{Ca}_4\text{Si}_2\text{O}_7\text{F}_2$ ) is the prevailing crystal phase in the crystalline layer. Casting alloyed steel grades may modify the structure of the crystalline layer. With increasing  $\text{Al}_2\text{O}_3$  content of the slag caused by interactions with the steel, nepheline ( $(\text{Na},\text{K})\text{AlSiO}_4$ ) will appear. When casting steel grades with increased Ti content, perovskite ( $\text{CaTiO}_3$ ) will be formed additionally to cuspidine in the crystalline layer.

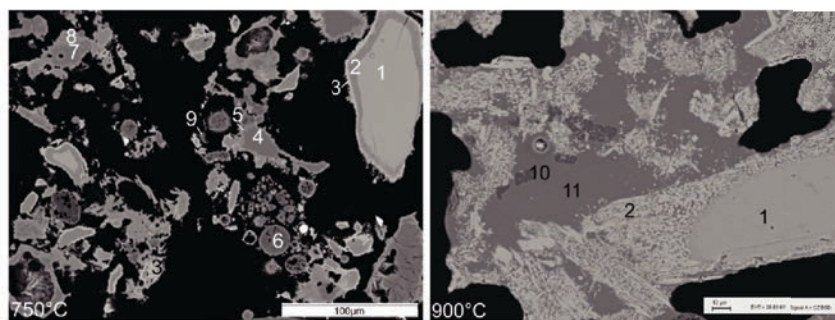


Figure 1. Backscattered electron image of a mould powder after heat treatment at 750 °C and 900 °C. Phases (1) wollastonite, (2) combeite, (3) cuspidine, (4) glass scrap, (5) sodium rich reaction zone around glass scrap (6) fly ash, (7) quartz, (8) sodium rich reaction zone around quartz, (9) alumina, (10)  $\text{NAS}_3$  ( $\text{Na}_2\text{Al}_2\text{Si}_3\text{O}_{10}$ ) and (11) glassy solidified liquid.



## KLEINE VORKOMMEN VON REDWITZITISCHEN MONZONITEN IM ÖSTLICHEN MÜHLVIERTEL

Matzinger, M.<sup>1</sup>, Finger, F.<sup>1</sup> & Reiter, E.<sup>2</sup>

<sup>1</sup>FB Materialforschung und Physik, Universität Salzburg, Hellbrunnerstr. 54, 5020 Salzburg, Österreich

<sup>2</sup>Institut für Chemische Technologie Anorganischer Stoffe, JKU Linz, Altenbergerstr. 69, 4040 Linz, Österreich  
e-mail: michael.matzinger@sbg.ac.at

Anlässlich einer systematischen Beprobung von dioritischen Gesteinsvorkommen auf Kartenblatt Steyregg (Südböhmischer Batholith) wurden Basite mit außergewöhnlich hohen  $K_2O/Na_2O$ -Verhältnissen gefunden (Abb.1), die als ultrapotassische Magmatite einzustufen sind (FOLEY et al., 1987). Sie zeichnen sich bei moderater Basizität ( $SiO_2$  meist 48-54 Gew.%) durch hohe  $MgO$ - (7-10Gew%),  $P_2O_5$ - (1,2-2,2Gew%),  $Ba$ - (1.900-6.300ppm),  $Cr$ - (140-500ppm) und  $Ni$ -Gehalte (70-250ppm) aus.

Makroskopisch weisen die Proben große, auffällig sperrige Biotite (bis 8mm) in einer feinkörnigen, grünlichgrauen Matrix auf (Redwitzitgefüge nach TROLL, 1968). Im Dünnschliff finden sich hohe Anteile mafischer Komponenten (30-50%), wobei neben Biotit stets grüner Amphibol sowie manchmal auch etwas Klinopyroxen zu beobachten sind. Apatit und Titanit sind häufige Akzessorien, fallweise wurde auch Orthit beobachtet. Das Verhältnis Kalifeldspat/Plagioklas bewegt sich meist um 1 und Quarz spielt nur eine sehr untergeordnete Rolle, sodaß die Gesteine als Monzonite angesprochen werden können. Die Monzonite intrudieren den Weinsberger und Engerwitzdorfer Granit und repräsentieren vermutlich Magmen aus einer phlogopitführenden, lithosphärischen Mantelquelle.

Der Schwerpunkt der Vorkommen ist im Gusental nahe St. Georgen. Weitere Fundpunkte liegen nahe Gallneukirchen (Autobahnanschlussstelle) und bei Holzgassen.

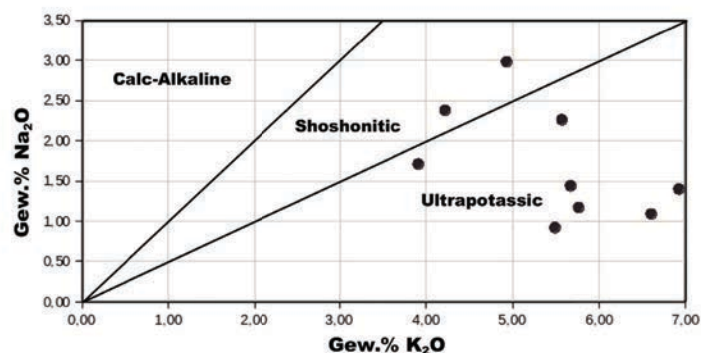


Abbildung 1:  $K_2O/Na_2O$ -Verhältnisse der redwitzitischen Monzonite auf Blatt Steyregg.

FOLEY, S.F., VENTURELLI, G., GREEN, D.H., TOSCANI, L. (1987): Earth-Science Reviews, 24, 81–134.

TROLL, G. (1968): Bayer. Akad. Wiss., Math.-Nat. Kl., Abh., N.F., 133, 86 S., München



**STABLE ISOTOPE FRACTIONATION OF ALKALINE EARTH METALS DURING  
CARBONATE MINERAL PRECIPITATION, DISSOLUTION AND AT  
EQUILIBRIUM**

Mavromatis, V.<sup>1</sup>, Stammeier, J.<sup>1</sup>, Konrad, F.<sup>1</sup> & Dietzel, M.<sup>1</sup>

<sup>1</sup>Institute of Applied Geosciences, Graz University of Technology, Rechbauerstrasse 12, 8010 Graz, Austria  
e-mail: mavromatis@tugraz.at

The interpretation of the stable isotope composition of natural carbonates, either they have been formed biotically or abiotically, relies on two major assumptions. The first one, which actually acts as the foundation for all the carbonate mineral-based paleo-environmental and paleo-temperature reconstructions, is that once a mineral is precipitated, it retains its original isotopic signal and preserves pristine information about its formation conditions. The second assumption is that stable isotope signatures are transferred conservatively in the fluid phase during congruent mineral dissolution. This assumption is the basis for tracing fluid flow pathways and characterizing the origin of fluids in natural systems.

From a thermodynamic point of view the first assumption appears problematic. Indeed temperature changes and fluid interaction with a sedimentary rock, may provoke an isotopic disequilibrium of carbonate mineral phases with their co-existing fluids. Thus in order for the isotopic composition of the mineral phase to remain unaltered, it requires the fluid-rock system to be set out of isotopic equilibrium for significant (i.e. geologic) timeframes. Along the same line the second assumption contradicts a main thermodynamic principle that of the backward reaction during dissolution in the near equilibrium regime.

In order to test those two widely adopted assumptions we studied the chemical and isotopic behaviour of alkaline earth metal carbonates (e.g. calcite, witherite, hydromagnesite) during dissolution, precipitation and at chemical equilibrium at ambient temperature in closed-system mineral-fluid experiments. The obtained results indicate that in less than a month-long period i) alkaline earths metals (i.e. Ca, Mg, Ba) are not conservatively transferred during stoichiometric mineral dissolution, ii) the isotopic composition of the carbonate mineral phase and its co-existing reactive fluid continue to evolve after fluid has retained its chemical equilibrium with respect to the alkaline earth metal carbonate mineral present and iii) kinetically induced isotopic signatures obtained during rapid mineral precipitation are eventually erased by the continuous isotopic re-equilibration between mineral and fluid. Moreover our results indicate that: i) kinetic isotope signals can be detected in elements with large masses such as Ba, in the witherite fluid system, and ii) owing to the large variations on the exchange of water molecules between the hydration spheres of free aqueous  $\text{Me}^{2+}$  and the aqueous fluid observed between Mg and the other alkali earths (i.e. Ca, Ba, Sr), a distinct behaviour in the isotopic composition of the fluid at the onset of congruent dissolution of Mg-bearing carbonates is observed compared to other alkaline earth metal carbonate minerals. This observation may have significant importance for the interpretation of the isotopic composition of natural fluids during carbonate mineral weathering.

## GOLD AND PLATINUM FROM THE RHINE RIVER

Melcher, F.<sup>1</sup>, Wotruba, H.<sup>2</sup>, Oberthür, T.<sup>3</sup> & Brauns, M<sup>4</sup>

<sup>1</sup>Lehrstuhl für Geologie und Lagerstättenlehre, Montanuniversität Leoben  
(Peter-Tunnerstraße 5, 8700 Leoben, Austria)

<sup>2</sup>Aufbereitung mineralischer Rohstoffe (AMR), RWTH Aachen (Lochnerstr. 4-20, 52064 Aachen, Germany)

<sup>3</sup>Bundesanstalt für Geowissenschaften und Rohstoffe (Stilleweg 2, 30655 Hannover, Germany)

<sup>4</sup>Curt-Engelhorn-Zentrum Archäometrie (D6, 3, 68159 Mannheim, Germany)  
mail: frank.melcher@unileoben.ac.at

For centuries, the “Rheingold” has fascinated and inspired people. Panning of gold along the Rhine river dates back to Celtic times, and historians estimate that about 1000 kg of gold have been recovered (ELSNER, 2009). Today, some gold is produced from fine fractions in sand and gravel operations that contain from 0.05 to 11 mg gold per ton of gravel.

Gold grains are usually less than 0.3 mm in size and reveal variable compositions depending on location along the river, ranging from a few up to 20 wt% Ag (on average 4-6% Ag). The median composition from LA-ICP-MS analysis of 116 gold grains from Rheinzabern is: 3.8% Ag, 60 ppm Cu, 3.5 ppm Pd, 15 ppm Sn, 60 ppm Pb. Commonly, elevated concentrations of Hg are detected (up to 1400 ppm).

First studies of opaque minerals accompanying gold in heavy mineral fractions of the Rhine gravels date back to RAMDOHR (1965). A suite of detrital grains upgraded from a professional gold extraction plant at Kieswerk Rheinzabern at the AMR was investigated using microscopy, electron beam and laser beam methods (OBERTHÜR et al., 2015). The grains comprise, among more common heavy minerals, platinum-group minerals (PGM), cassiterite, columbite-group minerals, tapiolite and uraninite. The PGM assemblage (0.05-0.3 mm) is dominated by grains of Ru–Os–Ir alloys (~70 %), followed by Pt–Fe alloys (15%), laurite, sperrylite and rare other PGM. One grain of an Os–Ir–Mo–W–Re alloy phase probably represents the very rare mineral hexamolybdenum.

Pt–Fe alloys and sperrylite may originate from various sources; however, the predominant Ru–Os–Ir alloy grains point to an origin from ophiolite sequences of unknown age (but likely pre-Alpine; Variscan or older). The exact locations of the primary sources and the complex, prolonged sedimentary history of the detrital PGM with possibly multiple intermittent storages remain unknown. Detrital cassiterite grains were dated by the U–Pb method using LA-ICP-MS. They largely overlap with zircon age distributions (KRIPPNER & BAHLBURG, 2013) by peaking at ca. 325 Ma, thereby implying a predominantly Variscan age of the cassiterite grains and possible derivation from mineralization in the Black Forest area. Tantalum oxides are dominantly tapiolite originating from pegmatites. Rare uraninite grains attest that this mineral experienced rapid erosion, transport and deposition in a reducing environment.

ELSNER, H. (2009): Commodity Top News 30

KRIPPNER, A., BAHLBURG, H. (2013): Int. Jour. Earth Sci. (Geol. Rundschau) 102: 917-932

OBERTHÜR, T., MELCHER, F., GOLDMANN, S., WOTRUBA, H., GERDES, A., DIJKSTRA, A., DALE, C. (2015): Int. Jour. Earth Sci. (Geol. Rundschau) DOI 10.1007/s00531-015-1181-3

RAMDOHR, P. (1965): Jh. Geol. Landesamt Baden-Württemberg 7: 87-95.

## FINE-STRUCTURAL ANOMALIES IN THE COMPRESSION BEHAVIOUR OF GYPSUM

Mirwald, P.W. & Paulini, P.

Material Technology Innsbruck, University of Innsbruck  
e-mail: peter.mirwald@uibk.ac.at

We performed a compression study on gypsum, up to 1,5 GPa at room temperature in connection with ultra sonic measurements. The experiments were conducted in a piston cylinder apparatus where piston displacement (volume change) is monitored by an external electrical transducer system. The us-measurements (excitation frequency 150 MHz) were performed in a transit configuration. Since multiple conversions between longitudinal and shear waves in the experimental setup impairs the determination of sound velocity, a relative parameter, the zero crossing of the wave signal has been chosen instead.

The detailed evaluation of the compression-decompression tracks reveals small but distinct and reproducible changes in the compressibility; no structural change is observed. These changes in compressibility may be visualized by a difference calculation between the raw data and a polynomial fit of 2<sup>nd</sup> order to the raw data. The compression-decompression data show three significant changes in the course of the difference curve (Fig.1). The ultrasonic data confirm the findings.

Similar volume anomalies also have been discovered by detailed analysis of  $C_p$  and thermal expansion data from the literature. This suggests that the P-V-T behaviour of gypsum is characterized by subtle P-V-T changes that do not affect the structural symmetry. We assume that these effects are related to non-continuous changes in the lattice vibrations of gypsum at changing P-T conditions.

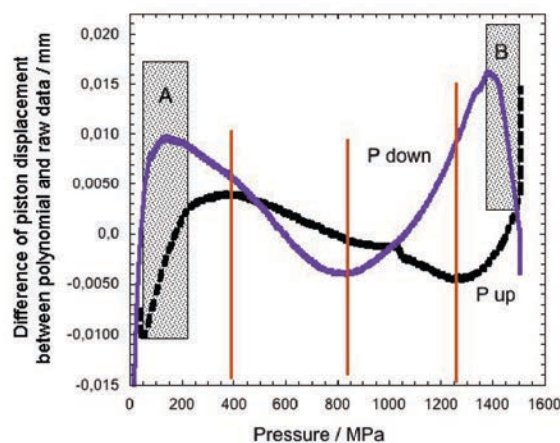


Fig.1 shows the result of a compression-decompression run at 26° C. The change in the V-P-behaviour of gypsum, located by difference calculation, shows three significant slope changes at 350–450, 850 and at 1250 MPa. A: range of pressurization / depressurization of the vessel; B: range of relaxation at beginning of P down.

**STRUCTURAL DISEQUILIBRIUM IN CORDIERITES FROM LONG-DURATION  
EXPERIMENTS USING CRYSTAL CHEMICAL CONSTRAINTS**

Mirwald, P.W.<sup>1</sup> & Tropper, P.<sup>1</sup>

<sup>1</sup>Institute of Mineralogy & Petrography, University of Innsbruck  
e-mail: peter.mirwald@uibk.ac.at

In an experimental examination of sodium incorporation in cordierite for a re-appraisal of the Na-in cordierite thermometer (MIRWALD, 1986), two batches of natural quartzphyllite starting materials (1: poor in albite; 2: rich in quartz) were used. Surprisingly, while the data obtained with material (1) confirmed previous results, significantly higher Na-incorporation was obtained when using material (2). Raman spectra showed that both types of cordierites are not fully ordered with respect to Si-Al, in particular not those of batch (2), when compared with pure synthetic Mg-cordierite and natural samples from the literature. Cordierite shows three different structural cation sites: Si<sup>4+</sup> and Al<sup>3+</sup> are tetrahedrally coordinated, Mg, Fe<sup>2+</sup>, Mn<sup>2+</sup> occur on the [6]-sites and Na<sup>+</sup>, K<sup>+</sup>, Ca<sup>2+</sup>(?) as well as fluid components (H<sub>2</sub>O, CO<sub>2</sub>, noble gases) are accommodated in different interstitial positions in the channels of this framework structure. This circumstance implies that cation incorporation, distribution and ordering processes are essential factors during nucleation and crystal growth of cordierite, basically governed by the electrical charges balance within the anion oxygen sublattice. The vacancies on the Si sites are counterbalanced by excess Al reflecting the substitution reaction  $\text{Si} = \text{Al}^{3+} + \text{Na}^+$  or  $\text{Al}^{3+} + \text{ChC}^+$  (channel components) respectively. In most cases the amount of the sum of the ChC exceeds  $\text{Al}^{3+}/3$ ; this applies also for the Na<sup>+</sup> component below the line of beginning melting at 660°C. A striking feature is 2-valent vacancies on the [6]-position. The final charge balance calculation, which includes the octahedral vacancies and the channel positions therefore yields a slight deficit in positive charges below 660°C and a slight excess above. This fact also must imply an equivalent compensation in the oxygen sublattice. These observations indicate that nucleation and crystal growth of cordierite in a complexly composed natural rock can be kinetically hampered and hence even very long duration experiments may not achieve complete equilibration.

MIRWALD, P.W. (1986): Fortschr. Mineral., 64, Beih.1, 113

**EVIDENCE FROM CHLORITOID SCHISTS FOR MULTI-STAGE  
METAMORPHISM IN THE MT. MEDVEDNICA AREA (ZAGORJE MID  
TRANSDANUBIAN ZONE, N-CROATIA)**

Mišur, I.<sup>1</sup>, Belak, M.<sup>2</sup>, Klötzli, U.<sup>3</sup> & Balen, D.<sup>2</sup>

<sup>1</sup>Croatian Geological Survey, Milana Sachsa 2, HR - 10 000 Zagreb, Croatia

<sup>2</sup>University of Zagreb, Faculty of Science, Department of geology, Horvatovac 95, HR – 10 000 Zagreb, Croatia

<sup>3</sup>University of Vienna, Department of Lithospheric Research, Althanstrasse 14, 1090 Vienna, Austria

e-mail: imisur@hgi-cgs.hr

Chloritoid schists form a part of the Palaeozoic - Mesozoic succession and represent one of the oldest lithology in the Mt. Medvednica area in N Croatia. Regionally Mt. Medvednica belongs to the Zagorje Mid Transdanubian zone, a transition area between the Alps and the Dinarides. The presented results are a part of an ongoing study of metasedimentary rocks of Mt. Medvednica. Samples were collected from the SE slopes of Mt. Medvednica. They are categorized as chloritoid-chlorite-quartz-muscovite schists, chlorite-muscovite-quartz schists, chlorite-muscovite-quartz-chloritoid schists and intercalations of marbles. Accessory minerals in the chloritoid-bearing schists are tourmaline, zircon, apatite, monazite, xenotime and rutile. XRD, XRF, LA-MC-ICP-MS, SEM, electron microprobe and microstructural investigations were used to determine the chemical composition, microstructural features, thermobarometric conditions and the morphology of zircons of the chloritoid schists. Chlorite-chloritoid thermometry (VIDAL et al., 1999) and intersection of phengite, chlorite and chloritoid isopleths in the MnNCKFMASHTO pseudo-section suggests the presence of a relict high-pressure metamorphic event at approximately 13-14kbar and 410-440°C and equilibration of chlorite and white mica within subsequent greenschist-facies P-T conditions at approximately 8kbar and 350-400°C. Thermometry of chlorite and chloritoid give unexpectedly high temperatures over 500°C. Zircon typology suggests that there could be at least two sources of zircon grains based on the Pupin classification (PUPIN, 1980). One source is possibly detrital made up by plutonic, stubby zircons. The other source of zircon grains could be of volcanic, with typically elongated crystals showing growth spindle inclusions. Based on the results of microstructural analysis the possible protolite of the chloritoid-bearing schists could be argillaceous sandstones. Geochemical data suggest that these could be derived from acid magmatic rocks. The whole rock composition of La-Th-Sc and Th-Sc-Zr/10 suggests that possible depositional environment very likely represents a continental arc environment (BATHIA & CROOK, 1986). Carbonate intercalations within the argillaceous sandstones could indicate deposition in a marine environment. Zircon typology indicates the input of volcanic material during deposition. Pseudo-section modelling indicates that the P-T path probably is a result of multi-stage metamorphism.

BHATIA, M. R. & CROOK, K. A. W. (1986): Contrib. Mineral. Petrol., 92, 181-193.

PUPIN, J. P. (1980): Contrib. Mineral. Petrol., 73, 207-220.

VIDAL, O., GOFFE, B., BOUSQUET, R., PARRA, T., (1999): J. Metamorph. Geol., 17, 25-39.

**CRYSTAL GROWTH, STRUCTURAL CHARACTERIZATION AND HIGH-TEMPERATURE BEHAVIOR OF  $\text{Na}_3\text{TmSi}_3\text{O}_9$  – A CHAIN SILICATE WITH A PERIODICITY OF 24**

Mörtl, A.<sup>1</sup>, Kahlenberg, V.<sup>1</sup> & Krüger, H.<sup>1</sup>

<sup>1</sup>Institute of Mineralogy and Petrography, University of Innsbruck, Innrain 52, A-6020 Innsbruck  
e-mail: volker.kahlenberg@uibk.ac.at

Luminescent materials play a major technological role concerning the development of novel devices and circuits for electronic, optoelectronic as well as communications industries. Applications span a wide field from cathode ray tubes, infrared amplifiers and X-ray detectors up to light-emitting diodes in flat panel displays of television screens, just to mention a few (KITAI, 2008). Rare earth element (REE) containing silicates are one class of inorganic metal oxide-based phosphors that have been intensively studied for these purposes. A promising silicate material that allowed a wide-range tuning of the optical properties from blue emitters and IR S-band amplifiers to X-ray phosphors depending on the type and the content of the REE cation was reported by ANANIAS et al. (2003):  $\text{Na}_3(\text{Y}_{1-x}\text{M}_x)\text{Si}_3\text{O}_9$  (M:  $\text{Tm}^{3+}$ ,  $\text{Tb}^{3+}$ ;  $x=0-1$ ).

In the course of an ongoing research project on the synthesis of rare earth element containing silicates from alkali fluoride fluxes single-crystalline material of several new silicates has been obtained in dimensions up to 500  $\mu\text{m}$  in diameter. The present contribution reports the results of structural investigations of the  $\text{Tm}^{3+}$  containing compound  $\text{Na}_3\text{TmSi}_3\text{O}_9$ . At 25°C, the compound has the following basic crystallographic data: space group  $P2_12_12_1$ ,  $a=15.1681(3)\text{\AA}$ ,  $b=15.0855(3)\text{\AA}$ ,  $c=14.9937(3)\text{\AA}$ ,  $V=3430.83(12)\text{\AA}^3$ ,  $Z=16$ . Structure solution was based on direct methods. The subsequent refinement calculations resulted in a residual of  $R(\text{IFl})=0.039$  for 9159 independent observed reflections with  $I>2\sigma(I)$  and 579 parameters. From a structural point of view,  $\text{Na}_3\text{TmSi}_3\text{O}_9$  belongs to the group of single-chain silicates. The periodicity of the extremely folded chains has a value of 24. The compound is isostructural with the corresponding yttrium phase. Alternatively, the structure can be described as a mixed octahedral-tetrahedral framework, for which a detailed topological analysis is presented.

The high-temperature behavior of  $\text{Na}_3\text{TmSi}_3\text{O}_9$  was investigated by *in-situ* single-crystal X-ray diffraction in the range between 25 and 700°C. No anomalies in the lattice parameters and unit cell volume vs. temperature curves were observed, pointing to the absence of structural phase transitions. From the evolution of the lattice parameters, the thermal expansion tensor  $\alpha_{ij}$  has been determined. Thermal expansion shows a pronounced anisotropy. In the whole temperature region, the largest values are observed along [010] (parallel to the single-chains).

ANANIAS, D., FERREIRA, A., CARLOS, L.D., ROCHA, J. (2003) Adv. Mater., 15, 980-984.

KITAI, A. (ed.) (2008): Luminescent materials and applications. John Wiley & Sons Ltd., Chichester.



**GEOCHEMICAL CHARACTERISTICS OF TWO PHOSPHORITE OCCURRENCES  
FROM THE TRANSDANUBIAN MOUNTAIN RANGE (NW HUNGARY)**

Molnár, Zs.<sup>1</sup>, Kiss, G. B.<sup>1</sup>, Zaccarini, F.<sup>2</sup>, Dunkl, I.<sup>3</sup>, Czuppon, Gy.<sup>4</sup> & Dódoný, I.<sup>1</sup>

<sup>1</sup>Dep. of Mineralogy, Eötvös Loránd Univ., Pázmány P. str. 1/C, H-1117 Budapest, Hungary

<sup>2</sup>Dep. of Applied Geosciences and Geophysics, Univ. of Leoben, A-8700 Leoben, Peter Tunnerstr. 5, Austria

<sup>3</sup>Dep. of Sedimentology and Environmental Geology, Geoscience Center, Univ. of Göttingen, Goldschmidtstr. 3,  
D-37077 Göttingen, Germany

<sup>4</sup>Inst. for Geological and Geochemical Research Centre for Astronomy and Earth Sciences, Hungarian Academy  
of Sciences, Budaörsi str. 45, H-1112 Budapest, Hungary  
e-mail: molnarzsuzsa89@gmail.com

The carbonate-dominated Mesozoic sequence of the NW Hungarian Transdanubian Mountain Range contains layered phosphorite in Triassic and nodular phosphorite in Cretaceous limestone (at Pécsely and Tata, respectively). Uranium enrichment was proven in the Triassic phosphorite layers (KISS & VIRÁGH, 1959, FÜLÖP, 1975), however, the chemical composition of the Cretaceous formation has not been studied yet.

The depositional age of the Triassic phosphorite is well constrained by marine biostratigraphy. The LA-ICP-MS U-Pb age  $237 \pm 11$  Ma coincides with the stratigraphic age – indicating negligible ion exchange during the burial history. The main mineral is carbonate-fluorapatite, but calcite and rarely hematite also occur. According to EPMA analyses, the U enrichment in the phosphorite layer is most likely related to the carbonate-fluorapatite, as it contains 0.023-0.3 mass% U, whereas no other U-bearing minerals were observed. In contrast, the Cretaceous nodular phosphorite occurs at the basis of the Aptian gray, Crinoidea-bearing limestone. The main minerals of the crust around the bio- and siliciclasts are apatite, calcite, quartz, mica and Fe-oxides, hydroxides. Based on EPMA studies, it contains a small amount of U (<0.041 mass%). The structure and the texture of the Cretaceous phosphorite strongly differ from the Triassic one, indicating substantial differences in their formations.

The EPMA mapping of REE and U elements revealed homogenous distribution in the measured crystals for both localities. According to the ICP-MS and ICP-OES analyses, many similarities and differences can be observed. A total REE (REE+Y) content of 116-158 ppm (Triassic) and 1235 ppm (Cretaceous) were detected. The patterns of the REE distribution diagrams are very similar, however some differences appear when the concentrations are normalized to North Atlantic Shale Composite (NASC). The Triassic phosphorite is slightly depleted relative to the NASC, in contrast the Cretaceous phosphorite shows strong enrichment. While the Triassic samples indicate negative Ce and Eu anomaly, the Cretaceous ones show positive anomaly. Based on the redox-sensitive proxies defined by MORFORD & EMERSON (1999), such as Th/U, V/Sc ratios and REEs, both phosphorite occurrences formed in anoxic environment, however the Cretaceous was closer to the suboxic conditions. The  $\delta^{13}\text{C}$  and  $\delta^{18}\text{O}$  stable isotope data may result in further refinement regarding the formation circumstances.

FÜLÖP, J. (1975): *Geol. Hung.*, 16, 1-225

KISS, J., VIRÁGH, K. (1959): *Bull. Hung. Geol. Soc.*, 89, 85-97

MORFORD, J.L., EMERSON, S. (1999): *Geochim. Cosmochim. Acta*, 63, 1735-1750

## **Rb<sub>2</sub>Ca<sub>2</sub>Si<sub>3</sub>O<sub>9</sub>: THE FIRST RUBIDIUM CALCIUM SILICATE**

Müllner, M.<sup>1</sup>, Schmidmair, D.<sup>1</sup>, Kahlenberg, V.<sup>1</sup> & Perfler, L.<sup>1</sup>

<sup>1</sup>Institute of Mineralogy and Petrography, University of Innsbruck, Innrain 52, A-6020 Innsbruck  
e-mail: volker.kahlenberg@uibk.ac.at

The last ten years have seen a revival of interest in the ternary systems containing silica and alkali as well as alkaline-earth oxides. While the system Na<sub>2</sub>O–CaO–SiO<sub>2</sub> has been in the focus of applied mineralogy and inorganic chemistry for decades due to its fundamental importance for glass industry, the remaining systems have been relegated to the backwaters of silicate research. However, this situation has gradually changed. For the system K<sub>2</sub>O–CaO–SiO<sub>2</sub>, for example, more than nine compounds have been structurally characterized only recently. The results of these investigations correct older phase analytical studies not only what concerns the number of existing compounds but also what concerns their melting behaviour. It has to be emphasized that these findings are of fundamental importance for any thermodynamic modeling of multinary systems implemented in software packages such FactSage or ThermoCalc which are frequently used in computational thermochemistry.

In the course of an ongoing research project on the compound formation in the abovementioned systems we synthesized the first rubidium calcium silicate with composition Rb<sub>2</sub>Ca<sub>2</sub>Si<sub>3</sub>O<sub>9</sub>, the crystal structure of which has been characterized by X-ray diffraction techniques. Crystal growth was accomplished by the flux technique in closed platinum capsules using a ceramic precursor as well as RbCl as a mineralizer. The crystal structure was solved from a single-crystal diffraction data set acquired at 23°C and refined to a final residual of R(|F|) = 0.022 for 1871 independent reflections. Basic crystallographic data are as follows: monoclinic symmetry, space group type *P1n1*, *a*=6.5902(3)Å, *b*=7.3911(3)Å, *c*=10.5904(4)Å, β=93.782(3)°, *V*=514.72(3)Å<sup>3</sup>, *Z*=2. With respect to the silicate anions the compound can be classified as a sechser single-chain silicate. The undulated chains run parallel to [101] and are connected by Rb and Ca cations, which are distributed among four crystallographically independent sites. In a first approximation the coordination polyhedra of the two different calcium ions in the asymmetric unit can be described by distorted trigonal prisms and tetragonal pyramids, respectively. The two rubidium sites exhibit more irregular coordination spheres with 8–9 neighbors. Structural investigations on the new phase were completed by solid state Micro-Raman spectroscopy.

## SILICATES – A NEW CHALLENGE FOR MINERAL PROCESSING AT LKAB IN KIRUNA, NORTHERN SWEDEN.

Niiranen, K.<sup>1</sup>

<sup>1</sup>Specialist in Process Mineralogy / LKAB, SE-98186 KIRUNA, Sweden  
e-mail: kari.niiranen@lkab.com

LKAB (Luossavaara-Kiirunavaara AB) is operating an underground iron ore mine, three concentration and three pelletizing plants in Kiruna. Methods of mineral processing consist of wet low intensity magnetic separation (WLIMS) and reverse apatite flotation, in which magnetic separation is regarded as the crucial part of silicate mineral separation. The high-grade iron ore deposit at Kiirunavaara has today a rather low grade of silica *in situ*, approximately 2.3 to 3.3 % SiO<sub>2</sub>. However, the silica grade is expected to increase in incoming material to cobbing plant in the future based on information generated from exploration and grade control drilling. The iron ore deposit is used to be divided into three ore types based on their chemistry and mineralogy: ore type B1 (low P, low SiO<sub>2</sub>), ore type B2 (low P, high SiO<sub>2</sub>) and ore type D (high P, low to high SiO<sub>2</sub>). The ore types B2 can be regarded as critical related to the problem with high SiO<sub>2</sub> grade. Because the silicate minerals and quartz are the only source of silica (SiO<sub>2</sub>) in the crude ore, the mineralogy of silicates impacts undoubtedly the silica grade in the final product, i.e. the iron ore pellets. It was essential to investigate the mineralogy of silicates and their behaviour in laboratory scale mineral processing tests with a focus on the ore B2.

The mineralogical analysis with QEMSCAN was an essential part of the mineralogical investigations not only for determining the modal mineralogy, distribution of silicates and deportment of silicon (Si), but also for the investigation of the degree of liberation and intergrowth of magnetite with various silicates. Magnetite (Fe<sub>3</sub>O<sub>4</sub>) is the only ore mineral of economic value in the deposit. Besides apatite, green minerals of the amphibole group, mostly actinolite, are the most common gangue minerals. Phlogopite, titanite, ilmenite, rutile, quartz, talc, albite and Ca-sulphates may occur, but commonly in lesser quantities as well as carbonates and sulfide minerals.

As an important conclusion can be noted the discovery of two separate subtypes (B2-a and B2-b) within the ore type B2 based on the mineralogical data, which also seem to differ in the mineral processing properties. The subtype B2-a is characterized by actinolite and the subtype B2-b by phlogopite and quartz, but also by albite in some cases. As second conclusion can be noted that the degree of the liberation of magnetite seems to be high for most cases especially in the finest particle size classes. When not liberated, the binary intergrowth of magnetite and the silicates is the most common type of mineral association. The intergrowth of magnetite and two or more silicates (ternary) appears to be rare. Intergrowth of magnetite and actinolite is the most common type in the subtype B2-a, but also magnetite and phlogopite in some cases. Intergrowth of magnetite and actinolite is presumably also the most problematic regarding to magnetic separation and to the SiO<sub>2</sub> grade in the magnetite concentrate at the beneficiation plants. In the subtype B2-b intergrowths of magnetite and phlogopite, but also of magnetite and chlorite are the most common. Albite and quartz seems to be often fully liberated.

## PRODUCTION OF CORDIERITE / INDIALITE REFRACTORY AGGREGATE BY ELECTRIC ARC MELTING

Nilica, R.

RHI Technology Center, Magnesitstrasse 2, 8700 Leoben, Austria  
e-mail: Roland.Nilica@rhi-ag.com

Due to its unique properties cordierite is an interesting refractory material. Usually, cordierite is formed during the sintering process by mixing raw materials corresponding to the chemical composition of cordierite. These might be pure oxides or mixtures e.g., of kaoline, clay, talc, sepiolite and chlorite. In the course of cordierite formation the ceramic body shows a softening behavior, which sometimes has a negative impact in the refractory production. Additionally, a high cordierite content of the sintered body is desired. The aim of this work is to develop a refractory aggregate with high cordierite content. Beside sintering the use of electric arc furnaces is a common technique for the production of refractory aggregates. Especially for compounds showing congruent melting behavior like  $\text{MgO}$ ,  $\text{Al}_2\text{O}_3$  or  $\text{MgAl}_2\text{O}_4$  this route is widely implemented. In most cases it is practically impossible to produce incongruent melting phases. Stoichiometric cordierite, respectively its high temperature modification indialite, is an incongruent melting compound but it is an option to use its ability to form mixed crystals. Based on literature data there are solid solutions, which are located in the primary indialite phase field within the ternary system  $\text{MgO-Al}_2\text{O}_3\text{-SiO}_2$ . Another difficulty for production is the high electric conductivity of melts with cordieritic composition which causes strong interactions with the carbon electrodes used for melting. This work shows a possible way to overcome difficulties of incongruent melting of cordierite. Furthermore, the influence on phase paragenesis due to strong reducing conditions is shown.



Figure 1. Fusion of ca. 400kg cordierite.

## THE HIGH-TECH METAL POTENTIAL OF PB-ZN MINERALIZATIONS IN THE EASTERN ALPS

Onuk, P.<sup>1</sup> & Melcher, F.<sup>1</sup>

<sup>1</sup>Lehrstuhl für Geologie und Lagerstättenlehre, Montanuniversität Leoben (Peter-Tunner-Straße 5, 8700, Leoben, Austria)

e-mail: peter.onuk@unileoben.ac.at

The “Ad-Hoc working Group on defining critical raw materials” of the European Union (EU) has identified twenty commodities as being critical; some of them are used in high-technology products and green technologies (EU, 2014). Austria hosts numerous mineralizations with significant potential of the rare high-tech metals germanium, gallium, indium and cobalt, as indicated by chemical data of sulphide ore concentrates. In the beginning of the 1990s, the long-lasting experience of Austrian companies in base metal mining from domestic sources was terminated by the closure of the zinc-lead mine at Bleiberg-Kreuth. Zinc, copper, lead and silver were the major commodities mined in deposits within Austria.

Erich Schroll was the first to analyze trace metals in domestic ores (SCHROLL, 1954; CERNY & SCHROLL, 1995). Modern, systematic research using state-of-the-art analytical methods, however, is almost completely missing. First LA-ICP-MS data from sphalerite, which is a major host for some high-technology metals, are presented as part of a re-evaluation of three major types of base metal deposits in the Eastern Alps.

- (1) Carbonate-hosted “Alpine-type” or “Bleiberg-type” deposits hosted by Triassic limestones and dolomites are characterized by low Fe, high Cd (~2000 ppm), Ge (200–400 ppm) and Tl concentrations (~100 ppm) in sphalerite and by the absence of Co, Cu, Ni and Ag.
- (2) Sedimentary exhalative deposits such as those found in the Pb-Zn district of the Graz Paleozoic formed during the Lower Devonian in an euxinic environment and are associated with submarine alkaline volcanism (WEBER, 1990). Our LA-ICP-MS investigations of sphalerite collected in the Silberberg exploration adit indicate up to 9 ppm Ge, 8 ppm Ga, 7 – 17 ppm In, 3–93 ppm Co, ~4wt% Fe and 2000 ppm Cd.
- (3) Vein deposits of different genesis and age are widespread in the Eastern Alps. Pb-Zn-mineralization at Meiselding located in the Gurktal Nappe is classified as a metamorphically overprinted SEDEX deposit, whereas the Pb-Zn mineralization of Vellach-Metnitz in the same tectonic unit shows vein-like NW-SE trending structures (WEBER, 1997). High indium concentrations have been previously reported for the Zn-Cu-Pb veins of Koprein (Paleozoic of the Karawanken Range). LA-ICP-MS analyses of sphalerite show between 10 and 40 ppm In (maximum 300 ppm), Ge up to 2 ppm, Ga up to 10 ppm, Co 250 – 850 ppm, Cd 1120 – 3560 ppm, and Fe 2.8 – 6.5 wt%.

The re-evaluation of the most significant base metal sulphide occurrences in the Eastern Alps will provide valuable data for strategic planning related to the use of domestic resources.

CERNY, I., SCHROLL, E., (1995): Archiv für Lagerstättenforschung Geologische Bundesanstalt, 18, pp 5–33

EU (2014) : <http://ec.europa.eu/enterprise/policies/raw-materials/files/docs/crm-report>

SCHROLL, E., (1954): Mitteilungen der Österreichischen Mineralogischen Gesellschaft, Sonderheft 3, Wien

WEBER, L., (1997): Archiv für Lagerstättenforschung Geologische Bundesanstalt, 19, pp 1–607

## MINERALOGISCHE STREIFZÜGE ZU LAGERSTÄTTEN DER SILBER-ZINN FORMATION UND SELENVORKOMMEN BOLIVIENS UND NW-ARGENTINIENS

Paar, Werner H.

Pezoltgasse 46, 5020 Salzburg, Austria

Im Zeitraum von 1993 bis 2008 wurden zahlreiche Lagerstätten der Silber-Zinn-Formation und Selenvorkommen Boliviens und NW-Argentiniens im Rahmen von zwei FWF-Projekten und Projekten der Kommission für Rohstoffforschung der ÖAW lagerstättenkundlich untersucht. Besonderes Augenmerk galt der Rohstoffmineralogie, vor allem in Hinblick auf seltene Elemente. Die Lagerstätten der Silber-Zinn-Formation zählen zu den epimesothermalen Bildungen, sind gangförmig ausgebildet und polymetallisch. Sie stehen im genetischen Zusammenhang mit dem jungen Vulkanismus der Anden. In Abhängigkeit von den Hauptmetallen und dem Alterationstypus (high sulfidation, intermediate sulfidation) unterscheidet man Gold-, Gold-Kupfer-, Silber-Zinn- und Silberlagerstätten. Im Vortrag werden Beispiele der beiden letztgenannten Typen vorgestellt. Im einzelnen werden die Lagerstätten Porco (Bolivien) und Pirquitas (NW-Argentinien) mit ihrer exotischen Erzmineralogie präsentiert. In Porco wurde erstmals eine ausgedehnte Indium- und Germaniumführung festgestellt. Erstere ist auf indiumreichen Sphalerit und Roquesit, letztere auf den Germaniumträger Argyrodit zurückzuführen. Die Silber-Zinn-Zink-Blei-Lagerstätte Pirquitas zeichnet sich durch eine besonders komplexe Erzmineralogie aus, die durch das Auftreten von Zinnkiesen (Stannit, Kesterit, Ferrokesterit, Hocerit-Pirquitasit), zinnhaltigen Sulfosalzen (Kylindrit, Potosit, Teallit), Te-Canfieldit, Ag-Sb- und Ag-Bi- Sulfosalzen neben Sphalerit, Galenit und sehr vielen anderen Komponenten gekennzeichnet ist. Suredait und das Sulfosalz Coirait („Arsen-Franckit“) sind wichtige Zinnträger in den Abbauerzen und bislang nur aus Pirquitas bekannt (PAAR et al., 2008). Eine ausgedehnte Indiumanomalie ist auf indiumreichen Sphalerit und Kassiterit sowie auf indiumhaltigen Petrukit sowie Sakuraiit zurückzuführen. Die polymetallischen Lagerstätten von Capillitas, Catamarca, wurden kürzlich im Rahmen einer Dissertation lagerstättenkundlich und erzmineralogisch untersucht (PUTZ, 2005). Dabei wurde eine signifikante Germaniumanomalie diagnostiziert, die auf Briartit und die neuen Spezies Putzit, Catamarcait sowie „Ge-Stannoidit“ zurückgeführt werden kann. Spektakuläre Freigoldfunde aus unverritzten oberflächennahen Gangabschnitten sind hervorzuheben. Die telethermalen Selenvorkommen der Provinz La Rioja, Argentinien, zählen weltweit zu den wichtigsten Anreicherungen dieses Elementes. Im Vortrag wird auf die Selenerzvererzungen in der Sierra de Umango und von Los Llanenes eingegangen, die sich durch eine bedeutende Edelmetallführung (Gold, Silber, Platin, Palladium) auszeichnen.

PAAR, W.H., MOELO, Y., MOZGOVA, N.N., ORGANOVA, N.I., STANLEY, C.J., ROBERTS, A.C., CULETTO, F.J., EFFENBERGER, H.S., TOPA, D., PUTZ, H., SUREDA, R.J. & BRODTKORB, M.K.de (2008): Mineralogical Magazine, 72(5), 1083-1101.

PUTZ, H. (2005): Ph.D. thesis, Universität Salzburg, Austria. 293 p.



**MODAL AND CRYPTIC METASOMATISM IN LITHOSPHERIC MANTLE  
WEDGE BENEATH COMALLO, RIO NEGRO PROVINCE, ARGENTINA**

Papadopoulou, M.<sup>1</sup>, Ntaflos, T.<sup>1</sup>, Bjerg, E.<sup>2</sup>, Gregoire, M.<sup>3</sup> & Hauzenberger C.<sup>4</sup>

<sup>1</sup>Department of Lithospheric Research, University of Vienna, Althanstrasse 14, 1090 Vienna, Austria

<sup>2</sup>INGEOSUR (CONICET-UNS) and Departamento de Geologia, Universidad Nacional del Sur, San Juan 670,  
8000 Bahia Blanca, Argentina

<sup>3</sup>GET, OMP, University of Toulouse III-CNRS-IRD, France

<sup>4</sup>Institute for Earth Sciences, University of Graz, Heinrichstrasse 26, 8010 Graz, Austria  
e-mail: a0904343@unet.univie.ac.at

Xenoliths from Comallo, N. Patagonia, are sp-lherzolites, sp-harzburgites, dunites, wehrlites and clinopyroxenites. The rock-forming minerals are olivine, ortho- and clinopyroxene and spinel. Amphibole and phlogopite are present as relicts, suggesting that the region was affected by modal metasomatism. The majority of xenoliths show a dominant well-equilibrated equigranular texture. Small rounded spinels and sulfides enclosed within olivine as well as amphiboles enclosed in clinopyroxenes indicate that these xenoliths were recrystallized. The recrystallized samples show secondary protogranular textures. The amphibole inclusions in clinopyroxenes indicate that the peridotite has experienced a dehydration reaction during the recrystallization process. Amphibole and phlogopite, where present, have been destabilized and show breakdown reactions at the margin, forming secondary ol, cpx and sp.

The clinopyroxene REE patterns display a concave-up shape in LREE and MREE whereas the HREE abundances are low. Depending on the presence or absence of amphibole and/or phlogopite the cpx REE patterns can be divided into two different groups, both of which show absence of Sr- and weak Zr, Hf and Ti-negative anomalies. These features combined with the REE patterns highlight a cryptic metasomatic event due to melt infiltration of alkali basaltic composition. The differences occurring between the two groups may indicate a differentiation at distance from the percolation front. A third group with steep patterns, negative slope and slightly positive Eu anomaly shows a progression from LREE enrichments to depleted HREE. A carbonatitic metasomatism is evidenced by the LREE enrichment as well as a positive Eu-anomaly combined with a negative Ti-anomaly.

Calculated equilibrium temperatures at 1.5 GPa using the cores of crystals range between 790°C and 950°C, whereas the estimated temperatures using the rims are ~70°C higher. Such temperatures are relatively low for the lithospheric mantle below Comallo indicating a cold environment which, combined with the fact that spinel and amphibole are frequently enclosed within olivine and clinopyroxene, suggest that recrystallization and re-equilibration took place at relatively low temperatures. Based on these calculations, lherzolites show lower equilibrium temperatures than most of the harzburgites, suggesting transport of harzburgites due to convection flows to deeper mantle areas, where the rocks have experienced a hydration process. This can be supported also by the fact that the modal metasomatism represented by the occurrence of disseminated amphibole and/or phlogopite appears to be related to the downgoing subducted Pacific slab. A model for peridotite phase melting trends in opx shows that the studied xenoliths have been affected by partial melting ranging between 18 and 25%.

## INVERSE MODELLING OF TI DIFFUSION IN OLIVINE

Petrishcheva, E.<sup>1</sup>, Jollands, M.<sup>2</sup> & Abart, R.<sup>1</sup>

<sup>1</sup>University of Vienna, Department of Lithospheric Research, Althanstrasse 14, A-1090, Vienna, Austria

<sup>2</sup>Research School of Earth Sciences, Australian National University, Canberra, ACT 0200, Australia

e-mail: elena.petrishcheva@univie.ac.at

The behaviour of trace elements in mantle minerals is of key importance in geochemistry and mantle petrology. In this study we investigate diffusion of titanium in olivine. Experimental observations, modelling, and computer simulations are presented. Titanium is initially deposited on the surface of oriented olivine single crystals in the form of buffer assemblages defining different silica activities. Our analysis reveals two principal features of the diffusion process at hand. On one hand a relatively high initial concentration of titanium on the crystal surface results in pronouncedly nonlinear diffusion. The measured volume distribution of titanium is far from being described by a simple solution of a linear diffusion equation, such as the standard error function. A dependence of diffusivity on concentration is revealed using a proper modification of the Boltzmann-Matano analysis. On the other hand an observed tail of the titanium concentration far inside the crystal shows a sudden jump from larger to lower values. We explain this behaviour by the effect of traps related to Al incorporation on the tetrahedral site. These traps are constantly filled by titanium, which only diffuses on the octahedral sub-lattice. The Ti trapped on tetrahedral sites becomes “inactive” in terms of diffusion but is detected in chemical analysis. The jump occurs at a position where free traps are still available. We discuss how the observed titanium concentration profiles can be derived from a mathematical model. The latter couples a nonlinear diffusion equation with a simple description of trap concentration. Finally we present the composition dependent diffusivities of Ti for different buffer assemblages and oxygen fugacities.

## AMBIGUOUS PORE PLUGGING DURING GEOTHERMAL REINJECTION – 3D-SANDSTONE CHARACTERIZATION AND EXPERIMENTAL SIMULATIONS

Petschacher, N.<sup>1</sup>, Hippler, D.<sup>1</sup>, Eder, M.<sup>1</sup>, Brunner, R.<sup>3</sup>, Böchzelt, B.<sup>2</sup> & Dietzel, M.<sup>1</sup>

<sup>1</sup>Institute of Applied Geosciences, Graz University of Technology, Rechbauerstrasse 12, 8010 Graz, Austria

<sup>2</sup>Technisches Büro Böchzelt, Ludersdorf 69, 8200 Gleisdorf

<sup>3</sup>Materials Center Leoben Forschung GmbH, Roseggerstraße 12, 8700 Leoben, Austria

e-mail: petschacher@hydro.or.at

The significant reduction of permeability of rocks during the reinjection of thermal water is a common and crucial phenomenon. The reduction can be attributed to (i) mobilization/re-deposition of fine particles, e.g., clay minerals, particulate metal (hydro-) oxides, within the pore space and/or (ii) temperature and pressure induced mineral precipitation. Although permeability decrease by above clogging mechanisms within the pore system causes high maintenance action and at times a breaking off criteria, individual causations are mostly not well established as e.g., local rocks might be highly heterogeneous, difficult to access and reaction paths and mechanisms are complex. In order to get insights into the potential clogging mechanisms several sandstone plugs and thermal solutions from Austrian and German geothermal sites were sampled for analyses, (hydro-) geochemical modeling, and conducting flow-through experiments.

Results from aqueous chemistry and modeling using PHREEQCI code indicate that a permeability reduction as a consequence of mineral precipitation is of minor importance for the selected sites. Thus flow-through permeability experiments for potential pore structure changes were carried out. Synthesized fluids containing NaCl and CaCl<sub>2</sub> at various concentrations and the sandstone plugs were used for the experiments, where temperatures ranged between 20 and 90°C and pressure gradients and fluid flow rates were monitored. Selected sandstone samples were - besides mineralogical and chemical bulk analyses - characterized before and after the experiment by (i) petrographic and scanning electron microscopy, (ii) HPHT fluidpermeameter, and (iii) X-ray microtomography. The latter was used to obtain a 3D-illustration of the pore structure and to map local arrangements and orientations of particles within the sandstone pore network. In the present contribution preliminary results of combined permeability data and pore micro-structure imaging are used to evaluate ambiguous pore plugging during geothermal reinjection in the aspects of permeability reduction as a function of temperature, pressure and ion composition of the thermal water as well as of the mineralogical composition of the sandstone.

**PETROLOGY AND GEOCHEMISTRY OF THE VIJAYAN COMPLEX  
(SRI LANKA)**

Petschnig, P.<sup>1</sup>, Hauzenberger, C. A.<sup>1</sup> & Fernando, G.W.A.R.<sup>3</sup>

<sup>1</sup>Institute of Earth Sciences, University of Graz (Universitätsplatz 2, 8010 Graz, Austria)

<sup>2</sup>Faculty of Geology, Hanoi University of Science (Hanoi, Vietnam)

<sup>3</sup>Department of Physics, Open University of Sri Lanka, Colombo, Sri Lanka  
e-mail: christoph.hauzenberger@uni-graz.at

Sri Lanka, with its central position within the Africa-India-Madagascar and East Antarctica collage of the late Neoproterozoic supercontinent of Gondwana, provides essential insights into the growth of the Neoproterozoic Earth. In respect to that the high grade basement of Sri Lanka is interpreted as a crustal segment of East Gondwana. The Precambrian basement of Sri Lanka is subdivided into four major terrains, from west to east: The Wannai Complex (WC), the Kadugannawa Complex (KC), the Highland Complex (HC) and the Vijayan Complex (VC). The HC is dominantly composed of meta-quartzites, marbles, calc-silicates, metapelites and charnockites gneisses. The granulite facies rocks were studied in detail and UHT metamorphism with T of up to 1150°C reported. The age could be constrained by U/Pb dating of zircon with ~550Ma.

In contrast, the metamorphic history of the Vijayan Complex, which consists mainly of migmatic orthogneisses, is poorly understood. While the age of metamorphism is similar to the Highland Complex, the grade of metamorphism seems to be lower. Garnet bearing gneisses as well as charnockitic layers in migmatic orthogneisses were investigated to constrain the PT conditions of this complex. We present results from geothermobarometry and P/T modelling using Perple\_X of several unique samples from different parts of the Vijayan Complex.

**EVOLUTION OF NANOSTRUCTURE AND SPECIFIC SURFACE AREA  
DURING THERMALLY DRIVEN DEHYDRATION OF  $\text{Mg}(\text{OH})_2$**

Pimminger, H.<sup>1</sup>, Freiberger, N.<sup>2</sup>, Habler, G.<sup>1</sup> & Abart, R.<sup>1</sup>

<sup>1</sup>University of Vienna, Department of Lithospheric Research, Althanstrasse 14 (UZA 2), 1090 Vienna, Austria

<sup>2</sup>RHI Technology Center, Magnesitstrasse 2, 8700 Leoben, Austria

e-mail: Norbert.Freiberger@rhi-ag.com

The thermally induced dehydration of micrometer sized particles of  $\text{Mg}(\text{OH})_2$  was investigated experimentally at ambient pressure and temperatures ranging from 350°C to 1300°C. Reaction progress is correlated with the evolution of the specific surface area and of the particle internal nanostructure. The maximum specific surface area of about 320 m<sup>2</sup>/g corresponding to a 70-fold increase relative to the starting material is obtained after heat treatment at 350°C for about two hours. This is due to the formation of a highly porous, particle-internal nanostructure comprised of newly crystallized strictly aligned, cube-shaped and nm sized crystals of MgO and about 50 vol. % porosity. Associated with the dehydration intensive fracturing and defoliation occurs parallel to the (0001) plane of the original  $\text{Mg}(\text{OH})_2$  or (111) of the topotactically grown MgO. After heat treatment at increasingly higher temperatures enhanced coarsening and sintering of the MgO crystals and healing of cracks leads to a successive decrease of the specific surface area. After heat treatment at 1300°C for two and a half hours the specific surface area has decreased to 5 m<sup>2</sup>/g close to the value typical for the original  $\text{Mg}(\text{OH})_2$ .

## SENSITIVE ORBICULAR DUNITE XENOLITHS FROM THE BASAL COMPLEX OF LA GOMERA

Pribil, B.<sup>1,2</sup>, Bakker, R.J.<sup>2</sup> & Zaccarini, F.<sup>2</sup>

<sup>1</sup>RHI Technology Center Leoben, Magnesitstr. 2, A-8700 Leoben, Austria

<sup>2</sup>Chair of Resource Mineralogy, Montanuniversität Leoben, Peter-Tunner-Str. 5, A-8700 Leoben, Austria

Exotic orbicular rock fragments of olivine grains (up to 3cm in length) have been found at the Playa de Vallehermoso, in the Miocene Basal Complex, which is the oldest geological unit of La Gomera (Canary Islands). The orbicular fragments are nodules of dunitic xenoliths, which are embedded in a fine-grained matrix of kaersutite, with minor amounts of chlorite, zoisite, sphe, diopside, calcite, magnetite and ilmenite. The contact between these zones is formed by narrow reaction rims, which have been generated by modal metasomatic reactions (olivine + kaersutite → tremolite + chlorite + titanite + magnetite). The complete mineralogy of the reaction rim is: tremolite, chlorite, sphe, magnetite, pyrite, chalcopyrite as well as relics of not completely reacted kaersutite.

The relatively Fe rich and coarse grained olivines of the dunites are characterised by a Fo# of 82%, i.e. Mg/(Fe+Mg), Ca contents of 500-5700µg/gram, NiO of 0.13-0.28mass% and MnO of 0.15-0.35mass%. Furthermore, the olivines are marked by an enrichment in incompatible (LREE, Th, U, Ta, Nb) and mobile (K, Rb, Ba) elements due to metasomatic processes, compared to chondrite, PM and MORB contents. Visible evidences of the metasomatism are magnetite and carbonatic precipitates in fluid inclusions within the olivines. Based on this data, a formation of the dunites as restites through a melting process of mantle peridotite can be excluded. Instead the genesis of the originally dunite is determined by olivine accumulation in a fractionating OIB melt. Naturally decorated dislocations, occurring in dense networks within the olivines, act as documents of a strong plastic deformation affecting the olivines before they were carried to the surface. Most of the dislocations have been identified as mixtures of edge and screw dislocations. The idiomorphic spinel phases, which are included in the olivines are mainly chromium-rich ferro- magnetites. Particularities are spinel phases revealing a “donut texture”. These are specific spinels of circular shape, which contain inclusions of intergrowth of pargasite and glass phases.

Calcite veins, which cross most of the plutonic rocks, are hosting a large number of elongated and regularly shaped fluid inclusions with an aqueous fluid. The average salinity of the fluids is 0.66mass% NaCl, the molar volume is ± 21.0cm<sup>3</sup>/mol and the density is 0.87g/cm<sup>3</sup>. The fluid's homogenisation temperature has been determined at 200 to 210 °C. The veins formed due to hydrothermal alteration cells of infiltrating sea-water and degassing CO<sub>2</sub> in the basic rocks. The veins can be interpreted as the result of metasomatism, which liberated Ca-ions from the host rock that combined with CO<sub>2</sub> from a magmatic source to carbonic veins.



**MARMORA CUM RADIIS VERNANTUR, CERNE, SERENIS  
- FINGERPRINTING OF ANCIENT MARBLES**

Prochaska, W.

Department of Applied Geosciences and Geophysics, University of Leoben  
Peter Tunner Straße 5, A-8700 Leoben, Austria  
e-mail: walter.prochaska@unileoben.ac.at

The topic of this paper is to give an overview of the methods to pinpoint the origin of white marbles and to discuss the progress made in this field during the last years. To define the place of origin of the marble of an artefact to an area or even to a special quarry may be of appreciable importance in investigating ancient trading routes and trade relations. A material-specific classification can be conducive to understand if the workshops of an area used marbles of acceptable quality from local quarrying areas or if they used imported marbles in or without combination with local ones. Furthermore during restoration activities the knowledge of the origin of the marbles used in architecture may be of importance for supplying more or less original types of marbles. The knowledge of the marble provenance may also be of interest and of considerable importance for evaluating the authenticity of an artefact.

With the advent of stable isotope analysis of carbonate rocks, a new method seemed to be at the archaeologists' hand to assign a marble sample precisely to its origin. However, with the rapidly increasing number of historical marble quarrying sites and with the increasing number of analysed samples in general, the compositional fields in the isotope diagram became larger and many classical marbles showed relatively large ranges of overlap.

Additional variables can be obtained by chemical analysis of the marbles. Because of their relatively homogeneous distribution, only those elements were analysed that are incorporated into the carbonate lattice (Mg, Fe, Mn, Sr and Zn).

A technique for characterizing marbles was developed which can be used in concert with the established methods. The proposed method is based on the "crush and leach" analysis of extractable total dissolved solids -TDS- from marbles and carbonate rocks in general. Samples available from sculptures etc. are very limited in size. Therefore heterogeneity is one of the main problems of conventional provenance detection methods, using the chemical or isotopic composition of marbles to identify their origin. Metamorphism is an isochemical process and does not homogenize the chemical differences of the protolith (carbonate sediments in the case of marbles). The results from fluid inclusion investigations of carbonate rocks show that the fluid phase is usually relatively uniform with respect to its chemical composition.

To demonstrate the usability of this method several case studies will be presented. These will include examples of the use of the above mentioned methods in the detection of forgeries and replicas. The recent discovery of an ancient marble quarrying region in Asia minor which supplied the most important portrait marble in roman imperial times and the diachronic change of portrait marble of the imperial portraits throughout 5 centuries will be discussed.

## MONITORING THE MINERALOGICAL PATHWAY OF AMORPHOUS CALCIUM CARBONATE TRANSFORMATION USING IN SITU RAMAN SPECTROSCOPY

Purgstaller, B.<sup>1</sup>, Mavromatis, V.<sup>1</sup>, Konrad, F.<sup>1</sup> & Dietzel, M.<sup>1</sup>

<sup>1</sup>Graz University of Technology, Institute of Applied Geosciences, Rechbauerstraße 12, 8010 Graz, Austria  
e-mail: bettina.purgstaller@tugraz.at

It has been earlier postulated that amorphous calcium carbonate (ACC) plays a significant role in  $\text{CaCO}_3$  biomineralization processes (ADDADI et al., 2003). The transformation pathways of ACC (e.g. to calcite or aragonite) are likely affected by various physicochemical parameters including aqueous Mg and pH.

In order to better understand the mechanisms controlling ACC formation and transformation, precipitation experiments were carried out under controlled physicochemical conditions (constant pH and  $T = 25^\circ\text{C}$ ). The precipitation of  $\text{CaCO}_3$  was induced by the addition of a 0.6 M  $(\text{Ca,Mg})\text{Cl}_2$  solution at distinct Mg/Ca ratios (1:4 to 1:8) into a 1 M  $\text{NaHCO}_3$  solution. During the synthesis, the pH of the reactive solution was kept constant at 7.8, 8.3 or 8.8 by the addition of a 1 M NaOH solution using an automated  $\text{pH}_{\text{stat}}$  titration unit. The temporal evolution of mineral precipitation was monitored by *in situ* Raman spectroscopy.

The results revealed two pathways of ACC transformation. In experiments with Mg/Ca ratios of 1:4 and 1:6 at pH 8.8, Mg-rich ACC acts as a precursor phase for monohydrocalcite formation (Figure 1). In a second stage, this monohydrocalcite transformed to aragonite. In contrast, in experiments with Mg/Ca ratios of 1:4 and 1:6 at pH 8.3 and at the lowest Mg/Ca ratio of 1:8 at pH 8.8, Mg-rich calcite formed via an intermediate Mg-rich ACC phase. The formation of ACC could not be detected by Raman spectroscopy in experiments that were carried out at pH 7.8 and in the experiment with a Mg/Ca ratio of 1:8 at pH 8.3.

The results are discussed in the light of Mg and pH effect on ACC precipitation environments and transformation to distinct carbonate mineral phases.

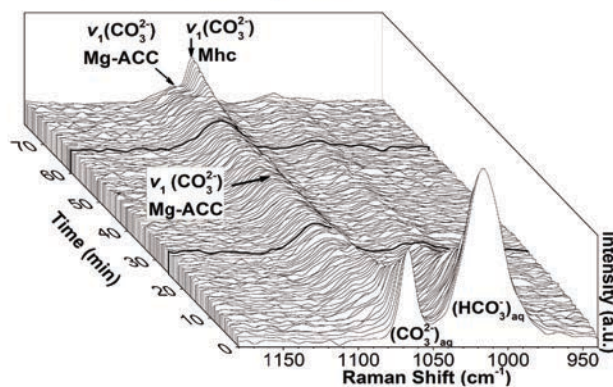


Figure 1. Waterfall plot of *in situ* Raman spectra collected for 75 min of reaction time of the experiment with Mg/Ca ratio 1:4 and pH 8.8.

ADDADI, L., RAZ, S., WEINER, S. (2003): Adv. Mater., 15, 959-970.

**PETROLOGICAL AND GEOCHEMICAL COMPARISON OF MEGACRYSTS  
FROM VIETNAM, LAOS AND THAILAND**

Raič, S.<sup>1</sup>, Hauzenberger, C.A.<sup>1</sup>, Konzett, J.<sup>2</sup>, Hoang, N.<sup>3</sup> & Khoi, N.N.<sup>4</sup>

<sup>1</sup>University of Graz, Universitätsplatz 2, 8010 Graz, Austria

<sup>2</sup>University of Innsbruck, Innrain 2, 6020 Innsbruck, Austria

<sup>3</sup>Vietnam Academy of Science & Technology, 84 Chua Lang, Dong Da, Hanoi, Vietnam

<sup>4</sup>Hanoi University of Science, 334 Nguyen Trai, Thanh Xuan, Hanoi, Vietnam

e-mail: sara.raic@edu.uni-graz.at

Neogene alkali basalts are commonly found within the Indochina Plate and are known to contain various megacrysts and mantle xenoliths. While lherzolitic and harzburgitic xenoliths represent the underlying mantle, the formation and origin of megacrysts is less well understood. Therefore a number of megacrysts (clinopyroxene, spinel and zircon) and some associated mantle xenoliths (spinel lherzolite) from different localities in Vietnam, Laos and Thailand was sampled, in order to compare their origin, genesis, as well as characterize their textural and compositional variations. Petrographic features of megacrysts from the southern and southeastern parts of Vietnam (Ba Ria – Vung Tau province, Dalat province, Dak Nong province and Gia Lai province), the southern Laos region (Attapeu and Champasak), and the Bo Phloi District in Thailand revealed the following textural varieties: Large black to smoky-brown, subhedral fractured clinopyroxene crystals and orange to reddish coloured zircon are typically the most abundant megacryst phases. Clinopyroxene megacrysts can reach up to 4cm with a few hosting small inclusions of sulfide-patches (chalcopyrite + pentlandite) rimmed by ilmenite and magnetite. Light orange colored zircon (up to 1cm) is optically zoned (darker cores); smaller (up to 0.3cm) fractured one is dark orange to deep red in colour and hosts oxide inclusions along rims. Spinel megacrysts appear as gray to almost opaque fragments (up to 0.7cm). Large olivine crystals are found in basaltic rocks which are fractured and show commonly altered rims to iddingsite.

Characterization of mineral composition, a comparison of trace element concentrations in megacrysts, as well as the modelling of parent magma compositions will be performed, in order to describe the nature of the lithospheric mantle beneath the Indochina plate along a W-E-profile (Thailand to Vietnam). The financial support by the Austrian Academy of Sciences and ASEA-Uninet is gratefully acknowledged. This is a contribution to IGCP 557.

**CONTROLS ON MINERALIZATION IN THE BATHTUB INTRUSION, BABBITT DEPOSIT (DULUTH COMPLEX, MINNESOTA, USA): HALOGEN VARIATIONS IN APATITE AND COEXISTING FLUID INCLUSIONS**

Raič, S.<sup>1</sup>, Mogessie, A.<sup>1</sup> & Krenn, K.<sup>1</sup>

<sup>1</sup>University of Graz, Universitätsplatz 2, 8010 Graz, Austria  
e-mail: sara.raic@edu.uni-graz.at

The Cu-Ni ± PGE Babbitt deposit (Bathtub intrusion) of the 1.1 Ga old Duluth Complex (NE-Minnesota) is known for its mineralized structurally affected heterogeneous basal units (troctolite, gabbro, norite) with metasedimentary hornfelsic footwall inclusions, as well as underlying footwall portions (Virginia Formation). Horizons of massive sulfides are restricted to underlying footwall units (Virginia Formation) and follow the direction of an E-W trending anticline within the footwall rocks. This distribution of mineralization is thought to be associated with the N-trending Grano Fault that was reactivated during the emplacement of the Duluth Complex. Assemblages of composite sulfide patches (pyrrhotite + pentlandite + chalcopyrite + cubanite) represent the main phases of the primary magmatic sulfide mineralization within troctolitic hosts. Platinum group minerals are either associated with the primary magmatic mineralization or found within hydrothermally altered portions, indicating the potential role of aqueous complexes in the transport and redistribution of PGEs (platinum-group elements).

Analysis of apatite from troctolites show pronounced trends in halogen contents: along an E-W-profile away from the Grano Fault the Cl-content in apatite is decreasing (from 1.6 wt. % to 0.2 wt. %) with increasing fluorine composition (from 2.2 wt. % to 3.3 wt. %). With increasing structural height above the mineralized basal Babbitt units similar trends of halogens are displayed by apatite. Textural differences of magmatic apatite grains are shown by detailed back scattered electron (BSE) imaging comprising euhedral inclusions in olivine or plagioclase with growth zonation, subhedral grains between olivine-plagioclase interfaces or overgrowth textures, larger fractured or acicular inclusions in plagioclase and pyroxene. Concentric or oscillatory zoned apatite inclusions (with regard to La<sub>2</sub>O<sub>3</sub>, Ce<sub>2</sub>O<sub>3</sub> and Nd<sub>2</sub>O<sub>3</sub> contents) are thought to represent the effects of magmatic differentiation; overgrowth textures could be linked to late hydrothermal processes.

The presence of primary and secondary fluid inclusions and fluid inclusion planes hosted by quartz, plagioclase, pyroxene and apatite from footwall units (Virginia Formation and underlying Biwabik Iron Formation) and overlying troctolites, as well as the Cl-enrichment in apatite in ore-bearing rocks suggests the involvement of aqueous complexes in the transport and redistribution of platinum group elements. FWF (P23157-N21) financial support to A. Mogessie is acknowledged.

## Nb-Ta MINERALISATION IN LITHIUM PEGMATITES IN THE EASTERN ALPS

Raith, J.G.<sup>1</sup>, Ahrer, S.<sup>1</sup>, Mali, H.<sup>1</sup>, Stocker, K.<sup>1</sup>, Melcher, F.<sup>1</sup>,  
Sitnikova, M.<sup>2</sup> & Hauzenberger, C.A.<sup>3</sup>

<sup>1</sup> Department of Applied Geosciences and Geophysics, Montanuniversität Leoben (Peter-Tunner Straße 5, 8700 Leoben, Austria)

<sup>2</sup> Bundesanstalt für Geowissenschaften und Rohstoffe (Stilleweg 2, 30655 Hannover, Germany)

<sup>3</sup> Institute of Earth Sciences, University of Graz (Universitätsplatz 2, 8010 Graz, Austria)

e-mail: johann.raith@unileoben.ac.at

Results are presented on the evaluation of pegmatites in the Eastern Alps for niobium-tantalum (coltan) mineralisation. Spodumene bearing pegmatites were studied at Hohenwart, Lachtal, Mitterberg, Garrach, and the lithium deposit at Weinebene/Koralpe. All these pegmatites are of Permian age and occur in the Austroalpine Koralpe-Wölz nappe, which is characterised by Permian low-P and Eoalpine high-P metamorphism. The immediate host rocks of the often (sub)-concordant, normally zoned pegmatites are metapelites and metacarbonate rocks.

Heavy mineral concentrates were extracted from several kg of pegmatite material, using different beneficiation methods, and then investigated (polished grain mounts) by optical microscopy, EMPA, MLA and LA-ICP-MS techniques (AHRER, 2014). SEM-based determination of the modal mineralogy by MLA allowed to quantify the amounts of Nb-Ta minerals and, in combination with EMPA, to identify the Nb-Ta phases. Higher amounts (up to 16 %) of Nb-Ta minerals were found in the Wölzer Tauern area (Hohenwart, Lachtal). The Nb-Ta mineralogy is variable and seems to be influenced by the pegmatite host rocks. Whereas in micaschist-hosted pegmatite samples columbite-tantalite group minerals dominate, a few samples from Hohenwart hosted in marbles show predominance of pyrochlore- and microlite-group minerals. The Mn/(Mn/Fe) of columbite-tantalite ranges between 27-73%, Ta/(Ta+Nb) between 6-63%. Different types of zoning are recorded by columbite-tantalite.

Major and trace element concentrations determined in muscovite by LA-ICP-MS and ratios (K/Rb, K/Tl) can be successfully used as a proxy for pegmatite fractionation although these parameters are not well correlated with Nb and Ta concentrations in mica. Nevertheless, these parameters can be used as a guide to Nb-Ta mineralized pegmatite bodies/zones. Samples with K/Rb less than ~40 always contained distinct Nb-Ta minerals.

Funding of this project by FFG (#838953) within the „Produktion der Zukunft“ scheme is gratefully acknowledged.

AHRER, S. (2014): Masterarbeit, Montanuniversität Leoben, 105 S.

## CHEMICAL INDUCED CRACK PROPAGATION IN Na-K EXCHANGED ALKALI FELDSPAR

Rieder, M.<sup>1</sup> & Abart R.<sup>1</sup>

<sup>1</sup>Department of Lithospheric Research, University of Vienna, Althanstraße 14, 1080 Wien, Austria  
e-mail: m.rieder@univie.ac.at

The lattice parameters of alkali feldspar show considerable composition dependence. As a consequence any compositional gradient within a single crystal of alkali feldspar induces coherency stress, which may lead to fracturing, if the mechanical strength of the crystal is exceeded. We investigated chemically-driven crack propagation in partially ion-exchanged alkali feldspar. For this purpose gem-quality alkali feldspar from Volkesfeld (Eifel, Germany) with initial composition  $X_{Or}=0.85$  and with either (010) or (001) surfaces polished was exchanged with NaCl-KCl salt melt at 850°C and ambient pressure. Two different salt compositions with  $X_{KCl}=0.25$  and  $X_{KCl}=0.3$  were used. Salt was applied in excess to ensure equilibrium compositions of  $X_{Or}=0.50$  and  $X_{Or}=0.65$ , respectively, for exchanged alkali feldspar. Run durations were 2, 4, 8 and 16 days. In all experiments sets of parallel cracks evolved parallel to the [010] direction of alkali feldspar, which are inclined by about 99°, measured from the positive [100] direction towards the positive [001] direction. In all experiments crack lengths increased, and the rate of crack propagation decreased with time. For given run duration and polished surface, cracks were longer when exchanging with the more sodium-rich melt ( $X_{KCl}=0.25$ ) than when exchanging with the less sodium-rich melt ( $X_{KCl}=0.30$ ). For a given run duration and salt composition cracks emanating from polished (001) surfaces were considerably longer than cracks emanating from polished (010) surfaces. Element distribution maps revealed Na-rich halos accompanying these cracks. These halos are relatively narrow and hardly overlap between neighbouring cracks emanating from (010) surfaces, and they are wider and show substantial overlap between neighbouring cracks emanating from (001) surfaces. As a consequence compositional gradients perpendicular to the (010) surface and, hence, driving force for Na-K interdiffusion in this direction are less pronounced in the crystal domains between cracks emanating from (010) surfaces than for cracks emanating from (001) surfaces. Overall Na-K exchange in the alkali feldspar domains between neighbouring cracks is less efficient for cracks emanating from polished (010) surfaces than for cracks emanating from polished (001) surfaces. As a consequence there is overall less compositional strain and thus less need for stress relaxation by fracturing for cracks emanating from (010) surfaces than for cracks emanating from (001) surfaces. This is in line with the systematic difference in length between cracks emanating from the (001) and (010) surfaces.

It is interesting to note that cracks emanating from (010) surfaces propagate in the direction perpendicular to the (010) plane, whereas the propagation direction of cracks emanating from (001) surfaces lies within the (010) plane. Na-K interdiffusion in alkali feldspar is highly anisotropic with diffusion along the [010] direction being relatively slow and diffusion for most of the directions within the (010) plane relatively fast. Thus the rates of crack propagation show similar direction dependence as Na-K interdiffusion in alkali feldspar suggesting that the rate of crack propagation is controlled by Na-K interdiffusion.



**RADIOMETRIC DATING AND ENVIRONMENTAL INFORMATION  
FROM TWO ACTIVE STALAGMITES IN KATERLOCH CAVE**

Sakoparnig, M.<sup>1</sup>, Boch, R.<sup>1</sup>, Wang, X.<sup>2</sup>, Spötl, C.<sup>3</sup> & Dietzel, M.<sup>1</sup>

<sup>1</sup>Institute of Applied Geosciences, Graz University of Technology, Rechbauerstraße 12, 8010, Graz, Austria

<sup>2</sup>Earth Observatory of Singapore, Division of Earth Sciences, 50 Nanyang Av., 639798, Singapore

<sup>3</sup>University of Innsbruck, Institute of Geology, Innrain 52, 6020, Innsbruck, Austria

e-mail: marlene.sakoparnig@edu.uni-graz.at

Katerloch Cave located north of Graz at the SE-rim of the Alps is well known for its impressive dripstone occurrence, e.g. up to several metres tall candle-stick-type stalagmites. Research activities in recent years focused on utilizing such speleothems from Katerloch as a high-resolution paleoclimate archive (Boch et al., 2009) and for studying the particular stalagmite growth dynamics and omnipresent seasonal lamination found in these chemical sediments (Boch et al., 2011).

In the course of a M.Sc. thesis project, we collected two actively-forming stalagmites from different cave sections combined with monitoring of major environmental parameters including automatic logging of drip-rates and temperature, as well as chemical- and isotopic compositions of drip waters. Stalagmite K10 (71 cm in length) was recovered from the deepest cave section showing a nearly constant temperature of 5.7 °C, while K8 (40 cm) was located in the largest chamber growing at 3.7 °C. In order to constrain the age of the growth inception and older stalagmite portions we applied MC-ICP-MS <sup>238</sup>U-<sup>234</sup>U-<sup>230</sup>Th dating in connection with careful petrographic inspection. K10 revealed relatively low U concentrations of 19-127 µg/kg and low detrital Th contributions, resulting in typical age-uncertainties (2σ) of 0.7 to 3 %. Several time intervals from 129.1 ± 1.2 kyr before present (Last Interglacial) up to now are represented in the stalagmite calcite separated by distinct growth interruptions and mostly reflecting relatively warm and humid climate intervals favourable for speleothem deposition. Stalagmite K8, in contrast, captured a relatively short time interval of the last ca. 2000 years, but suffers from overall less precise age constraints.

Focusing on the most recent, historical and Late Holocene time intervals of stalagmite growth and associated (paleo) environmental conditions we conducted high-resolution, micromill-based carbonate sampling along the stalagmite growth axes for stable carbon and oxygen isotope analyses. K10 isotope profiles obtained at 0.25 mm resolution show δ<sup>13</sup>C values ranging from -9.3 to -4.6 ‰ and δ<sup>18</sup>O from -8.0 to -5.1 ‰ VPDB. K8 (0.1/1 mm res.) revealed values from -11.0 to -3.8 ‰ and -7.4 to -4.5 ‰ for δ<sup>13</sup>C and δ<sup>18</sup>O, respectively. These highly variable isotopic compositions are discussed with regard to temporal variations of the determining environmental conditions, as well as spatial differences within the cave system. Moreover, the isotopic composition and evolution of the younger stalagmites K10 and K8 are compared to data from Katerloch stalagmites of older time intervals and further to multi-annual monitoring data.

BOCH, R., SPÖTL, C., KRAMERS, J. (2009): *Quat. Sci. Rev.*, 28, 2527-2538.

BOCH, R., SPÖTL, C., FRISIA, S. (2011): *Sedimentology*, 58, 508-531.

# HIGH PRESSURE GRANULITES FROM THE SOUTHEASTERN MARGIN OF THE BOHEMIAN MASSIF, AUSTRIA

Schantl, Ph.<sup>1</sup>, Hauzenberger, Ch.<sup>1</sup> & Linner, M.<sup>2</sup>

<sup>1</sup>Institute of Earth Sciences, University of Graz, Universitätsplatz 2, A-8010 Graz, Austria

<sup>2</sup>Geologische Bundesanstalt, Neulinggasse 38, A-1030 Wien, Austria

e-mail: philip.schantl@edu.uni-graz.at

High pressure granulites play a key role in the geodynamic reconstruction of deep subducted or overthickened continental crust. One of the most spectacular areas to study such enigmatic rocks is the southeastern margin of the Bohemian Massif (BM) in Lower Austria, close to the River Danube. There, the BM is occupied by the high grade Gföhl Nappe System of the Moldanubian Zone which exposes predominately fresh leucocratic granulites accompanied by subordinate amounts of mesocratic pyroxene bearing granulites in its uppermost position. Both granulite types outcrop in locally separated massifs which, from south to north, are the Pöchlarn-Wieselburg, the Dunkelsteinerwald and Zöbing massifs. Ultra high temperature (UHT) conditions of 950-1150°C and 20-22kbar have been calculated from leucocratic granulites comprising the mineral assemblage quartz + ternary feldspar (now mesoperthitic K-feldspar) + garnet + kyanite + rutile (Fig.1A). Garnet zoning profiles display a distinct grossular plateau with high  $X_{\text{Grs}}$  values of about 0.3, in contrast to values of about 0.05 at the outermost rim (Fig. 1B). The pronounced zoning in garnet indicates that the UHT event must have been short lived since diffusion in this temperature region is usually sufficient fast to homogenize any prograde zoning pattern. However, the homogeneous cores might also be interpreted as the result of homogenization and the zoning pattern at the rims is the result of an additional growth phase which is obscured by additional diffusional processes. The general mineral assemblage of mesocratic pyroxene bearing granulites consists of quartz + mesoantiperthitic plagioclase + orthopyroxene + garnet. The presence of orthopyroxene and the lack of clinopyroxene, indicates reequilibration at medium pressure where orthopyroxene forms after garnet, clinopyroxene and quartz (e.g. GREEN & RINGWOOD, 1967).

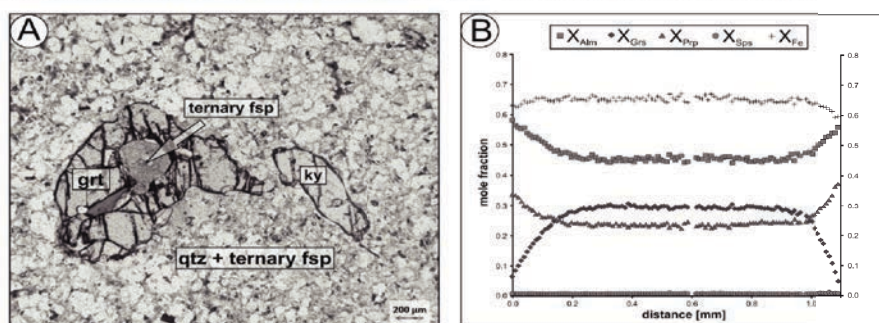


Figure 1. (A) High pressure mineral assemblage of leucocratic granulites from the Dunkelsteiner Wald Massif and (B) Garnet profile with grossular plateau indicating high pressure metamorphic conditions for core growth.

### THREE PHASE GARNET GROWTH IN THE SOUTHEASTERN GRAZ PALEOZOIC AND ADJACENT ANGER CRYSTALLINE UNIT

Schantl, Ph.<sup>1</sup>, Röggla, M.<sup>1</sup>, Schuster, R.<sup>2</sup>, Krenn, K.<sup>1</sup>, Hauzenberger, Ch.<sup>1</sup> & Hoinkes, G.<sup>1</sup>

<sup>1</sup>Institute of Earth Sciences, University of Graz, Universitätsplatz 2, A-8010 Graz, Austria

<sup>2</sup>Geologische Bundesanstalt, Neulinggasse 38, A-1030 Wien, Austria

e-mail: philip.schantl@edu.uni-graz.at

Chemical zoning patterns as well as textural evidence from garnet porphyroblasts from the Raasberg Mountain (Styria/Austria) in the southeastern part of the Graz Paleozoic (GP) point to a polymetamorphic evolution. Similar patterns are also found in the underlying Austroalpine crystalline complexes, referred to as Anger Crystalline Unit (ACU). The investigated micaschists of the GP belong to the Gösselhof Lithodeme, which is part of the uppermost Gschnaidt Nappe which is underlain by the Schöckel Nappe and the lowermost Gasen Nappe (MATURA & SCHUSTER, 2014). The underlying ACU consists of the Rossegg, Rappold, Wölz and Schoberkogel complexes belonging to nappes of the Koralpe-Wölz Nappe System. Similarities of garnet zoning patterns from micaschists of the Gösselhof Lithodeme (Fig. 1A) and the Schoberkogel Complex (Fig. 1B) include low  $X_{\text{Grs}}$  values of about 0.05-0.10 in the core and discontinuous eo-Alpine (Cretaceous) rims with significantly higher  $X_{\text{Grs}}$  values of about 0.20. Between the garnet core and eo-Alpine rim another discontinuous growth zone can be observed. The three stage growth pattern of garnets raises the question about the polymetamorphic history of the GP and adjacent ACU and may indicate three different metamorphic events (Variscan, Permian, eo-Alpine). However, it may also represent a two stage growth during the Permian event possibly due to a change in the garnet forming reaction followed by the eo-Alpine overprint. Only Permian ages of ~270Ma were obtained from garnet cores of the Rappold and Wölz complexes using the Sm/Nd method and are supported by U/Pb microprobe ages of monazite inclusions. The comparable growth pattern may have important consequences for the internal nappe structure between the eastern margin of the GP and its underlying ACU.

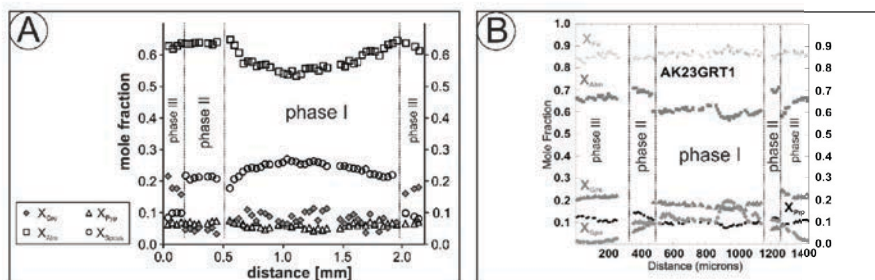


Figure 1. Garnet profiles indicate a three phase growth for the (A) Gösselhof Lithodeme/GP and (B) Schoberkogel Complex/ACU.

MATURA, A., SCHUSTER, R., 2014: Geologische Karte der Republik Österreich 1:50000, Blatt 135 Birkfeld. Verlag der Geologischen Bundesanstalt, Wien.

### Spurenelemente in Quarz aus alpinen Klüften

Schifferle, L.<sup>1</sup>, Tropper, P.<sup>1</sup>, Ungerank, W., Leitner, W. & Hauzenberger, C.<sup>2</sup>

<sup>1</sup>Institut für Mineralogie und Petrographie, Universität Innsbruck, Innrain 52, 6020 Innsbruck, Österreich

<sup>2</sup>6274 Aschau im Zillertal, Österreich

<sup>3</sup>Institut für Archäologien, Langer Weg 11, Universität Innsbruck, 6020 Innsbruck, Österreich

<sup>4</sup>Institut für Erdwissenschaften, Bereich Mineralogie und Petrologie, Universitätsplatz 2, A-8010 Graz, Österreich

e-mail: lukas.schifferle@student.uibk.ac.at

Im Rahmen des Forschungszentrums HiMAT (Historical Mining Activities in Tyrol and Adjacent Areas) werden Untersuchungen im Zuge des Projektteiles „Urgeschichtlicher Silex- und Bergkristallbergbau in den Alpen“ vom Institut für Archäologien der Universität Innsbruck in Kooperation mit dem Institut für Mineralogie und Petrographie der Universität Innsbruck hinsichtlich einer Herkunftsbestimmung für Bergkristall durchgeführt. Diese Untersuchungen beinhalten die petrographische als auch geochemische Charakterisierung von Kluftquarzen aus dem Bereich des Alpenhauptkamms. Mittels Elektronenstrahlmikrosonde und LA-ICP-MS wurden in-situ Messungen an hydrothermalen Quarzen aus alpinen Klüften durchgeführt. Mehrheitlich stammen die Proben aus dem Tiroler und Südtiroler Anteil des Tauernfensters.

Die ersten Ergebnisse weisen auf eine ausgeprägte Heterogenität innerhalb der Quarzkristalle des Probenmaterials hin, wobei das Gesamtbild dennoch Gemeinsamkeiten aufzeigt. Die vergleichsweise besten Nachweisgrenzen wurden mit der LA-ICP-MS erreicht, wobei aber die Spotgröße wesentlich größer ist, als jene der Mikrosonde; außerdem führt die Dekripitation der Flüssigkeitseinschlüsse zum Abplatzen größerer Teilbereiche. Aus diesen Gründen eignet sich die LA-ICP-MS eher dazu, Mittelwerte über größere Volumina zu liefern, was auch im Vergleich mit den Spot-Messungen der Elektronenstrahlmikrosonde sichtbar ist. Letztere Messungen weisen z.T. deutlich höhere chemische Variabilität auf, was als Hinweis auf - in den Proben nur selten sichtbare - Wachstumszonierungen aufgefasst werden kann. Im Gegensatz zu den klaren Quarzen (var. Bergkristall) weisen die trüben Quarze (var. Milchquarz) praktisch immer erhöhte Al-Gehalte auf. Vergleichsproben, die nicht aus alpinen Klüften stammen, sind aufgrund ihres probenspezifisch deutlich erhöhten Spurenelementgehaltes in der Regel einfach von den alpinen Kluftquarzen unterscheidbar.

## METAMORPHOSEGESCHICHTE DES MÜHLVIERTELS: NEUE DATEN AUS DER ZONE VON HERZOGSDORF

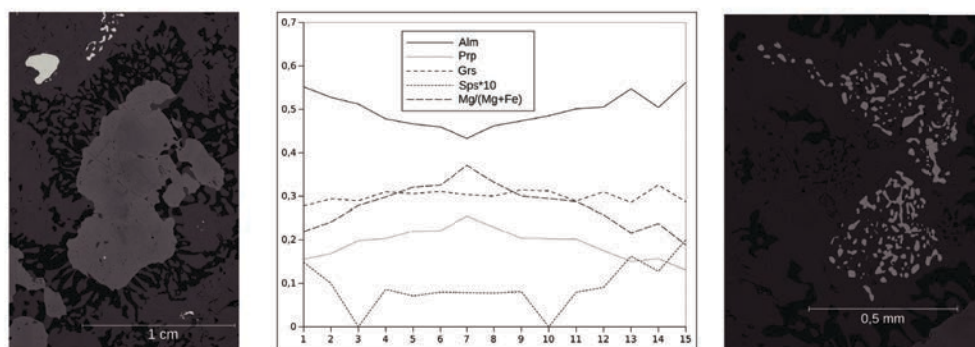
Schiller, D.<sup>1</sup>, Hauzenberger, Ch.<sup>2</sup> & Finger, F.<sup>1</sup>

<sup>1</sup>Universität Salzburg, FB Materialforschung und Physik, Hellbrunnerstraße 34, 5020 Salzburg

<sup>2</sup>Universität Graz, Institut für Erdwissenschaften, Universitätsplatz 2, 8010 Graz

e-mail: David.Schiller@stud.sbg.ac.at

Im Zuge der Kartierung von Blatt Haslach (westliches Mühlviertel) wurden Metamorphite aus der “Zone von Herzogsdorf” petrologisch untersucht. Während die Hauptmasse der Metamorphite des Mühlviertels von weitgehend uniformen, anatektischen Quarz-Feldspat-Biotit±Crd-Gneisen repräsentiert wird (Perlgneis; Metamorphosealter ~315-330 Ma), findet sich in der Zone von Herzogsdorf eine variabelere Lithologie mit Hornblende-Schiefer, Kalksilikat, Graphitschiefer und Amphibolit. Ebenso wie die Perlgneise sind diese Gesteine von der penetrativen LP-HT Metamorphose der bavarischen Orogenese (FINGER et al., 2007) geprägt. In einem Granat-Amphibolit aus der Zone von Herzogsdorf konnten nun, erstmals im Mühlviertel, Relikte einer älteren HP-HT Metamorphose nachgewiesen werden. Die Granate zeigen im Kern hohe Pyrop (26 %) und Grossulargehalte (bis 34%), was bei der gegebenen Gesamtgesteinschemie auf Metamorphosetemperaturen von ~1000°C und Mindestdrucke von ~11kbar schließen lässt (CAPITANI & PETRAKAKIS, 2010). Die Granatränder haben eine Zusammensetzung von etwa  $\text{Alm}_{0.59}\text{Gr}_{0.26}\text{Py}_{0.13}\text{Sp}_{0.02}$  (Fig. 1b) und sind an die Niedrigdruck-Bedingungen der bavarischen Regionalmetamorphose (Finger et al., 2007) angepasst. In Zusammenhang mit dem Abbau von Granat entstanden dabei charakteristische symplektitische Koronastrukturen bestehend aus Plagioklas und Amphibol (Fig. 1a). Anhäufungen von Ilmenitkörnern markieren vermutlich die Umrisse ehemaliger Ti-reicher Pyroxene (Fig. 1c).



Figur 1. Granat mit symplektitischem Plagioklassaum (a), chemisches Profil durch Granat (b), Ilmenit-anhäufungen pseudomorph nach Pyroxen (c).

DE CAPITANI, C., PETRAKAKIS, K. (2010): Am. Min., 95, 1006-1016.

FINGER, F., GERDES, A., JANOUŠEK, V., RENÉ, M., RIEGLER, G. (2007): J. Geosci., 52, 9-28.



ON THE CRYSTAL STRUCTURE OF THE NEW POTASSIUM CALCIUM  
SILICATE FLUORIDE  $K_7Ca_9[Si_2O_7]_4F$

Schmidmair, D.<sup>1</sup>, Dorn, T.<sup>1</sup>, Kahlenberg, V.<sup>1</sup> & Tribus, M.<sup>1</sup>

<sup>1</sup>Institute of Mineralogy and Petrography, University of Innsbruck, Innrain 52, 6020 Innsbruck, Austria  
e-mail: Volker.Kahlenberg@uibk.ac.at

In the course of a series of flux synthesis experiments aiming on the production of new compounds in the ternary system  $K_2O$ - $CaO$ - $SiO_2$ , crystals of a novel potassium calcium silicate fluoride,  $K_7Ca_9[Si_2O_7]_4F$ , were formed.  $KF$  was used as the flux substance and it occurred that fluorine was incorporated into the new material.

Applying direct methods it was possible to solve the crystal structure of the above mentioned compound from single-crystal diffraction data. Structure solution was complicated due to pseudo-merohedral twinning of three individuals.  $K_7Ca_9[Si_2O_7]_4F$  crystallizes in the monoclinic space group  $P2_1/m$ . Unit cell parameters are:  $a=5.6122(2)\text{\AA}$ ,  $b=13.8143(5)\text{\AA}$ ,  $c=9.8016\text{\AA}$  and  $\beta=90.255(4)^\circ$ . Electron microprobe analyses were performed to check the chemical composition and yielded an atomic ratio normalised on 28 oxygen atoms for  $K:Ca:Si:O:F$  of 6.732(1):8.904(1):7.866(0):28:1.120(1).

$K_7Ca_9[Si_2O_7]_4F$  belongs to the group of sorosilicates and is built up of  $Si_2O_7$ -groups. Potassium and calcium cations are distributed among five crystallographically independent cation positions, which are either coordinated by distorted octahedra, trigonal prisms and more irregular polyhedra. By sharing common faces, octahedra and trigonal prisms form infinite columns running parallel to  $[010]$ . These columns are connected to the  $Si_2O_7$ -groups through common corners. Fluorine positions are located in voids between the  $Si_2O_7$ -groups and the columns.

The present compound is structurally related to  $K_2Ca_2Si_2O_7$  (ARROYABE et al., 2011) and  $K_3REESi_2O_7$  (with REE = Gd, Tb, Dy, Ho, Er, Tm, Yb) (VIDICAN et al., 2003).

ARROYABE, E., KAHLENBERG, V. (2011): Eur. J. Mineral., 23, 101-110.

VIDICAN, I., SMITH, M.D., zur LOYE, H.C. (2003): J. Solid State Chem., 170, 203-210.



**THE PLANKOGEL DETACHMENT OF THE EASTERN ALPS: PETROLOGICAL  
EVIDENCE FOR AN OROGENY-SCALE EXTRATCION FAULT**

Schorn, S.<sup>1</sup> & Stüwe, K.<sup>1</sup>

<sup>1</sup>Institute of Earth Sciences, University of Graz, Universitätsplatz 2, A-8010 Graz, Austria

Email: [simon.schorn@edu.uni-graz.at](mailto:simon.schorn@edu.uni-graz.at)

The Saualpe and Koralpe regions are characterized by Cretaceous high-pressure metamorphism that occurred around 90Ma (e.g. THÖNI et al., 2008) in response to the onset of Eoalpine intracontinental subduction, but also experienced an earlier metamorphic event in the Permian (SCHUSTER et al., 2001). In both, the southern Saualpe and the Koralpe regions, eclogite-facies high-pressure rocks occur in sharp contact with amphibolite-facies metapelites. The contact is of tectonic nature. In the southern Koralpe it is referred to as the Plankogel detachment. While any traces of older metamorphic events have been erased by the Eoalpine event in the eclogite-facies units, the lower-grade metapelites preserve complexly zoned garnets as an expression of the conspicuously different pressure-temperature conditions of both the Permian- and Eoalpine metamorphic events. During the Eoalpine evolution, both units have been subducted to different crustal levels as inferred by pseudosection modelling combined with conventional geothermobarometry. Despite the different peak metamorphic conditions, ranging from ~2.3GPa and 680°C for the eclogite-facies units and ~1.3GPa and 550-580°C for the amphibolite-facies metapelites, both units display a common retrograde overprint at conditions around 1.0GPa and 580-650°C. From this, we infer a two-stage exhumation process. We interpret this two stage exhumation process to be a reflection of slab extraction (FROITZHEIM et al., 2003), during early Eoalpine subduction. We suggest that the first stage of exhumation occurred due to the extraction of a crustal boudin that was localized in the trace of the Plankogel detachment. This would define the latter as an extraction fault in the sense of FROITZHEIM et al. (2006). In view of the fact that the Plankogel detachment is directly related to the Plattengneiss shear zone, we also suggest that our model may solve the long-standing discussion about the enigmatic shear sense of the Plattengneiss shear zone.

FROITZHEIM, N., PLEUGER, J. & NAGEL, T.J. (2006): *Journal of Structural Geology*, 28, 1388-1395.

FROITZHEIM, N., PLEUGER, J., ROLLER, S. & NAGEL, T.J. (2003): *Geology*, 31, 925-928.

SCHUSTER, R., SCHABERT, S., ABART, R., FRANK, W. (2001): *Mitteilungen der Geologie und Bergbau Studenten Österreichs*, 44, 111-141.

THÖNI, M., MILLER, C., BLICHERT-TOFT, J., WHITEHOUSE, M. J., KONZETT, J., ZANETTI, A. (2008): *Journal of Metamorphic Geology*, 26, 561-581.

## X-RAY LINE PROFILE ANALYSIS OF CALCITE DEFORMED BY HIGH-PRESSURE TORSION

Schuster, R.<sup>1</sup>, Schafler, E.<sup>2</sup> & Abart, R.<sup>1</sup>

<sup>1</sup>Dept. of Lithospheric Research, Univ. of Vienna, Althanstrasse 14, 1090, Vienna, Austria

<sup>2</sup>Faculty of Physics, Univ. of Vienna, Boltzmannngasse 5, 1090, Vienna, Austria

e-mail:roman.schuster@univie.ac.at

X-ray line profile analysis (XLPA) is a powerful tool for investigating the microstructure and dislocation structure of highly deformed materials (UNGAR, 2004). This method allows to relate the characteristic broadening of Bragg peaks due to lattice defects and the finite size of the coherent scattering domains (CSD) to physical parameters such as dislocation density and the distribution of crystallite size.

In this study calcite samples subjected to torsional deformation under confining pressures in the GPa range to shear strains of up to 100 at temperatures between room temperature and 450°C were measured at the High Energy Materials Science Beamline at Petra III at DESY in Hamburg as well as the Microdiffraction Beamline at the ALS in Berkeley. The powder diffractograms were then evaluated by means of the convolutional multiple whole profile fitting procedure (CMWP-fit; RIBARIK et al., 2004). CMWP-fit permits fitting of a theoretical Bragg profile calculated from physical parameters to the measured diffractograms. The results show that at high deformation temperatures the CSD size as well as the dislocation density saturate at low strains and strain rates, whereas grain refinement as determined by EBSD continues to much higher strains. The dynamic recovery at these elevated temperatures also shows a significant dependence on the confining pressure. At low temperatures no saturation can be seen, leading to significantly higher dislocation densities and reductions in CSD size. Through the analysis of the anisotropy of the lattice strain caused by dislocations the dominant slip system active during deformation could be established.

UNGAR, T. (2004): Scripta Mat., 51, 777-781.

RIBARIK, G., GUBICZA, J., UNGAR, T. (2004): Mater Sci. Eng. A, 387-389, 343-347.

# FIRST OCCURENCE OF PLATINUM-GROUP MINERALS IN SALZBURG: THE HAIDBACHGRABEN Cu-Ni-Co DEPOSIT, PINZGAU

Schwabl, S.<sup>1</sup>, Melcher, F.<sup>1</sup> & Grill, H.A.<sup>2</sup>

<sup>1</sup> Montanuniversität Leoben, Peter Tunner-Straße 5, 8700 Leoben, Austria

<sup>2</sup> Schurfgemeinschaft Zinkwand, Birkenweg 2, 8820 Neumarkt in der Steiermark, Austria  
sonja.schwabl@stud.unileoben.ac.at

WEBER et al. (1997) report on concentrations of platinum-group elements (PGE) in Cu-Ni mineralization south of Mittersill. At the location “Gaiswände” in the Haidbach valley (“Haidbachgraben”), exploration has been conducted for Cu and Ni between 1911 and 1939. The stratiform deposit is hosted by greenschists of the pre-Variscan Habach Group which is part of the Subpenninic Venediger nappe system.

Polished sections of mineralized schists reveal pyrrhotite, pyrite and chalcopyrite as the major sulphides, with less abundant pentlandite that is commonly replaced by violarite. As accessory phases, the following minerals have been observed: Ni-Fe-Co sulfarsenides (gersdorffite, arsenopyrite), sphalerite (6-7% Fe, 1% Cd), hessite Ag<sub>2</sub>Te, Pd-melonite (Ni,Pd)(Te,Bi)<sub>2</sub>, merenskyite Pd(Te,Bi)<sub>2</sub>, sperrylite PtAs<sub>2</sub>, testibiopalladinite PdSbTe and gold (Fig. 1). Zinc-bearing chromian spinel occurs as inclusions in base metal sulphides. Grain sizes of the precious metal-bearing phases are up to 20 µm. Palladium minerals are invariably hosted by pyrrhotine and chalcopyrite, and are intergrown with sphalerite and Ni-Fe-Co sulpharsenides, whereas sperrylite is commonly present as single euhedral to subhedral grains along sulphide grain boundaries and in the silicate matrix.

Mineralized samples were analysed by XRF and ICPMS methods and yielded the following concentrations: 13-18% Fe, 0.2-4% Cu, 0.5-1.5% Ni, 300-3000 ppm Co, 100-400 ppm Zn, 50-120 ppm Se, up to 80 ppm Mo, 4-30 ppm Ag, up to 1.1 ppm Pd, up to 8.5 ppm Pt, and up to 0.6 ppm Au. Pt shows a strong nugget effect in different aliquots of the same sample.

Despite a number of sulphide occurrences associated with metabasic rocks in the Tauern Window, the Ni-Cu-Co mineralization at Haidbachgraben is unique in the presence of discrete PGM. The goals of an ongoing study are to describe the geological and structural setting of the mineralization, its trace element chemistry and mineralogy, and to model its genesis.

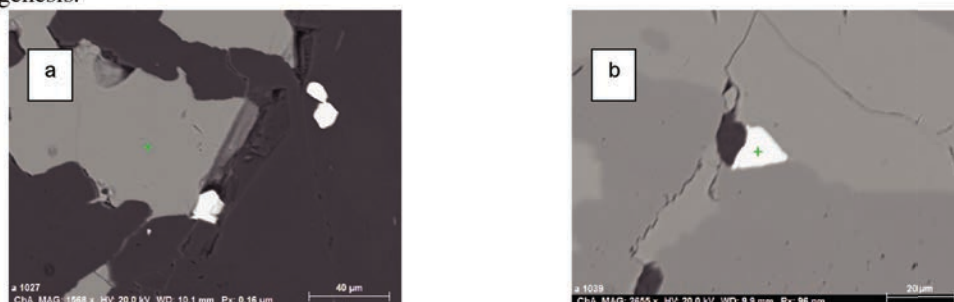


Figure 1. (a) Sperrylite (bright) next to chalcopyrite and amphibole; (b) Pd-melonite between pyrrhotine (light grey) and pyrite (dark grey)

WEBER et al. (1997): Archiv für Lagerstättenforschung Geol. B.-A. 19, 1-607.

## CHROMIUM CONTAMINATED SITE – BUT WHERE IS THE CHROMIUM?

Sedlazeck, K.P.<sup>1</sup>, Höllen, D.<sup>1</sup> & Pomberger, R.<sup>1</sup>

<sup>1</sup>Chair of Waste Processing Technology and Waste Management, Montanuniversität Leoben,  
 Franz-Josef-Str. 18, 8700 Leoben, Austria  
 e-mail: philipp.sedlazeck@unileoben.ac.at

Since 2013, a project dealing with the remediation of contaminated sites is established at the Chair of Waste Processing Technology and Waste Management of the Montanuniversität Leoben. In the course of a previous project, a unique technique was developed for remediation of heavy metal contaminated subsurfaces and contaminated industrial waters (ferroDECONT process). This technique is tested in the current project. A field scale pilot plant was installed at a chromium contaminated abandoned site in Klagenfurt, Carinthia; a former leather tannery where Cr(VI) bearing solid phases were used to produce tannery acid. This production led to a serious underground Cr(VI) as well as Cr(III) contamination.

In order to proceed with the project, new groundwater wells were drilled in the region of the assumed hot spot area and also outside of this area. Inside of the contaminated area, the color of the drill cores turned with increasing depth from brown via gray into deep black, the latter present in a layer with a thickness of up to 5 meters. This color change appeared successively below the groundwater level and was not present in the drill cores from the alleged non-contaminated area. Macroscopic observation of the black material revealed a smaller grain size compared to the brown material, but also certain parts where the color is not as dark.

Chemical analysis proved the assumption that the dark material represents the hot spot. Analyses were conducted for several drill cores - two representatives of each area were chosen for further investigation. The contaminated sample “A” contains almost 3g/kg of Cr, whereas the Cr-concentration of the non-contaminated sample “B” is 0.59g/kg.

XRD analysis (Fig. 1) showed that the samples consist of quartz, albite, muscovite and chlorite; sample B also contains of microcline. The fact that no Cr bearing phase has been found leads to the question of how the chemically detected Cr is present in the underground. One possibility could be that it precipitated as amorphous phase around the other minerals. Alternatively, the modal content of the Cr-bearing phase is below the detection limit of XRD (about 2wt%). Consequently, enrichment methods and more space-resolved techniques like electron microprobe analyses will be used to determine in which phase the chromium is present.

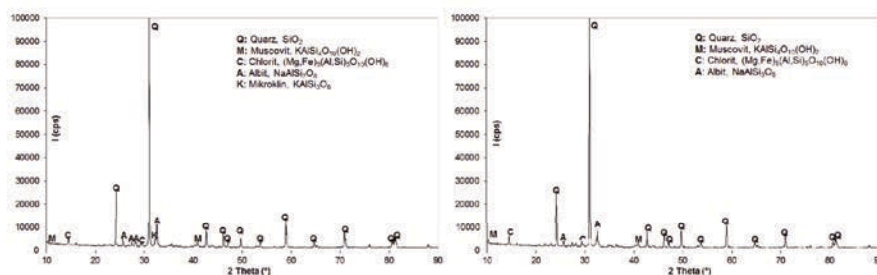


Figure 1. XRD pattern of sample A (left) and sample B (right).

## TWO PHASE GARNET GROWTH IN VARISCAN MIGMATITES FROM THE BAVARIAN UNIT, UPPER AUSTRIA

Sorger, D.<sup>1</sup>, Hauzenberger, C.<sup>1</sup>, Linner, M.<sup>2</sup> & Iglseder, C.<sup>2</sup>

<sup>1</sup>Institute for Earth Sciences, University of Graz (Heinrichstraße 26, 8010, Graz, Austria)

<sup>2</sup>Geological Survey of Austria (Neulinggasse 38, 1030, Wien, Austria)

e-mail: dominik.sorger@edu.uni-graz.at

Outcrops of garnet bearing cordierite migmatites are found mainly along the Danube valley west of Linz. The common formation of migmatites with well-developed leucosomes (K-feldspar, plagioclase, quartz) and melanosomes (garnet, cordierite, sillimanite, spinel, ilmenite,  $\pm$  biotite) indicate high temperature metamorphism. Most of the scarce garnets are characterized by a homogenous iron rich composition ( $X_{\text{alm}}=0.78-0.80$ ), moderate pyrope contents ( $X_{\text{prp}}=0.16-0.18$ ) and minor amounts of grossular and spessartine components ( $X_{\text{grs}}=0.028-0.032$ ,  $X_{\text{sps}}=0.020-0.024$ ). Large garnet porphyroblasts display an elevated Ca-plateau ( $X_{\text{grs}}=0.053-0.055$ ) and a slightly increased spessartine component ( $X_{\text{sps}}=0.030-0.035$ ) in the cores followed by a decrease towards the rim (Figure 1 A). The change in garnet composition from core to rim is directly related to a change in P and T conditions. Mineral inclusions in garnet cores (biotite+plagioclase+spinel+quartz+ilmenite $\pm$ rutile $\pm$ staurolite $\pm$ corundum) are different to matrix minerals and support the two stage metamorphic history. Multi equilibrium thermobarometry using winTWQ Version 2.34 (BERMAN, 1991) allowed to constrain metamorphic conditions of 850-900°C and 0.55-0.65 GPa for matrix and garnet rim composition (Figure 1 B). Geothermobarometric calculations using inclusions in garnet cores yielded P/T conditions of 600-650°C and 1.0-1.2 GPa (Figure 1 C). Calculated pseudo-sections using garnet core and rim compositions were used in addition to better constrain the P-T evolution where a medium T/high P metamorphic stage was subsequently followed by the well-established high T/low P stage, commonly found in the Bavarian unit (TROPPER et al., 2006).

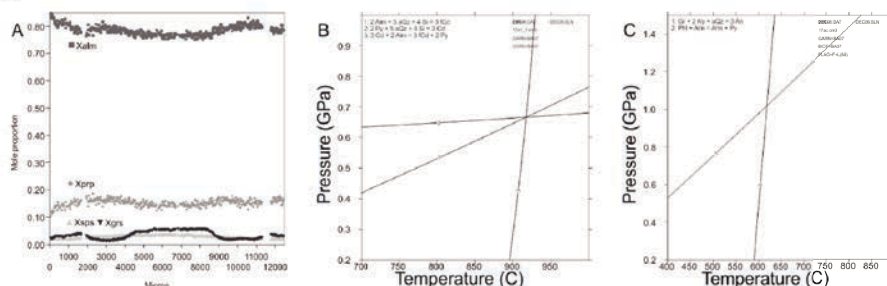


Figure 1. A) Chemical profile through a 12mm large garnet porphyroblast displaying an elevated Ca plateau in the core. B) Geothermobarometric calculations using the reaction  $\text{Grt}+\text{Sil}+\text{Qz}=\text{Crd}$  to obtain matrix P/T conditions. C) Geothermobarometric calculations using GASP barometer and Grt-Bt thermometer to obtain metamorphic conditions for garnet cores.

BERMAN, R.G. (1991): Canadian Mineralogist, 29, 833-855.

TROPPER, P., DEIBL, I., FINGER, F., KAINDL, R. (2006): Intern. J. Earth Sci., 95, 1019-1037.

**REE ABUNDANCES IN EDIACARAN TO EARLY CAMBRIAN PHOSPHATE  
DEPOSITS FROM CENTRAL AND SOUTH ASIA BY LA\_ICP\_MS**

Stammeier, J.<sup>1</sup>, Hippler, D.<sup>1</sup> & Dietzel, M.<sup>1</sup>

<sup>1</sup>Graz University of Technology, Institute of Applied Geosciences, Rechbauerstrasse 12, 8010 Graz, Austria  
e-mail: j.stammeier@tugraz.at

The Precambrian-Cambrian (PC-C) boundary has been earlier characterized by geochemical means for its unique environmental and evolutionary changes. Concomitant with these changes is the widespread formation of phosphate deposits in Central and South Asia. The most abundant mineral in sedimentary phosphorites is carbonate fluorapatite (CFA), which is either formed by (1) direct precipitation from aqueous solution, or indirectly through (2) microbial mediation or (3) replacement of carbonates. Moreover, these sedimentary phosphorites provide promising environmental archives of changes in ocean chemistry. We therefore applied LA-ICP mass spectrometry to investigate the abundances of rare earth elements (REE) and yttrium of phosphorite samples that represent different depositional facies: (i) phos-stromatoliths, (ii) phosphatic concretions, and (iii) phosphatic grainstones, all covering the PC-C boundary interval. REE abundances are sensitive to changes of numerous physicochemical conditions such as pH, temperature, aqueous complexation with organics and organic ligands. Among the most prominent parameters controlling their abundance in sedimentary apatite however is the redox condition of the fluid from which the mineral is formed. Within this study we thus aim to investigate the paleoenvironmental conditions occurring during the formation of phosphorites in Central and South Asia during the Ediacaran to Early Cambrian and Ediacaran using a unique set of geological samples. The main focus is laid on the conditions prevailing during CFA formation, the extent of diagenetic modification and the reconstruction of the temporal and spatial variability of sea- and porewater chemistry. By investigating different depositional facies and phosphorites from different microcontinents, we can further evaluate the facies-specific mechanisms of sedimentary apatite formation and their regional significance.

Most phosphorites display a distinctive REE distribution pattern involving enrichment of MREE. This feature has been earlier suggested as an indicator of post-depositional alteration (e.g. Shields and Stille 2001). Another fraction of the analysed phosphorite samples exhibit REE distribution patterns that resemble seawater-like REE distribution with an enrichment of HREE over LREE. Such distribution points towards a formation mechanism that implicates a dissolution/re-precipitation process and rapid phosphatization of marine carbonates in seawater-derived pore fluids. Financial support of the research project by DFG-FG 736, NAWI Graz and EFRI – Land Steiermark is kindly acknowledged. We further thank C. Hauzenberger for assistance with the LA-ICPMS analyses.

SHIELDS, G., STILLE, P. (2001): Chem. Geol., 175, 29-48.



## HIGH Nb-Ta CONCENTRATIONS IN STREAM SEDIMENTS IN THE BOHEMIAN MASSIF (AUSTRIA): INDICATORS OF COLTAN MINERALIZATION?

Stocker, K.<sup>1</sup>, Legerer P.<sup>1,3</sup>, Raith, J.G.<sup>1</sup>, Rantitsch, G.<sup>1</sup>, Rachetti, A.<sup>2</sup> & Neinavaie, H.<sup>4</sup>

<sup>1</sup>Department of Applied Geosciences and Geophysics, Montanuniversität Leoben,  
Peter-Tunner-Straße 5, 8700 Leoben, Austria

<sup>2</sup>Chair of General and Analytical Chemistry, Montanuniversität Leoben  
Franz Josef-Straße 18, 8700 Leoben, Austria

<sup>3</sup>Geological Survey of Austria, Neulinggasse 38, 1030 Vienna, Austria

<sup>4</sup>Rennfeld 28, 6370 Kitzbühl, Austria  
e-mail:kristina.stocker@unileoben.ac.at

The Bohemian Massif is part of the European Variscan orogenic belt and, in its Austrian part, includes the Moravian and Moldanubian zones. The latter is characterized by polyphase low-P high-T metamorphism and emplacement of voluminous granitoids formed due to extensive crustal melting between ~330 to 300 Ma (Gerdes 2003; Finger, 2007). The syn- to post-orogenic granitoids are exposed in large composite plutons such as the South Bohemian Batholith (SBB) with its three main suites (Gerdes 2003): (1) Weinsberg type granites (331-323 Ma); 2) Eisgarn type granites (328-327 Ma); 3) young biotite-bearing I-type granitoids of Mauthausen type (317-300 Ma).

Stream sediment data from the South Bohemian Pluton often show elevated contents of Nb, Ta ( $\pm$  REE, Sn, W etc.). In order to clarify whether these higher concentrations are caused by concealed mineralization (e.g., Nb-Ta pegmatites) or only represent regionally higher background values we compiled geological data on Nb-Ta occurrences, did a GIS-supported re-processing of existing chemical data from the Bohemian Massif and studied stream sediments from three selected areas; i.e. north of Sandl, south of Weitra and in an area north of Heidenreichstein and Litschau. At each sampling site the fine fraction (SF) and a heavy mineral concentrate (SM) were collected; in addition three samples of granite eluvium were taken. Chemical bulk analyses were combined with qualitative and quantitative mineralogy (optical microscopy, MLA) and mineral-chemical studies (EMPA). By applying this multi-method approach it could be demonstrated that geochemical anomalies of Nb ( $\pm$  La, Ce, Sn, W etc.) in the Bohemian Massif reflect *different* sources and provenance. Some regional “anomalies” within the Weinsberg Granite (Sandl, Weitra) are caused by incorporation of higher contents of Nb and Ta in Ti oxides, especially in ilmenite, which become concentrated in the heavy mineral fraction of the stream sediments and reflect regionally higher background values. In contrast, anomalies in the Eisgarn granite, such as the one north of Litschau in the Rottal area, are caused by presence of distinct Nb-Ta-(Sn) phases. There, tiny inclusions of columbite-tantalite group minerals were observed within cassiterite as well as larger grains of columbite. We propose a flowchart allowing for discriminating these different sources that will be tested in future mineral exploration in this area.

FINGER, F. et al. (2007): J. Geosci. 52, 9-28

GERDES, A. et al. (2003): J. Czech Geol. Soc. 48, 53-54

## TOWARDS AN INDUSTRIAL NITROGEN CYCLE USING NATURAL ZEOLITES

Stocker, K.<sup>1</sup>, Lubensky J.<sup>2</sup> & Ellersdorfer, M.<sup>2</sup>

<sup>1</sup>Chair of Resource Mineralogy, Montanuniversität Leoben, Peter-Tunner-Straße 5, 8700 Leoben, Austria

<sup>2</sup>Chair of Process Technology and Industrial Environmental Protection, Montanuniversität Leoben,

Franz Josef-Straße 18, 8700 Leoben, Austria

e-mail: kristina.stocker@unileoben.ac.at

Liquid digestate from biogas plants contains significant amounts of ammonia, which has to be removed in order to close in-plant water circulation without the risk of inhibiting the anaerobic digestion processes. Liquid/solid separation and clarification of the liquid phase of digestates by winning and recycling of ammonium for industrial NO<sub>x</sub> removal is a way to avoid problems, which arise from the output of digestate on agricultural areas, for example legal restrictions concerning regional N-capacity, seasonal output limitations as well as N-losses or nitrate formation in groundwater. For this purpose, a new process for the production of an industrial DeNO<sub>x</sub>-agent suitable for catalytic and non-catalytic off-gas treatment is developed („ion exchanger-loop-stripping“). The ion exchanger-loop-stripping process combines ammonia preconcentration via solid ion exchanger beds, where zeolite is used, followed by air stripping. In laboratory experiments, required contact times, performance and exchange capacities as well as various desorption and pretreatment options of different natural zeolites (clinoptilolite, phillipsite, chabazite) combined with simultaneous air stripping were investigated. Exchange capacities up to 8 mg NH<sub>4</sub><sup>+</sup>/g natural zeolite can be achieved in packed bed columns if the regeneration/pretreatment is performed with concentrated NaOH-solutions. We present ammonia ion exchange capacities of different natural zeolites, adsorption and desorption isotherms as well as their eligibility for denitrification of wastewaters deriving from biogas plants and municipal sewage works. In order to reuse adsorbed ammonia in offgas treatment, laboratory experiments were done in several cycles of loading and regeneration of natural zeolites. For this purpose natural zeolites of different origins as well as artificial zeolites were characterized by XRD analysis, DTA-TG and semiquantitative microprobe analysis. In order to fulfill the requirements to this very special demand, zeolite samples were also tested under acidic and alkaline conditions. First results show that natural clinoptilolite is a stable and well-suited ion exchanger for ammonia removal from digestate under alkaline conditions. Furthermore, exchange performance of natural clinoptilolite increases over several adjacent adsorption/desorption cycles.

## CRYSTAL STRUCTURE OF ARGENTOBAUMHAUERITE

Topa, D.<sup>1</sup> & Makovicky, E.<sup>2</sup>

<sup>1</sup>Zentrale Forschungslaboratorien, Naturhistorisches Museum, Burgring 7, A-1010 Wien, Austria

<sup>2</sup>Department of Geoscience and Resource Management, University of Copenhagen,

Østervoldgade 10, DK-1350, Copenhagen K, Denmark

e-mail: dan.topa@nhm-wien.ac.at

The name ‘argentobaumhauerite’ replaces the preliminary name ‘baumhauerite-2a’ (IMA-CNMNC; accepted proposal 15-F). The mineral was described by PRING et al. (1990), with the unit-cell parameters determined by means of transmission electron microscopy and refined using powder diffraction data. They were accompanied by the EPMA data which indicated that ‘baumhauerite-2a’ is distinguished from baumhauerite (ENGEL & NOWACKI, 1969) by appreciable contents of silver (LAROUSSI et al., 1989). The hitherto unknown crystal structure of argentobaumhauerite  $\text{AgPb}_{22}\text{As}_{33}\text{S}_{72}$ , was solved by us using a crystal fragment, mechanically extracted from an EPMA pre-analysed polished section of Lengenbach (Binntal, Switzerland) material. The structure was refined in space group  $P-1$ ,  $a=7.9053(10)$ ,  $b=8.4680(10)$ ,  $c=44.4102(53)\text{Å}$ ,  $\alpha=84.614(2)^\circ$ ,  $\beta=86.469(2)^\circ$ ,  $\gamma=89.810(2)^\circ$ ,  $V_{\text{cell}}=2954.16\text{Å}^3$ , to  $R_1(F) = 3.9\%$  (SHELX-97) for 583 parameters. In contrast, the structure of baumhauerite,  $\text{Pb}_{12}\text{As}_{16}\text{S}_{36}$ , is triclinic,  $a=7.884(4)$ ,  $b=8.345(4)$ ,  $c=22.811(11)\text{Å}$ ,  $\alpha=90.069(8)^\circ$ ,  $\beta=97.255(8)^\circ$ ,  $\gamma=90.082(8)^\circ$ ,  $V_{\text{cell}}=1488.8(13)\text{Å}^3$  and space group  $P1$ . Both minerals are members of the sartorite homologous series (MAKOVICKY, 1997), in which only the members  $N=3$  and  $N=4$  are known, and the variety is created by combinations of these two unit homologue slabs in different ratios. Baumhauerite is the simplest of these combinations, namely  $N_{1,2} = 3;4$  (i.e. ..3,4,3,4,3,4..). In argentobaumhauerite the sequence is further modified by alternation of two distinct types of  $N = 4$  slabs, those with Pb present in the slab interior and those with the interior Pb substituted by Ag+As (i.e. ..3, 4',3, 4'',3,4',3, 4''..), with the same type of  $N=3$  slab as in baumhauerite. The argentobaumhauerite cell is a 2-fold supercell of the baumhauerite cell. The remarkable separation of Ag and surplus As *on a unit-cell scale* into an alternative set of  $N=4$  slabs, creating well localized Ag and As substitution sites (due to 2Pb for As+Ag substitution mechanism), and the difference of the length and arrangement of crankshaft chains of short As-S bonds between the  $N=4$  slabs of baumhauerite and argentobaumhauerite, are responsible for the doubling of the  $c$  parameter. The present study succeeded to make an independent mineral species with its own name, chemistry, structure, local configurations and symmetries from a questionable mineral ‘baumhauerite-2a’ (which was interpreted as a polytype of baumhauerite).

PRING, A., BIRCH, W.D., SEWELL, D., GRAESER, S., EDENHARTER, A., CRIDDLE, A. (1990): Am. Mineral., 75, 915-922.

LAROUSSI, A., MOËLO, Y., OHNENSTETTER, D., GINDEROW, D. (1989): C. R. Acad. Sci. Paris, 308, Sér. II, 927-933.

ENGEL, P., NOWACKI, W. (1969): Zeitschrift für Kristallographic, 129, 178-202.

MAKOVICKY, E. (1997): EMU Notes in Mineralogy, 1, 237-271.

## UTILIZATION POTENTIAL OF ULTRAMAFIC ROCKS IN AUSTRIA IN VIEW OF HYDROMETALLURGICAL PROCESSING AND MINERAL CARBONATION

Treimer, R.<sup>1</sup>, Melcher, F.<sup>2</sup>, Moser, P.<sup>1</sup>, Niesenbacher, I.<sup>3</sup>, Lehner, M.<sup>3</sup> & Höllen, D.<sup>4</sup>

<sup>1</sup>Chair of Mining Engineering and Mineral Economics, Montanuniversität Leoben, Austria

<sup>2</sup>Chair of Geology and Economic Geology, Montanuniversität Leoben, Austria

<sup>3</sup>Chair of Process Technology and Industrial Environmental Protection, Montanuniversität Leoben, Austria

<sup>4</sup>Chair of Waste Processing Technology and Waste Management, Montanuniversität Leoben, Austria

e-mail: robert.treimer@unileoben.ac.at

Anthropogenic carbon dioxide emissions are the main driving force for global warming, therefore the reduction of these emissions is indispensable in order to mitigate the threatening climate change with all its ecological, economic and social consequences. An important approach for mitigating CO<sub>2</sub>-emissions is the use of CO<sub>2</sub> as feedstock for the production of carbon-based products (CCU-carbon capture and utilization). One of the most interesting CCU-options in future is mineral carbonation (MC), which offers the possibility for sequestration of CO<sub>2</sub> in form of synthetic carbonates based on the fundamental principle of the reaction of CO<sub>2</sub> with Mg or Ca and the formation of the corresponding carbonates which can be applied as industrial minerals or construction materials.

Mg-rich ultramafic rocks, such as peridotites, dunites or serpentinites are the main primary resources for the MC-technology. By means of hydrometallurgical processing (HP) primary rocks are separated into their compounds, such as magnesium, silicates (leaching residues) and metals (Fe, Ni, Cr, Al, Mn, Co). Subsequently, Mg is carbonated with captured CO<sub>2</sub> under formation of synthetic magnesium carbonate.

The most important deposits of peridotites and serpentinites in Austria occur in the Speik Complex in Styria, especially at Kraubath and Pernegg. In the scope of this study, selected samples of these deposits will be investigated particularly in view of the utilization potential for hydrometallurgical processing and mineral carbonation. The mineralogical and mineral-chemical aspects of the primary rocks as feedstock for HP and MC, as well as the mineralogical and mineral-chemical composition of the mineral fractions from the process technology will be investigated by means of optical microscopy, electron microprobe and scanning electron microscopy.

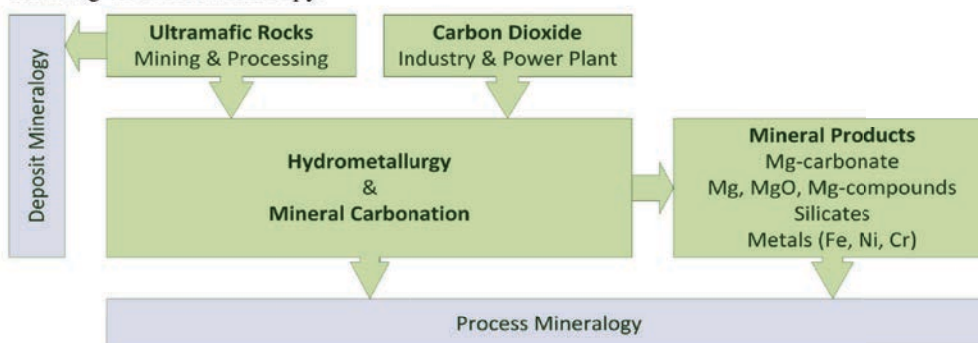


Figure 1. Principle of utilization of ultramafic rocks for hydrometallurgical processing and mineral carbonation and corresponding mineralogical investigations.

**THE USE OF TI-PHASE (RUTILE, ILMENITE, TITANITE) INTERGROWTHS AS  
PETROGENETIC INDICATORS IN METABASITES (ECLOGITES,  
AMPHIBOLITES) FROM THE TEXEL COMPLEX (SOUTH-TYROL, ITALY)**

Tribus, M.<sup>1</sup> & Tropper, P.<sup>1</sup>

<sup>1</sup>Institute of Mineralogy and Petrography, University of Innsbruck, Innrain 52, A-6020 Innsbruck, Austria  
e-mail: martina.tribus@uibk.ac.at

The polymetamorphic basement rocks SE of the Ötztal complex have been overprinted by a HP-metamorphic event in the Cretaceous and were interpreted as part of the “Eo-Alpine High Pressure Belt”. The Texel Complex is composed mainly of paragneisses with minor intercalations of micaschists, orthogneisses bodies, amphibolites and eclogites. The eclogites contain the peak mineral assemblage omphacite + amphibole + garnet + clinozoisite/epidote + quartz + titanite ± ilmenite ± rutile. Thermobarometric calculations with multi-equilibrium geothermobarometry using an H<sub>2</sub>O-bearing invariant point yielded *P-T* conditions of 1.8–2.2 GPa and 560–600°C. During decompression, diopside-rich clinopyroxenes + albite-rich plagioclase + Ca-amphiboles form. Coexisting amphibolites contain the mineral assemblage amphibole + clinozoisite + garnet + titanite + rutile + ilmenite + quartz and represent *P-T* conditions of ca. 600°C and 1 GPa. Both rocks contain complex Ti-phase intergrowths and it is the aim of this study to test the petrogenetic use of these aggregates by applying Zr-in-rutile and Zr-in-titanite geothermometry as well as Schreinemaker's analysis. The growth sequence in both rock types is always ilmenite ± rutile ⇒ titanite. The observation of the growth sequence of the Ti-phases such as ilmenite ⇒ rutile also allows to put constraints on the shape of the *P-T* paths, obtained from these rocks. Calculations of model reactions in the system CaO-FeO-TiO<sub>2</sub>-Al<sub>2</sub>O<sub>3</sub>-SiO<sub>2</sub>-H<sub>2</sub>O assuming a monometamorphic evolution and considering the mineral assemblage amphibole + plagioclase + clinozoisite + quartz ± garnet ± rutile ± ilmenite ± titanite yields constraints on the transitions rutile ⇒ titanite, ilmenite ⇒ rutile and ilmenite ⇒ rutile ⇒ titanite. These calculations indicate that rutile is not always the high-*P* phase and that titanite has a large stability field which also extends to high-*P* as well as to high *T*. Ilmenite by itself though, always seems to be associated with low-*P*. Zr-in Ti-phase geothermometry was applied to rutile/titanite intergrowths in both rock types. In the amphibolites, Zr-in-rutile yielded 600°C indicating that rutile was stable during peak metamorphism. Titanite rims did not yield any results, indicating that they did not grow in equilibrium with zircon, or their *T* of formation was simply too low. In the eclogites, Zr-in-rutile also yielded ca. 600°C and Zr-in-titanite yielded ca. 600°C but only if the calculations were done at low pressures of ca. 0.5 GPa or extremely low *a*SiO<sub>2</sub>. Since quartz is present throughout the rocks this suggests that titanite rims could only have grown during the retrograde stage at much lower *P* possibly indicating an isothermal decompression *P-T* path perhaps even associated with heating. Nonetheless, these first results show that the use of these Ti-phase aggregates is still hampered by precise constraints on *a*SiO<sub>2</sub> and the polymetamorphic nature of the rocks.

## THE DUBIOUS ROLE OF CALIBRATIONS AND ACTIVITY MODELS IN *P-T* CALCULATIONS OF METABASITES

Tropper P.<sup>1</sup>

<sup>1</sup>Institute of Mineralogy and Petrography, University of Innsbruck, Innrain 52, 6020, Innsbruck, Austria  
e-mail: peter.tropper@uibk.ac.at

Geothermobarometric investigations of metamorphic rocks have evolved over the years from using simple phase equilibria to constrain the metamorphic peak *P-T* conditions to complex calculations utilising phase equilibria or thermodynamically stable mineral assemblages involving internally-consistent databases. One characteristic feature occurred over the years: while in the beginning limiting pressure estimates could only be obtained, calculations of the actual pressures using a multitude of phases and reactions yielded oftentimes increasing pressure estimates over the years which are the result of different calibrations and the use of different activity models. A very characteristic example is the Texel Complex: initially (1991) limiting pressures of 1.1 to 1.2 GPa were obtained using the breakdown of albite to jadeite+quartz. Then (2006) pressures (although again only limiting) increased to 1.2 to 1.4 GPa in order to increase (2008) to *P-T* conditions of 1.8-2.2 GPa and 560-600°C. These calculations involved the mineral assemblages garnet+omphacite+epidote+quartz and garnet+omphacite+Na-Ca amphibole+epidote+quartz. In 2013 the *P-T* conditions of eclogites from the Texel Complex climbed to 2.65-2.90 GPa and 630-690°C by using the garnet – omphacite – phengite ± kyanite ± quartz/coesite geothermobarometer. Recalculating a sample from this UHP study yielded an enormous spread in *P* from 2.6 to 4.1 GPa! This is a total variation: 1.5 GPa! Besides using different calibrations, the use of different activity models also has a strong influence on the results. The spread in  $a_{\text{Grs}}$  and  $a_{\text{Py}}$  is huge and  $a_{\text{Grs}}$  even doubles!

The second example is from the Amdo metamorphic complex, located along the Bangong Suture Zone in central Tibet. Garnet-amphibolites provide a record of high-grade metamorphism. Peak *P-T* conditions of gneiss within the metamorphic complex are constrained by conventional as well as multi-equilibrium (THERMOCALC v.3.21 and v.3.33) geothermobarometry of two samples of garnet-amphibolite. Using conventional geothermobarometry one sample yielded *P-T* conditions of 1.01±0.03 GPa and 737±17 °C and the other 0.95±0.04 GPa and 719±19 °C, statistically equal. Whereas THERMOCALC v.3.21 yielded similar results of 0.83±0.06 GPa and 646±33 °C and 0.97±0.06 GPa and 704±35 °C, respectively, when using THERMOCALC v. 3.33 *P-T* conditions dramatically changed to 0.52±0.06 GPa and 701±57 °C and 0.60±0.07 GPa and 674±46 °C, respectively, mostly due to the change in the amphibole activity model used. The aim of this presentation is not to verify or falsify existing *P-T* data but to document the pitfalls in the application of geothermobarometry by pointing out caveats such as the influence of *a-X* relations and different calibrations on the results.



**THERMODYNAMIC MODELLING OF BIOTITE-PLAGIOCLASE  
MICRODOMAINS IN METAPELITES FROM VAL SAVENCA (SESLIA ZONE,  
WESTERN ALPS)**

Tropper, P.<sup>1</sup>

<sup>1</sup>Institute of Mineralogy and Petrography, University of Innsbruck, Innrain 52f, A-6020 Innsbruck, Austria  
e-mail: peter.tropper@uibk.ac.at

A common feature of HP and UHP terranes is the subduction of lower crustal rocks to great depths. Previous investigations have shown that this process is triggered by fluids present during an eclogite-facies metamorphic overprint. If the amount of fluid is low, protolith mineral assemblages will remain and only partial transformations will occur. A key example of these processes is exposed in the metapelites at Val Savenca in the Sesia-Lanzo Zone, Italy, where Alpine eclogite-facies metamorphism and restricted fluid flow led to partial transformation of Variscan amphibolite-eclogite facies metapelites (garnet+biotite+sillimanite+K-feldspar+plagioclase+quartz) to zoisite±jadeite+kyanite+phengite+quartz. This transformation took place under *P-T* conditions of 1.7–2.1 GPa at 600°C and low *a*(H<sub>2</sub>O) of 0.3–0.6. The textures in the Val Savenca metapelites show relict igneous biotite which is rimmed by a thin rind of garnet. Biotite is replaced by the assemblage phengite+omphacite±kyanite±garnet if it is adjacent to former plagioclase, otherwise by phengite + rutile/titanite, or only by phengite. These omphacitic areas contain no zoisite. Thermodynamic modelling of biotite-plagioclase micro-domains was done by calculating pseudo-sections of stoichiometric mixtures of biotite and plagioclase using the ratios 1:1, 1:2, 1:3, 1:5 and 1:10 using the program THERIAK-DOMINO (De CAPITANI & PETRAKAKIS, 2010). Protolith plagioclase composition was calculated using image analysis and yielded a plagioclase composition ranging of around 50% anorthite component. Calculations using a biotite-plagioclase ratio of 1:1 yielded biotite still to be stable. The ratio 1:2 yielded the mineral assemblage garnet+omphacite+phengite+zoisite+rutile but no kyanite. The ratio of 1:3 yielded the same assemblage but with kyanite stable only at low H<sub>2</sub>O contents. Higher ratios yielded only more complex assemblages also involving two micas. The calculations reveal that 1.) plagioclase reacts to a higher extent than biotite which is obvious since no relict plagioclase is left anymore, whereas biotite relicts frequently occur; 2.) the amount of coexisting H<sub>2</sub>O was very low since kyanite occurs in the microdomains, and 3.) garnet also forms in the domains but only nucleates on the sites of pre-Alpine garnet rims around biotite. This study shows that reproduction of the observed mineral assemblage in the plagioclase-biotite microdomains is quite successful and provides estimates on the amount of fluid present during eclogitization.

DE CAPITANI, PETRAKAKIS, K. (2010): American Mineralogist, 95, 1006–1016.

## EXPERIMENTAL INVESTIGATION OF THE HIGH-P STABILITY OF MONAZITE AT 600°C USING NATURAL STARTING MATERIALS

Tropper, P., Mair P. & Viehhauser A.<sup>1</sup>

<sup>1</sup>Institute of Mineralogy and Petrography, University of Innsbruck, Innrain 52, 6020, Innsbruck, Austria  
e-mail: philipp.mair@uibk.ac.at

Accessory minerals are major hosts of minor and trace elements such as Th, U, Y, and rare earth elements (REE). During subduction zone metamorphism these elements are redistributed and may be mobilized as a consequence of irreversible mineral reactions among accessory phases, several rock-forming minerals (e.g. feldspars), and fluids. Petrological investigations of rocks from paleosubduction zones reveal that allanite plays an important role. Allanite  $[\text{Ca}, \text{REE}, \text{Fe}(\text{Al}, \text{Fe})_2(\text{SiO}_4)_3\text{OH}]$  is an important accessory mineral in magmatic and metamorphic rocks and has been described from a range of HP rocks, including garnet-amphibolites, eclogites, and HP/UHP-gneisses. Allanite forms due to the high-P breakdown of monazite according to mineral reactions such as: monazite + Ca-silicate(?) + fluid  $\rightarrow$  allanite + apatite + thorite (REGIS et al., 2012). This feature has also been observed in the jadeite veins from partially transformed metapelites from Val Savenca (Sesia-Lanzo Zone), indicating that fluid composition indeed plays an important role in this reaction. This indicates that allanite is a major carrier of LREE and Th in subducted crustal material.

Until now no experiments concerning the high-P stability of monazite have been done. In this study we investigate the stability of monazite (beach sand monazite from North Carolina) in a natural orthogneiss (granulite-facies orthogneiss from the Gföhl Unit) in the presence of fluid as a function of P at 600°C by doing piston-cylinder experiments. So far two experiments were carried out: 600°C and 2 GPa and 600°C and 2.5 GPa. The experiments show that monazite breaks down to form the assemblage allanite + apatite, although the reaction products are extremely small (in the 600°C, 2 GPa experiment) and occur only very localized. Textures also indicate that protolith plagioclase takes part in the reaction. The inferred reaction therefore is: monazite + plagioclase +  $\text{H}_2\text{O} \rightarrow$  allanite + apatite. The formation of allanite also indicates that most of the REE will stay contained during eclogite-facies conditions at 2-2.5 GPa.

REGIS et al. (2012): Am. Mineral., 97, 315-328.

## MINERALOGY AND PETROLOGY OF THE CTD-IN/CHL-OUT ISOGRADE IN THE SOUTHERN ÖTZTAL COMPLEX

Tropper, P.<sup>1</sup>, Molenaar, A.<sup>1</sup>, Fügenschuh, B.<sup>2</sup>, Mair, V.<sup>3</sup>, Montresor, L.<sup>4</sup>, Morelli, C.<sup>3</sup>,  
Moretti, A.<sup>5</sup>, Pichin, G.<sup>6</sup>, Zanchetta, S.<sup>7</sup>

<sup>1</sup>Institute of Mineralogy and Petrography, University of Innsbruck, A-6020 Innsbruck, Austria

<sup>2</sup>Institute of Geology, University of Innsbruck, A-6020 Innsbruck, Austria

<sup>3</sup>Amt für Geologie und Baustoffprüfung, Eggentalerstrasse 48, I-39053 Kardaun (BZ), Italy

<sup>4</sup>Via G. Verga, 14, 35125 Padova (PD), Italy

<sup>5</sup>Via Liguria 34, 35030, Sarmeola di Rubano (PD), Italy

<sup>6</sup>Dolomiti Project srl, Via Paradiso 31, 32032 Feltre (BL), Italy

<sup>7</sup>Ricerca e Sviluppo nel campo della Geologia Via Verdi 2, Mandello del Lario (LC), Italy

e-mail: [peter.tropper@uibk.ac.at](mailto:peter.tropper@uibk.ac.at)

The Austroalpine nappe stack in the investigated area, located in the Vinschgau area (Southern Tyrol), comprises from bottom to top the Campo-Ortler (COC), the Texel (TC), the Ötztal (ÖC) complexes and the Matsch (M) nappe. All these units have been known for a long time and were essentially defined based on the degree and age of their metamorphic overprint. Their delimiting faults are only partly well known (e.g. Vinschgau shear zone (VSZ), Schneeberg Fault Zone (SFZ) while in other areas they are hard to pin down. This is partly due to the lack of obvious fault rocks such as mylonites or cataclasites as well as to missing petrological/geochronological data (e.g. the contact between TC and ÖC). The currently mapped sheet Schlanders (CARG 012) offers the chance to carefully investigate the above mentioned units and their tectonic contacts and to implement them into a tectonic model based on new petrological, geochronological and structural data.

The petrographical observations of Al-rich garnet-Staurolite-bearing micaschists from the southern Ötztal-Stubai Complex in the area of the CARG 012 sheet Schlanders resulted in the construction of the chloritoid isograd. Distinguished could be three Eo-Alpine mineral zones from west to east: 1) Variscan staurolite and kyanite breaking down to Eo-Alpine phyllosilicates such as chlorite, muscovite and margarite along a model reaction such as:  $10fst + 82an + 94H_2O = 8daph + 82ma + 51q$ , 2) Variscan staurolite breaking down to Eo-Alpine chloritoid, biotite and paragonite and the formation of garnet along a model reaction such as:  $6fst + 7ann + 2ab + 35H_2O = 7mu + 2pa + 45fctd$ , 3) the formation of Eo-Alpine staurolites in the vicinity of the Schneeberg Complex. The calculation of model reactions illustrating these mineral reactions using the software THERMOCALC v.3.33 yielded chlorite, paragonite and chloritoid phase stability fields in agreement with previously published P-T data of this region. A temperature of less than 500°C can be assumed based on literature data as well as the reaction kyanite + anorthite = margarite + quartz for the westernmost samples. Further to the East staurolite breaks down to chloritoid and Eo-Alpine garnet at around 520-540°C based on estimates from the COC. In the East new Eo-Alpine staurolite formed which indicates a maximum possible temperature of around 550-600°C. This staurolite is also very Zn-rich, indicated by its retrograde breakdown to Zn-spinel and chlorite.

## GRAPHIT GEOTHERMOMETRIE DER PB-ZN VERERZUNGEN DER LAGERSTÄTTE SCHNEEBERG AUS DEM PFLERSCHTAL

Ungerank, D. & Tropper P.

<sup>1</sup>Institut für Mineralogie und Petrographie, Universität Innsbruck, Innrain 52, 6020, Innsbruck, Österreich  
e-mail: peter.tropper@uibk.ac.at

Die Graphitschiefer im Pflerschtal stellen mit Sicherheit ehemalige Sapropel dar. Aufgeschlossen sind diese im ehemaligen Teilrevier „Röckengraben“ im Bachbett unweit der heutigen Bergstation der Ladurnser Bergbahnen. Die Graphitschiefer treten vorwiegend im Liegenden oder Hangenden der Vererzungen auf und zwar als Einschaltungen in den Paragneisen. Zusammenhänge zwischen den ursprünglichen bituminösen Schiefern und schichtgebundenen Sulfidvererzungen sind unübersehbar. Die Graphitschiefer zeigen eine ausgeprägte charakteristische Schieferung und Fältelung. Die Mächtigkeit beträgt im Schnitt weniger als einen Meter kann aber auch maximal einige Meter betragen. Die Graphitschiefer führen aufgrund ihrer Nähe zum Vererzungshorizont reichlich Bleiglanz (PbS), Zinkblende (ZnS), Pyrrhotin (FeS) sowie Chalkopyrit (CuFeS<sub>2</sub>). Ziel dieser Untersuchungen war es die *P-T* Bedingungen der Pb-Zn Vererzungen der Lagerstätte Schneeberg im Bereich Pflerschtal zu ermitteln. Die Proben, die für die vorliegende Arbeit untersucht wurden, stammen aus dem Pflerschtal (PF 4, KL I). Bei den beiden Proben handelt es sich um Proben die direkt an der Vererzung genommen wurden. In den zwei Proben im Pflerschtal konnten direkt neben der Vererzung Graphitschlieren und zahlreiche größere Graphiteinschlüsse gefunden werden. Das Interessante daran war, dass man aufgrund der Textur im Probenstück sehen konnte, dass sowohl Erz als auch der Graphit zeitgleich metamorph überprägt wurden, da sich beide konkordant zur Schieferung befanden. So war es erstmals möglich direkte Aussagen zur Bildungstemperatur der Vererzung zu machen.

Aus den Proben des Pflerschtales liegen die ermittelten Temperaturen zwischen 400 und 550°C. Die ermittelte durchschnittliche Temperatur über die 38 Messungen ergibt einen Wert von 470°C ( $\pm 50^\circ\text{C}$ ). Es handelt sich hier also nicht um die Temperatur, wie sie beim Metamorphosehöhepunkt der eo-alpidischen Orogenese geherrscht haben. Mittels Sphaleritgeobarometer konnte ein Druck von ca. 6 kbar berechnet werden. Die Vererzungen sowie die Graphite, die aufgrund struktureller und textueller Gemeinsamkeiten, gleichzeitig gebildet wurden, sind demnach also unter *P-T* Bedingungen entstanden, wie sie mit Sicherheit nach dem Metamorphosehöhepunkt geherrscht haben

# TH-U-PB ALTERSBESTIMMUNG VON MONAZIT IM RASTERELEKTRONENMIKROSKOP MIT EINEM EDS DETEKTOR

Waitzinger, M.<sup>1</sup> & Finger, F.<sup>1</sup>

<sup>1</sup>Universität Salzburg, FB Materialforschung und Physik, Hellbrunnerstraße 8, 5020 Salzburg  
e-mail: Michael.Waitzinger@sbg.ac.at

Die chemische Th-U-Pb Altersbestimmung von akzessorischen Monaziten in Gesteinsdünn-  
schliffen wird üblicherweise mit einer Elektronenmikrosonde im wellenlängendispersiven  
Analysemodus ausgeführt. Aber auch mit modernen energiedispersiven Detektoren lassen  
sich durchaus passable Ergebnisse erzielen. Eine entsprechende Testreihe mit Monazitpopula-  
tionen bekannten Alters (20Ma, 270Ma, 340Ma, 550Ma, 1400Ma, 1870Ma) wurde von uns  
an einem Zeiss ULTRA PLUS Rasterelektronenmikroskop mit dem EDX Detektor INCA  
Synergy 450X-Max 50 von Oxford Instruments durchgeführt. Die Datenauswertung erfolgte  
mit der Software Inca von Oxford Instruments Analytical Limited.

Um ausreichende Zählraten für Pb zu erzielen wurde eine hohe Anregungsspannung von  
25 kV gewählt. Die Zählzeiten pro Messpunkt wurden flexibel gestaltet, mit der Vorgabe,  
dass der individuelle Fehler beim Alter möglichst eine Größenordnung von 30-60Ma (1 $\sigma$ )  
nicht übersteigt. Bei Th(U)-reichen Monaziten mit hohem radiogenem Bleianteil kann dies  
u.U. bereits nach wenigen Minuten erreicht werden. Bei durchschnittlich Th(U)-hältigen  
Monaziten sind dafür Messzeiten von 15-60 Minuten pro Punkt einzuplanen. Bei 60 Minuten  
Zählzeit liegt der analytische Fehler für Pb bei etwa 0,01Gew%.

Bei den Tests wurden fünf Monazite pro Dünnschliff analysiert und daraus jeweils ein  
mittleres Monazitalter errechnet (Fehlerangabe 95% confidence interval). Wie Abbildung 1  
zeigt, konnten die Alter der einzelnen Monazitpopulationen innerhalb eines moderaten  
Fehlers korrekt erfasst werden. Diese Genauigkeit ist ausreichend um z.B. bei  
Monazitkörnern aus dem Alpenen Basement eine Zuordnung zu den wichtigsten  
Metamorphoseereignissen (z.B. känozoisch, kretazisch, permisch, karbon, ordovizisch)  
treffen zu können.

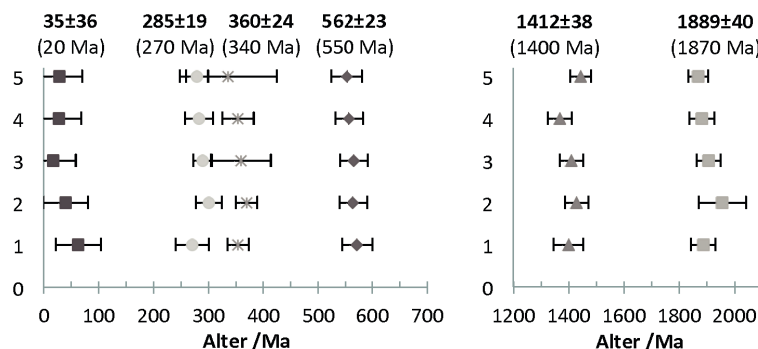


Abbildung 1. Ergebnisse der Monazit-Altersdatierungen mit gewichteten Mittelwerten für die sechs untersuchten  
Proben (Fehlerangabe: 95% confidence interval). Sollwerte der Monazitpopulationen in Klammer.

# **A PETROLOGICAL INVESTIGATION OF THE BLÅHØ NAPPE (SEVE NAPPE COMPLEX) IN SØR-TRØNDELAGE, NORWAY, WITH A PARTICULAR FOCUS ON GARNET IN DIFFERENT LITHOLOGIES**

Weigand, S.<sup>1</sup>, Hauzenberger, Ch.<sup>1</sup> & Gasser, D.<sup>2</sup>

<sup>1</sup>Institute of Earth Sciences, University of Graz, Universitätsplatz 2, 8010 Graz, Austria

<sup>2</sup>Geological Survey of Norway, Postboks 6315 Sluppen, 7491 Trondheim, Norway

e-mail: silvia.weigand@edu.uni-graz.at

The Seve Nappe Complex, primarily outcropping in Sweden, contains remnants of Ordovician HP and UHP metamorphism, overprinted by upper amphibolite facies metamorphism and anatexis during the Silurian. In Norway, in the hinterland of the Caledonian orogen, rocks of the Blåhø Nappe have been correlated with the Seve Nappe Complex, but their metamorphic history is much less investigated. The Blåhø Nappe is strongly overprinted by post-collisional extension, and it is unknown whether these rocks experienced the same high pressure conditions as the Seve Nappe Complex in Sweden.

Recent detailed mapping within the Blåhø nappe revealed that it mainly consists of micaschist, amphibolite, orthogneiss (felsic volcanites) and pegmatites. Garnet is commonly seen in the first two lithologies. Garnet zoning pattern from these two lithologies are used together with selected geothermobarometers and thermodynamic modelling to investigate whether the Blåhø Nappe experienced a similar metamorphic history as the Seve Nappe Complex. The micaschists comprise the mineral assemblage garnet+biotite+amphibole+quartz+plagioclase+muscovite+clinopyroxene+tourmaline+rutile (see Fig. 1A). Preliminary results show that garnet in the micaschist display a single phase prograde growth zoning pattern (Fig. 1B), while the metabasites, with the mineral assemblage amphibole+garnet+titanite+biotite+plagioclase+quartz show no or only slightly chemically zoned garnets.

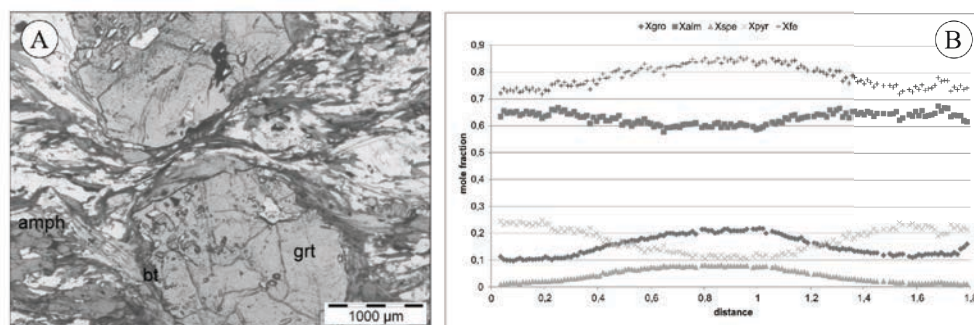


Figure 1. Mineral assemblage consisting of garnet+biotite+amphibole+quartz+plagioclase+muscovite+clinopyroxene+tourmaline+rutile and chemical garnet profile of micaschists from the Blåhø Nappe.



**THERMAL WATERS FROM SÃO MIGUEL (AZORES, PORTUGAL):  
HYDROCHEMICAL AND STABLE ISOTOPIC EVIDENCE FOR GAS-WATER-  
ROCK INTERACTIONS**

Woitischek, J.<sup>1</sup>, Dietzel, M.<sup>1</sup>, Cruz, J.V.<sup>2</sup> Leis, A.<sup>3</sup> & Böttcher, M.E.<sup>4</sup>

<sup>1</sup>Institute of Applied Geoscience, Graz University of Technology, Rechbauerstraße 12, 8010 Graz, Austria

<sup>2</sup>CVARG Department of Geoscience, University of Azores, Ladeira da Mãe de Deus,  
9501-855 Ponta Delgada, Portugal

<sup>3</sup>Institute of Water, Energy and Sustainability, Joanneum Research, Elisabethstraße 18, 8010 Austria

<sup>4</sup>Leibniz Institute for Baltic Sea Research (IOW), Geochemistry and Stable Isotope Biogeochemistry Group,  
D-18119 Warnemünde, Germany  
e-mail: j.woitischek@student.tugraz.at

Thermal waters of São Miguel have been analysed to decipher the geochemical and isotopic evolution to create a conceptual model for a geothermal system in an evolving basaltic ocean island. Besides waters, precipitates and local volcanic rocks were sampled for analyses in the area of Sete Cidades, Fogo and Furnas volcano. Thermal discharges were divided into springs (up to 75°C) and boiling pools, and classified by the dominant dissolved ions in Na-SO<sub>4</sub>, Na-HCO<sub>3</sub> and Na-Cl type waters. The pH-values of all thermal discharges range between 2.1 and 7.6. In Furnas, the concentrations of Si(OH)<sub>4</sub>, K<sup>+</sup> and Sr<sup>2+</sup> increased through intensive leaching of basaltic rocks at enhanced temperature, whereas Al<sup>3+</sup> and ΣFe concentrations decreased by precipitation of e.g. alunite. In Fogo, at higher altitude in particular CO<sub>2</sub> rich water at T≈20°C occurs. In this case HCO<sub>3</sub><sup>-</sup> concentration and its isotopic composition (δ<sup>13</sup>C(DIC)=-5±3‰V-PDB) reflect evolved uptake of volcanic CO<sub>2</sub> and subsequent leaching progress. The extent of basaltic rock leaching rather depends on uptake of volcanic CO<sub>2</sub> (calculated δ<sup>13</sup>C(CO<sub>2(gas)</sub>)) ranging between -3 and -4‰V-PDB than on temperature. High SO<sub>4</sub> concentration of up to 16.5mmolL<sup>-1</sup> with δ<sup>34</sup>S(SO<sub>4</sub>)=0.35±0.3‰V-CDT are reflecting a volcanic origin which mainly controls water chemistry of the boiling pools of both Fogo and Furnas lake. Low δ<sup>34</sup>S(SO<sub>4</sub>) values of -3.7‰V-CDT are accompanied by stromatolite-like microstructures in siliceous precipitates, which had been collected at the rim of domal mound. Microbial processes could trigger this low δ<sup>34</sup>S(SO<sub>4</sub>) values, but it is difficult to distinguish them from δ<sup>34</sup>S caused by magmatic processes because of their overlap. Therefore, we propose that the combined hydrochemical and stable isotope signature allow for an estimation of the overall distance to the magma sources and could be used as an indicator of volcanic activity itself. Ferraria water is discharging from a basal aquifer of Sete Cidades volcano and belongs to the Na-Cl type, where stable hydrogen and oxygen isotopes reveal mixing of meteoric and sea water. The molar Mg/Ca ratio (0.77) of all thermal discharges of São Miguel reflects leaching of the regional basalt (Mg/Ca≈0.78).

**STUDY OF THE VOLCANIC FACIES AND THE SUBMARINE HYDROTHERMAL PROCESSES OF THE JURASSIC BASALT AT SZARVASKŐ (NE HUNGARY)**

Zagyva, T.<sup>1</sup>, Kiss, G.B.<sup>1</sup> & Zaccarini, F.<sup>2</sup>

<sup>1</sup>Department of Mineralogy, Eötvös Loránd University, Pázmány P. stny. 1/c, Budapest, Hungary

<sup>2</sup> Department of Applied Geosciences and Geophysics, University of Leoben, Peter Tunner Str. 5,  
Leoben, Austria

e-mail: [tamas.zagyva@gmail.com](mailto:tamas.zagyva@gmail.com)

The Jurassic pillow basalt outcrops around Szarvaskő (NE Hungary) belong geologically to the Szarvaskő Unit, within the Bükk Unit and form a part of an incomplete ophiolitic sequence. According to the most recent studies, the origin of the magmatic rocks of Szarvaskő is related to a back-arc-basin or a marginal basin opening (AIGNER-TORRES & KOLLER, 1999). Though several studies were carried out about the basalt, the complex volcanic facies analyses of the outcrops within the village of Szarvaskő and its close vicinity, and the description of the primary submarine hydrothermal processes have not been performed.

Closely packed pillow and pillow-fragmented hyaloclastite breccia facies of a submarine basaltic lava flow have been identified. The relative distance between the different closely-packed pillow blocks and the central part of the basaltic lava flow has been determined, based on the size of the pillows and the amount of the inter-pillow hyaloclastite breccia. In the pillow-fragmented hyaloclastite breccia block, hydrothermal minerals and siliciclastic sediment were found, filling the space among the breccia clasts. Thus, this locality represents a transition between the pillow-fragmented hyaloclastite breccia and the peperitic facies s.l.

Chlorite, prehnite and quartz precipitated during the earlier, higher temperature part of the hydrothermal process, while later, at lower temperatures, pumpellyite±calcite precipitated. Minerals of a very low-grade metamorphic overprint were also identified.

Chlorite geothermometry, fluid inclusion microthermometry and Raman spectroscopy measurements have been performed in order to obtain temperature information about the different steps of the hydrothermal processes. Based on the composition of the early chlorite, an average formation temperature of 183°C±7°C was found using the geothermometer of ZANG & FYFE (1995). Fluid inclusion microthermometry measurements on quartz and calcite of the inter-pillow hyaloclastite breccia (closely packed pillow) and the pillow-fragmented hyaloclastite breccia facies characterise a later part of the hydrothermal processes. The characteristics of the fluid in the inter-pillow hyaloclastite breccia (Th(LV-L)=145-155°C, salinities ~6-8 NaClequiv.m%) and in the hyaloclastite breccia facies (Th(LV-L)=133-153°C) are similar than in the primary submarine hydrothermal minerals of a nearby Jurassic basalt locality (KISS et al., 2011), and different from the results obtained from the minerals of the Alpine regional metamorphic overprint (KISS et al., 2012). This research was granted by the Hungarian Science Foundation (OTKA, PD 112580) to G.B. Kiss.

AIGNER-TORRES, M. & KOLLER, F. (1999): *Ofioliti*, 24, 1-12.

KISS, G., MOLNÁR, F., KOLLER, F., PÉNTEK, A. (2011): *Mitt. Österr. Miner. Ges.*, 157, 43-69.

KISS, G., MOLNÁR, F., ZACCARINI, F. (2012): *Centr. Eur. J. Geosci.*, 261-274.

ZANG, W., FYFE, W. S. (1995): *Mineralium Deposita*, 30, 30-38.

**HIGH-RESOLUTION SEM STUDY OF AUTHIGENIC HIGH-MG CALCITE AND  
(PROTO-) DOLOMITE OF LAKE NEUSIEDL (AUSTRIA)**

Zünterl, A.<sup>1</sup>, Neuhuber, S.<sup>2</sup>, Kogelbauer, I.<sup>2</sup>, Ottner, F.<sup>2</sup>, Dietzel, M.<sup>1</sup> & Hippler, D.<sup>1</sup>

<sup>1</sup>Technische Universität Graz, Inst. Applied Geosciences, Rechbauerstraße 12, 8010 Graz, Austria

<sup>2</sup>Universität der Bodenkultur, Inst. Applied Geosciences, Peter-Jordan-Straße 70, 1190 Wien, Austria  
e-mail: dorothee.hippler@tugraz.at

Lacustrine environments provide an ideal setting to study the formation of authigenic high-Mg calcite/(proto-) dolomites. Within these settings carbonate mineral formation is highly controlled by the saturation state and reaction kinetics depending on e.g. (1) alkalinity, due to physico-chemical conditions or microbial activity, (2) degree of evaporation, and/or (3) mixing of different water bodies. Here, we present new results on the formation of authigenic carbonate precipitates of Lake Neusiedl (Austria) that were first noted in the early 70's. We performed high-resolution imaging and mapping on different size fractions of five sediment samples of Lake Neusiedl applying field emission SEM, equipped with SE and BSE detectors and an EDX system. The aim of our study is to better understand the mechanisms controlling the formation of Mg-rich carbonates in Lake Neusiedl, as a case study for low temperature (proto-) dolomite formation environment by investigating mineralogical and chemical composition, as well as their microstructure.

We found clear evidence for the authigenic origin of the investigated high-Mg calcite/(proto-) dolomites, which form spherical aggregates ranging in size from 0.4  $\mu\text{m}$  to 3  $\mu\text{m}$ . These aggregates are made of (i) cauliflower-arranged amorphous or cryptocrystalline precipitates or (ii) nano-sized rhombs ( $\leq 0.2 \mu\text{m}$ ). BSE imaging reveals no zoning, but homogenous distribution of Ca and Mg ions in the carbonate phases. The evaluation of the Mg to Ca ratio yields two types of high-Mg carbonate phases: Type 1 represents (proto-) dolomites with excess Mg over Ca (Mg:Ca = 1.1 to 1.5), and type 2 consists of the high-Mg carbonate solid phase calcite with a Mg:Ca ratio of 0.7. Interestingly, the sediment also contains framboidal pyrite besides quartz, feldspar, mica (smectite), and low-Mg calcite.

According to our findings, we propose that an amorphous precursor phase initiates precipitation of the Mg rich carbonate phase, which subsequently form (proto-) dolomite by suggesting dissolution-reprecipitation reactions. The occurrence of framboidal pyrite points to bacterial sulfate reduction, which likely stimulates high-Mg carbonate/(proto-) dolomite precipitation in particular in respect to the high alkalinity and elevated Mg/Ca ratio ( $> 5$ ) of the solution of Lake Neusiedl.

D.H., M.D. and A.Z. kindly acknowledge financial support through the TU Graz Anschubfinanzierung. We also thank S. Simic (FELMI) and G. Auer (Universität Graz) for assistance during SEM analyses. This is a contribution to NAWI Graz.

# ALPHABETICAL LISTING OF CONTRIBUTORS

|                         |   |
|-------------------------|---|
| Abart R.                | 15, 25, 39, 40, 76, 98, 101, 108, 116           |
| Ageeva O.               | 15  |
| Aldrian A.              | 16  |
| Ahrer S.                | 107   |
| Altenburger I.          | 16  |
| Anelli-Monti I.         | 60  |
| Artho R..               | 57  |
| Atzenhofer C.           | 17  |
| Bachhuber P.            | 18  |
| Bakker R.J.             | 19, 20, 102                                     |
| Baldermann A.           | 24, 69  |
| Balen D.                | 89  |
| Bau M.                  | 73, 74  |
| Bayer B.C.              | 21  |
| Belak M.                | 89  |
| Belic M.                | 22  |
| Bernhard F.             | 67  |
| Binder H.               | 49  |
| Bjerg E.                | 68, 97  |
| Boch R.                 | 23, 24, 44, 109                                 |
| Böchzelt B.             | 99  |
| Böhm A.                 | 33  |
| Böttcher M.E.           | 133   |
| Bourgin N.              | 25  |
| Brandstätter F.         | 26  |
| Braun D.E.              | 56  |
| Brauns M.               | 86  |
| Breiter K.              | 27  |
| Brosch E.               | 28  |
| Brunello E.             | 29  |
| Brunner R.              | 99  |
| Buda Gy.                | 52  |
| Butcher A.R.            | 41  |
| Buttinger-Kreuzhuber T. | 30  |
| Cruz J.V.               | 133   |
| Czuppon Gy.             | 91  |
| Dabić P.                | 47  |
| Danling Ch.             | 22  |
| Deák J.                 | 23  |
| Demarchi G.             | 62  |
| Demeny A.               | 23  |
| Dietzel M.              | 23, 24, 44, 69, 85, 99, 104, 109, 120, 133, 135 |
| Dobbe R.                | 41  |

|                   |                     |
|-------------------|---------------------|
| Dódony I.         | 91                  |
| Dorn T.           | 114                 |
| Dosbaba M.        | 38                  |
| Dong Y.           | 22                  |
| Đordevič T.       | 30                  |
| Dunkl I.          | 91                  |
| Eder M.           | 99                  |
| Effenberger H.    | 31                  |
| Ellersdorfer M.   | 122                 |
| Falschlunger H.   | 57                  |
| Feimuth M.W.      | 32                  |
| Fernando G.W.A.R. | 100                 |
| Finger F.         | 77, 84, 113, 131    |
| Fisslthaler E.    | 75                  |
| Flachberger H.    | 33, 75              |
| Franz G.          | 48                  |
| Freiberger N.     | 101                 |
| Fröschl H.        | 44                  |
| Fügenschuh B.     | 129                 |
| Ganwa A.A.        | 34                  |
| Gasser D.         | 132                 |
| Gerdes A.         | 72                  |
| Giestler G.       | 26                  |
| Girtler D.        | 35                  |
| Gobba J.M.        | 81                  |
| Goettgens V.      | 36                  |
| Göd R.            | 37                  |
| Goldbrunner J.    | 44                  |
| Götze L.C.        | 76                  |
| Gottlieb P.       | 38                  |
| Gravogl G.        | 39                  |
| Gregoire M.       | 97                  |
| Griffiths T.A.    | 40                  |
| Grill H.A.        | 117                 |
| Gröbner K.        | 70                  |
| Günes Z.          | 62                  |
| Gschiel S.        | 17                  |
| Haberlah D.       | 41                  |
| Habler G.         | 39, 40, 71, 76, 101 |
| Haeger T.         | 42, 45              |
| Hakim A.Y.A.      | 43                  |
| Hanel M.          | 58                  |
| Harlov D.         | 78                  |
| Harmuth H.        | 17, 59, 64, 83      |
| Haslinger E.      | 44                  |

|                        |   |
|------------------------|---|
| Hauzenberger C.A.      | 22, 28, 45, 70, 81, 97, 100, 105, 107, 110, 111, 112, 113, 119, 132 |
| Hejny C.               | 29, 47  |
| Heinisch M.            | 46  |
| Henn U.                | 42  |
| Hippler D.             | 48, 99, 120, 135  |
| Hoang N.               | 70, 81, 105   |
| Holzmann J.            | 51  |
| Höllen D.              | 16, 49, 50, 118, 124  |
| Hoinkes G.             | 46, 111   |
| Horvat M.              | 52  |
| Hoschek G.             | 53  |
| Hrstka T.              | 27  |
| Iglseder C.            | 119   |
| Jamičić D.             | 52  |
| Jank A.                | 57  |
| Jollands M.            | 54, 98  |
| Jerabek P.             | 76  |
| Jumanne R.             | 81  |
| Junge M.               | 55, 74  |
| Kahlenberg V.          | 29, 36, 47, 56, 57, 82, 90, 92, 114                                 |
| Kain-Bückner B.        | 58  |
| Kaindl R.              | 21  |
| Kärner K.              | 55  |
| Karlowski P.           | 42  |
| Karydas A.             | 26  |
| Khisina N.             | 39  |
| Khoi N.N.              | 70, 105   |
| Kircher V.             | 59, 64  |
| Kiss G.B.              | 91, 134   |
| Klammer D.             | 18, 60  |
| Kleindienst A.         | 61  |
| Klötzli E.             | 52  |
| Klötzli U.             | 34, 37, 52, 62, 71, 89  |
| Knaus R.               | 44  |
| Knebl U.G.             | 63  |
| Koeberl C.             | 26  |
| Kölbl N.               | 59, 64  |
| Kogelbauer I.          | 135   |
| Kolitsch U.            | 30, 32, 65, 66, 67  |
| Kolosova-Satlberger O. | 68  |
| Konrad F.              | 69, 85, 104   |
| Konzett J.             | 70, 81, 105   |
| Kopřiva A.             | 38  |
| Kovaleva E.            | 71  |
| Kozlik M.              | 72  |



|                    |                                       |
|--------------------|---------------------------------------|
| Kraemer D.         | 55, 73, 74                            |
| Krenn K.           | 46, 63, 70, 106, 111                  |
| Krois L.-M.        | 49                                    |
| Krüger H.          | 29, 90                                |
| Kuhnt-Saptodewo S. | 26                                    |
| Kurzweil H.        | 37                                    |
| Lämmerer W.        | 75                                    |
| Legerer P.         | 121                                   |
| Lehner M.          | 50, 124                               |
| Leis A.            | 23, 24, 44, 133                       |
| Leitner W.         | 112                                   |
| Lengauer C.L.      | 31, 32                                |
| Li C.              | 76                                    |
| Le Thi-Thu Huong   | 45                                    |
| Libowitzky E.      | 31                                    |
| Lindner M.         | 77                                    |
| Linner M.          | 110, 119                              |
| Lorenz C.          | 39                                    |
| Lubensky J.        | 122                                   |
| Mair P.            | 36, 78, 79                            |
| Mair V.            | 129                                   |
| Mali H.            | 58, 107                               |
| Makovicky E.       | 80, 123                               |
| Mamczek M.         | 48                                    |
| Mandl M.           | 81                                    |
| Mangler C.         | 76                                    |
| Manning C.E.       | 78                                    |
| Manninger T.       | 82                                    |
| Marbler H.         | 55                                    |
| Marschall I.       | 59, 83                                |
| Matzinger M.       | 84                                    |
| Mavromatis V.      | 69, 85, 104                           |
| Melcher F.         | 43, 50, 55, 75, 86, 95, 107, 117, 124 |
| Mindszenty A.      | 23                                    |
| Mirwald P.W.       | 87, 88                                |
| Mischitz R.        | 49                                    |
| Mišur I.           | 89                                    |
| Mitsche St.        | 75                                    |
| Mörtl A.           | 90                                    |
| Mogessie A.        | 61, 63, 106                           |
| Molenaar A.        | 129                                   |
| Molnár Zs.         | 91                                    |
| Montresor L.       | 129                                   |
| Morelli C.         | 129                                   |
| Moretti A.         | 129                                   |

|                    |              |
|--------------------|--------------|
| Moser P.           | 124          |
| Motl D.            | 38           |
| Müller P.          | 49           |
| Müllner M.         | 92           |
| Neinavaie H.       | 121          |
| Neuhuber S.        | 135          |
| Nguyen N.K.        | 45           |
| Nickel C.          | 18           |
| Niesenbacher I.    | 50, 124      |
| Niiranen K.        | 93           |
| Nilica R.          | 94           |
| Ntafos T.          | 39, 68, 97   |
| Oberthür T.        | 55, 74, 86   |
| Olbrich T.         | 49           |
| Onuk P.            | 95           |
| Orlova M.          | 56           |
| Ottner F.          | 135          |
| Paar W.H.          | 96           |
| Padilla-Alvarez R. | 26           |
| Papadopoulou M.    | 97           |
| Paulini P.         | 87           |
| Pačevski A.        | 30           |
| Pennycook T.J.     | 76           |
| Perfler L.         | 92           |
| Petrakakis K.      | 25           |
| Petrishcheva E.    | 98           |
| Petschacher N.     | 99           |
| Petschnig P.       | 100          |
| Pichin G.          | 129          |
| Pimminger H.       | 101          |
| Plank O.           | 44           |
| Pölt P.            | 24           |
| Pomberger R.       | 118          |
| Pribil B.          | 102          |
| Prochaska W.       | 103          |
| Purgstaller B.     | 104          |
| Putz H.            | 31           |
| Quick J.           | 62           |
| Rachetti A.        | 121          |
| Raič S.            | 61, 105, 106 |
| Raith J.G.         | 72, 107, 121 |
| Rantitsch G.       | 75, 121      |
| Reichl P.          | 24           |
| Reiter E.          | 84           |
| Rhede D.           | 40           |

|                      |   |
|----------------------|---|
| Rieck B.             | 66  |
| Rieder M.            | 108   |
| Röggla M.            | 111   |
| Rümmele F.           | 18  |
| Sakoparnig M.        | 109   |
| Sato K.              | 62  |
| Schachinger T.       | 67  |
| Schaffler E.         | 116   |
| Schantl Ph.          | 110, 111  |
| Schifferle L.        | 112   |
| Schiller D.          | 113   |
| Schilli S.E.         | 20  |
| Schmidmair D.        | 29, 36, 92, 114   |
| Schmidt-Balassari M. | 57  |
| Schmitz F.           | 42  |
| Scholger R.          | 60  |
| Schorn S.            | 115   |
| Schuster R.          | 111, 116  |
| Schwabl S.           | 117   |
| Schweiger G.         | 16  |
| Sedlazeck K.P.       | 118   |
| Shirbaz A.           | 44  |
| Sieberer A.-K.       | 70  |
| Sitnikova M.         | 107   |
| Sinigoï S.           | 62  |
| Sorger D.            | 119   |
| Spötl C.             | 109   |
| Stammeier J.         | 85, 120   |
| Stalder R.           | 70  |
| Stocker K.           | 107, 121, 122   |
| Stöllner M.          | 50  |
| Struck U.            | 48  |
| Stüwe K.             | 115   |
| Sutthirat C.         | 45  |
| Szanyi J.            | 23  |
| Tassinari C.         | 62  |
| Tessadri R.          | 57  |
| Topa D.              | 15, 31, 123   |
| Treimer R.           | 50, 124   |
| Tribus M.            | 29, 114, 125  |
| Többens D.M.         | 29  |
| Tropper P.           | 35, 46, 51, 78, 79, 88, 112, 125, 126, 127, 128, 129, 130 |
| Twrdy G.             | 75  |
| Ungerank W.          | 112, 130  |
| Vesseur E.J.         | 41  |

|               |              |
|---------------|--------------|
| Viehhauser A. | 128          |
| Visser S.     | 26           |
| Voudouris P.  | 66           |
| Waitzinger M. | 131          |
| Wang X.       | 109          |
| Wathankul P.  | 45           |
| Weigand S.    | 132          |
| Woitischek J. | 133          |
| Wyllidal S.   | 44           |
| Wotruba H.    | 86           |
| Zaccarini F.  | 91, 102, 134 |
| Zagyva T.     | 134          |
| Zanchetta S.  | 129          |
| Zöll K.       | 79           |
| Zünterl A.    | 135          |
| Zsolt B.      | 61           |

*Sponsors MinPet 2015 - Leoben*



Leading With Innovation



